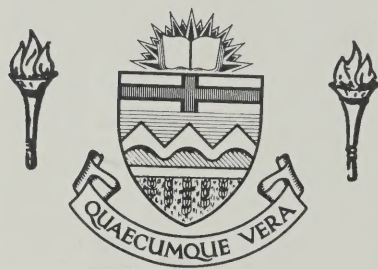



For Reference

NOT TO BE TAKEN FROM THIS ROOM

Ex LIBRIS
UNIVERSITATIS
ALBERTAENSIS





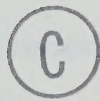
Digitized by the Internet Archive
in 2022 with funding from
University of Alberta Library

<https://archive.org/details/Hiob1980>

THE UNIVERSITY OF ALBERTA

RESONANCE RADIATION TRAPPING WITH APPLICATION TO
THE PHONON BOTTLENECK IN OPTICALLY PUMPED RUBY

by



ERIC ERWIN HIOB

A THESIS

SUBMITTED TO THE FACULTY OF GRADUATE STUDIES AND RESEARCH
IN PARTIAL FULFILLMENT OF THE REQUIREMENTS FOR THE DEGREE
OF DOCTOR OF PHILOSOPHY

IN

THEORETICAL PHYSICS

DEPARTMENT OF PHYSICS

EDMONTON, ALBERTA

FALL, 1980

ABSTRACT

The resonant interaction between radiation and two-level states, with application to the interaction between 29-cm^{-1} phonons and excited Cr^{3+} ions in optically pumped ruby, is studied via the Heisenberg equations of motion for the system. As a first example the spontaneous decay of a single two-level state is studied. Next a set of rate equations, rigorously valid for low densities of two-level states, is derived from the Heisenberg equations. The rate equations show that in the case of far-from-equilibrium initial conditions the system relaxes rapidly to an intermediate quasi-equilibrium with the density of electronic states in the upper level increasing with the density N^* of two-level states, i.e. Cr^{3+} ions in the case of optically pumped ruby, like $N^{*\frac{1}{2}}$ for large N^* . It is shown that spatial diffusion is ineffective as an escape mechanism for the phonons for large N^* . Thus the subsequent decay of the system is controlled by spectral diffusion of the phonons away from the resonance frequency due to repeated absorption and emission by the two-level states, with accompanying rearrangement of the phonon and electronic energies in the coupled mode. The phonon spectrum inside the excited region of the ruby crystal (with diameter b) is shown to suffer self-reversal and to broaden with time to a final width proportional to $(N^*b)^{\frac{1}{2}}$. The effects of the inhomogeneous broadening of the resonance, due to possible

random static strains in the ruby crystal, on the evolution of the electron-phonon system are also briefly examined. Finally some exact solutions of the Heisenberg equations are found and improvements on the rate equations suggested by field theory are studied.

ACKNOWLEDGEMENTS

I am indebted to my wife Lidia for the encouragement that she gave me and the sacrifices that she made during the course of my studies.

I would like to thank my supervisor, Dr. H.J. Kreuzer for his excellent guidance, encouragement and friendship.

I would also like to thank Bob Teshima (who never ceases to amaze me) for help with the numerics.

Finally I would like to thank Mrs. Mary Yiu for her great kindness in typing my thesis.

My appreciation is also extended to the National Research Council and the Province of Alberta for providing financial assistance.

TABLE OF CONTENTS

<u>Chapter</u>		<u>Page</u>
1	INTRODUCTION	1
	1.1 General Survey	1
	1.2 The Phonon Bottleneck in Ruby	13
	1.3 Aim and Scope of the Present Investigation	27
2	FIELD THEORETICAL DESCRIPTION OF THE PHONON BOTTLENECK (I)	28
	2.1 The Electron-Phonon Interaction	28
	2.2 Survey of Solutions to the Electron-Phonon Interaction Problem	35
	2.3 Linear Equations of Motion for the Electron-Phonon System	45
3	SPONTANEOUS DECAY OF A SINGLE TWO-LEVEL ATOM AND THE GENERAL THEORY OF THE DECAY OF UNSTABLE QUANTUM SYSTEMS	55
	3.1 Decay of a Two-Level Atom in a Finite Crystal	56
	3.2 Decay of a Two-Level Atom in an Infinite Crystal	66
	3.3 Notes on the General Theory of Decay of Unstable Quantum Systems	75
4	DERIVATION OF PHENOMENOLOGICAL RATE EQUATIONS FOR THE PHONON BOTTLENECK	78
	4.1 The Derivation	78
	4.2 Comparison with Pauli's Derivation of the Master Equation	87

<u>Chapter</u>		<u>Page</u>
5	SOLUTION OF THE RATE EQUATIONS	91
	5.1 The Solution and Comparison with Experiment	91
	5.2 Inclusion of Inhomogeneous Broadening	117
	5.3 Discussion	121
6	FIELD THEORETIC DESCRIPTION OF THE PHONON BOTTLENECK (II)	125
	6.1 General Description	125
	6.2 Exact Results	139
7	CONCLUSION	160
	REFERENCES	163
	APPENDIX. The Emitted Phonon Spectrum	169

LIST OF TABLES

<u>Table</u>		<u>Page</u>
4.1	Comparison of Pauli's master equation with phonon bottleneck equations.	90

LIST OF FIGURES

<u>Figure</u>		<u>Page</u>
1.1	Real and imaginary parts of function $c_0/c(\omega)$.	11
1.2	Energy levels of the Cr^{3+} ion.	14
1.3	Experimental arrangement to study phonon bottleneck.	17
1.4	R_2 signal found by Pauli. ²⁰	19
1.5	N_2^{eq}/N^* and T_S as functions of N^* .	21
1.6	Experimental results of Dijkhuis. ¹⁴	26
2.1	Phonon dispersion curves.	31
2.2	Energy levels in the Dicke model.	41
2.3	Perturbation tree for $S^-(t)$.	52
3.1	A single atom coupled to a single phonon mode.	58
3.2	Graphical solution for poles of $\mathcal{J}^-(x)$.	62
3.3	A single atom coupled to a finite number of phonon modes.	65
3.4	A single atom coupled to infinitely many phonon modes.	70
5.1	Graphical solution of the rate equations.	100
5.2	Time evolution of the phonon bottleneck.	103
5.3	T_S as a function of N^* .	105
5.4	Time evolution of the phonon spectrum.	110
5.5	N_2^{eq}/N^* as a function of N^* .	116
5.6	T_S vs. N^* for a Voigt profile.	119

<u>Figure</u>		<u>Page</u>
6.1	Fourier transform of the probability amplitude for the decay of an excited atom influenced by a nearby unexcited atom, to various approximations.	141
6.2	Fourier transform of Fig. 6.1.	142
6.3	Perturbation about the Dicke model.	155

CHAPTER 1

INTRODUCTION

1.1 General Survey

The interaction of radiation in resonance with a system of two-level atoms has long been a subject of interest. Resonance radiation refers to that part of the spectrum that is emitted by an atom in an electronic transition from some excited state to the ground state or a metastable state. If most of the atoms of the system are in the ground state (or the metastable state) then this radiation is highly absorbable and will very likely be absorbed by another atom after traversing a short distance, thus exciting that atom. This situation is referred to as the 'trapping' of the resonance radiation. By a 'random walk' process of emission and subsequent absorption by different atoms the radiation eventually reaches the boundary of the system and is lost into the bath.

If a phonon rather than a photon is emitted in the electronic transition, the resonance radiation trapping is referred to as the phonon bottleneck. In this case the decay of the two-level atoms leads to a transfer of energy to a narrow band of phonon modes near the resonance frequency ν_0 , which in turn deliver this energy to the thermal bath of the surrounding crystal. If the rate of decay of

the atoms is slower than the rate of delivery of energy to the bath by the phonons, then the phonon modes near resonance act as a reservoir i.e. they are almost always empty and can absorb all the energy emitted by the decaying atoms. We may say that the phonon modes are at the bath temperature of 0 K. Thus the excited two-level atoms can decay unhindered with their spontaneous decay rate $1/T_1$. On the other hand, if the rate of delivery of energy to the bath by the phonons, due to multiple absorption and emission, is slower than the rate of decay of the atoms, then the phonon modes near resonance will become effectively full. Before another atom can decay, it must wait for some of the phonon modes near resonance to empty their energy to the bath. Because of this phonon bottleneck the effective decay time T_s of the system is prolonged.

At first glance it might appear that since phonons are bosons an unlimited number can be put in any mode so that the two-level atoms should always be able to decay freely. However statistical considerations show that the phonons and atoms reach a quasi-equilibrium with the fraction of phonon modes near resonance that are occupied never exceeding the fraction of two-level atoms that are excited. We may say that the phonon modes near resonance, as measured by the occupation numbers, heat up to the temperature of the two-level atoms and no higher.

The earliest experiments on the trapping of resonance radiation were done on the optical resonance lines of

mercury and sodium vapor under low pressure¹. For example Webb² in 1924 and Zemansky³ in 1927 studied the trapping of the 2537 Å photon emitted in the $6^3P_1 \rightarrow 6^1S_0$ ground state transition of the mercury atom. They observed that the trapped radiation decayed in times of the order $T_s \approx 10^{-4}$ sec (which is 10^3 times longer than the lifetime $T_1 \approx 10^{-7}$ sec of the 6^3P_1 state), and that T_s increased with the density N^* of mercury atoms in the ground state for small N^* as one would expect. However at the largest densities N^* they found that T_s actually decreased very slowly with N^* . This rather surprising result was attributed either to pressure broadening or to the more frequent collisions at higher pressures causing non-radiative transitions from the radiating 6^3P_1 state to the metastable 6^3P_0 state 0.218 volts lower. In the former case, collisions with the radiating atom cut off the radiating wavetrain, thus increasing the natural linewidth (hence the name pressure broadening) and effectively reducing the lifetime T_1 of the excited state and presumably also the decay time T_s of the system. In the latter case, a competing process simply reduces the number of atoms in the radiating 6^3P_1 state. Aside from these factors one must take into account the hyperfine structure of the 2537 Å line, the Doppler broadening of the line due to thermal motion of the gas molecules, and a host of emission and absorption processes induced by atomic collisions. Thus we see that optical experiments on gases are very 'unclean' i.e. there are many complicating factors

that make interpretation of the experimental results difficult. We shall see shortly that many of these problems can be eliminated by doing similar experiments on magnetic impurity doped crystals at low temperatures.

The first theoretical treatments of resonance radiation trapping were given by K.T. Compton⁴ in 1922 and E. Milne⁵ in 1926 in connection with the transmission of light in the atmospheres of stars. They assumed that the radiation quanta propagated from atom to atom by a type of random walk. Thus the density of excited atoms N_2 could be described by the diffusion equation

$$\frac{\partial N_2(\underline{r}, t)}{\partial t} = \mathcal{D} \nabla^2 N_2(\underline{r}, t) , \quad (1.1)$$

with diffusion constant

$$\mathcal{D} = \frac{\Lambda \bar{c}}{3} , \quad (1.2)$$

where Λ is the mean-free-path of the quanta, and

$$\bar{c} = \frac{\Lambda}{T_1 + T_{ph}} \quad (1.3)$$

is the average velocity of the quanta taking into account the time of the collision i.e. the excited state lifetime T_1 as well as the propagation time between collisions T_{ph} . In the case of photons one can obviously neglect T_{ph} in comparison to T_1 . The treatment of Compton and Milne however did not take into account the fact that the mean-free-path of the quanta is not constant but highly frequency

dependent. The mean-free-path of radiation on resonance is very short whereas that of radiation far from resonance is very long and limited only by the dimension b of the container. Thus the meaning of Λ in Eq. (1.3) is unclear.

In 1947 Holstein⁶ derived an integral transport equation describing the time decay of the density of excited atoms $N_2(\underline{r}, t)$ taking into account the frequency dependence of the mean-free-path, namely

$$\frac{\partial N_2(\underline{r}, t)}{\partial t} = -\frac{N_2(\underline{r}, t)}{T_1} + \int_{\Omega} d^3 r' \int_0^{\infty} d\nu \frac{N_2(\underline{r}', t)}{T_1} f(\nu) \frac{e^{-\alpha(\nu) \cdot |\underline{r} - \underline{r}'|}}{4\pi |\underline{r} - \underline{r}'|^2} \alpha(\nu) . \quad (1.4)$$

The first term on the right hand side of (1.4) describes the spontaneous decay of excited atoms at position \underline{r} in time T_1 . The second term describes the excitation of atoms at position \underline{r} due to radiation coming from other atoms \underline{r}' . These atoms \underline{r}' decay in time T_1 emitting radiation with spectrum $f(\nu)$. We assume that $f(\nu)$ is strongly peaked about the resonance frequency ν and normalized to unity. The radiation is attenuated by a factor $e^{-\alpha(\nu) \cdot |\underline{r} - \underline{r}'|}$ due to absorptions in travelling from \underline{r}' to \underline{r} (here $\alpha(\nu) \equiv 1/\Lambda(\nu)$ is the frequency dependent absorption coefficient), and by a factor $1/4\pi |\underline{r} - \underline{r}'|^2$ due to spherical spreading of the photons outward from \underline{r}' . The radiation reaching position \underline{r} is then absorbed with probability $\alpha(\nu)$. Finally we integrate over all atoms \underline{r}' and all radiation frequencies ν . Implicit in Eq. (1.4) is the assumption that the radiation travels from \underline{r}' to \underline{r} instantaneously i.e. that $T_{ph} = 0$.

Thus this equation is appropriate for photon but not phonon radiation trapping.

Holstein⁶ solved Eq. (1.4) by assuming a solution exponentially decaying in time and using a variational method to find the associated time constant. Veklenko⁷ in 1959 provided an alternative solution of Eq. (1.4) which made use of the so-called Ambartsamyan transformation. In both cases the analysis is very complicated and the results cannot easily be generalized to arbitrary emission spectra $f(\nu)$.

We wish now to present a novel and very simple solution of Eq. (1.4). We can transform the integral equation (1.4) into a differential equation⁸ by assuming that N_2 is not too rapidly varying in space so that we may make a Taylor expansion of $N_2(\mathbf{r}', t)$ about $N_2(\mathbf{r}, t)$. Substituting

$$N_2(\mathbf{r}', t) \approx N_2(\mathbf{r}, t) + \sum_i (\mathbf{r}'_i - \mathbf{r}_i) \nabla_i N_2(\mathbf{r}, t) + \frac{1}{2} \sum_{ij} (\mathbf{r}'_i - \mathbf{r}_i) (\mathbf{r}'_j - \mathbf{r}_j) \times \\ \nabla_i \nabla_j N_2(\mathbf{r}, t) \quad (1.5)$$

under the integral in (1.4), we immediately get the result that

$$\frac{\partial N_2(\mathbf{r}, t)}{\partial t} = \mathcal{D} \nabla^2 N_2(\mathbf{r}, t) \quad , \quad (1.6)$$

where

$$\mathcal{D} = \int_0^\infty d\nu \, f(\nu) \frac{1}{3\alpha^2(\nu) T_1} \quad , \quad (1.7)$$

which is simply the frequency dependent diffusion coefficient

$1/3\alpha^2(\nu)T_1$ averaged over the emission spectrum $f(\nu)$. Eq. (1.6) is just the diffusion equation (1.1) with a now well-defined effective diffusion constant. Neglecting factors of order one we may replace ∇^2 by $1/b^2$, where b is the diameter of the container and find the result that N_2 decays with time constant

$$T_s = T_1 / \int d\nu \frac{f(\nu)}{(\alpha(\nu)b)^2} . \quad (1.8)$$

As soon as the emission spectrum $f(\nu)$ is specified (1.8) can be integrated. ($\alpha(\nu)$ is proportional to $f(\nu)$ in thermal equilibrium[†] according to Kirchoff's law.) For example if $f(\nu)$ is a delta function $\delta(\nu-\nu_0)$ or a rectangular line-shape, then

$$T_s \approx T_1 (\alpha(\nu_0)b)^2 , \quad (1.9)$$

which is the usual result for material particles. For Doppler and dispersion lineshapes we find that

[†]This is true for all frequencies ν for which $\alpha(\nu) > 1/b$. On the other hand for those frequencies ν far from resonance for which proportionality would imply that $\alpha(\nu) < 1/b$, we must set $\alpha(\nu) = 1/b$ since for those frequencies the mean-free-path $\Lambda(\nu) \equiv 1/\alpha(\nu)$ is limited by the size b of the container. This is not in contradiction of Kirchoff's law because these frequencies do not come into thermal equilibrium due to the absence of collisions.

$$T_S \approx T_1 \alpha(v_O) b \sqrt{\ln(\alpha(v_O) b)} \quad (1.10)$$

and

$$T_S \approx T_1 \sqrt{\alpha(v_O) b} \quad (1.11)$$

respectively, in agreement with the results of Holstein⁶ and Veklenko⁷.

Since we will derive an expression similar to (1.8) in Chapter 5 we defer a detailed discussion of it until then. For now we simply wish to remark that Holstein and Veklenko did not try to discover the physical basis of the different decay times (1.10,11) and that Eq. (1.4) could not give them any information on the radiation spectrum inside the container or emerging through the boundary of the container. We will try to answer these questions in Chapter 5.

A completely different semi-classical formulation of the trapping problem was given by Jacobsen and Stevens⁹ (1963) who were interested in the effects of a crystal lattice of paramagnetic spin 1/2 atoms immersed in a magnetic field on the propagation of phonons in the crystal. Their system is described by the Hamiltonian (we set $\hbar=1$)

$$\mathcal{H} = \sum_n \{ [\Delta S_n^z] + [\frac{P_n^2}{2m} + \frac{K}{2} (U_n - U_{n-1})^2] + [g(U_{n+1} - U_{n-1}) S_n^x] \}, \quad (1.12)$$

where the sum over n is over all lattice sites in the one-dimensional crystal; the first, second, and third terms in the square brackets are respectively the spin, phonon and spin-phonon interaction energies; P_n , U_n , and S_n^i are

respectively the momentum, displacement, and i^{th} component of spin of the n^{th} atom; and Δ , K and g are respectively the Zeeman splitting of the spin energy levels in the external field, the nearest neighbor restoring force, and the coupling between the strain and the spin at position n . The Heisenberg equations of motion for P_n , U_n and S_n^i (similar to the ones we derive in Chapter 2) can be combined to give a pair of wave equations for the displacements and spins, namely

$$\begin{cases} m\ddot{U}_n - K(U_{n+1} + U_{n-1} - 2U_n) = g(S_{n+1}^x - S_{n-1}^x) & , \end{cases} \quad (1.13a)$$

$$\begin{cases} \ddot{S}_n^x + \frac{2}{T_1} \dot{S}_n^x + (\Delta^2 + \frac{1}{T_1^2}) S_n^x = g\Delta (U_{n+1} - U_{n-1}) S_n^z . \end{cases} \quad (1.13b)$$

Here $T_1 = T_1(g)$ is the phenomenologically introduced lifetime of the spin against phonon emission. With no interaction (i.e. $g=0$ and hence $T_1 = \infty$), (1.13a) is the wave equation for the propagation of free phonons and (1.13b) is the equation for an undamped harmonic oscillator of frequency Δ . With the interaction switched on (g and T_1 finite) the right hand side of Eqs. (1.13a,b) act as sources and sinks for the phonons and spins. The interaction is non-linear due mathematically to the factor $(U_{n+1} - U_{n-1}) S_n^z$ and due physically to the existence of processes such as stimulated emission, etc. To solve Eqs. (1.13) we replace S_n^z by the c-number average $\langle S_n^z \rangle \approx -1/2$ for a normal population (i.e. few excited atoms) or $\langle S_n^z \rangle \approx +1/2$ for an

inverted population (few unexcited atoms), and assume that U_n and S_n^x both vary like $e^{i(\omega t - kna)}$ where na is the position along the chain of the n^{th} atom. This yields the dispersion relation

$$\frac{Ka^2}{m} \frac{k^2}{\omega^2} \equiv \left(\frac{c_o}{c}\right)^2 = 1 - \frac{4g^2 \frac{\Delta}{K} \langle S^z \rangle}{\Delta'^2 - \omega^2 + \frac{2i\omega}{T_1}}, \quad (1.14)$$

where

$$\Delta'^2 \equiv \Delta^2 + \frac{1}{T_1^2} + 4g^2 \frac{\Delta}{K} \langle S^z \rangle \approx \Delta^2 \quad (1.15)$$

is the shifted resonance frequency, and $c_o = a\sqrt{K/m}$ and $c(\omega) = \omega/k$ are respectively the speed of sound (phase velocity) for zero and non-zero spin-phonon coupling. In Figure 1.1 we have plotted the real and imaginary parts of $c_o/c(\omega) \equiv \delta(\omega) - i\alpha(\omega)$, corresponding respectively to the dispersion and attenuation of phonons of frequency ω .

In Fig. 1.1a the solid curve representing a normal population ($\langle S^z \rangle < 0$) has negative slope in the region around Δ' indicating anomalous dispersion where a group velocity cannot be defined. Outside this region the increasing positive slope as ω approaches Δ' indicates a decreasing group velocity of the coupled spin-phonon wave. This is due to the delay by a time T_1 of phonons every time they are captured by normal atoms, the resonant phonons being captured most often. On the other hand, for inverted populations the dashed curve of Fig. 1.1a indicates an increase in the group velocity near the resonance frequency beyond

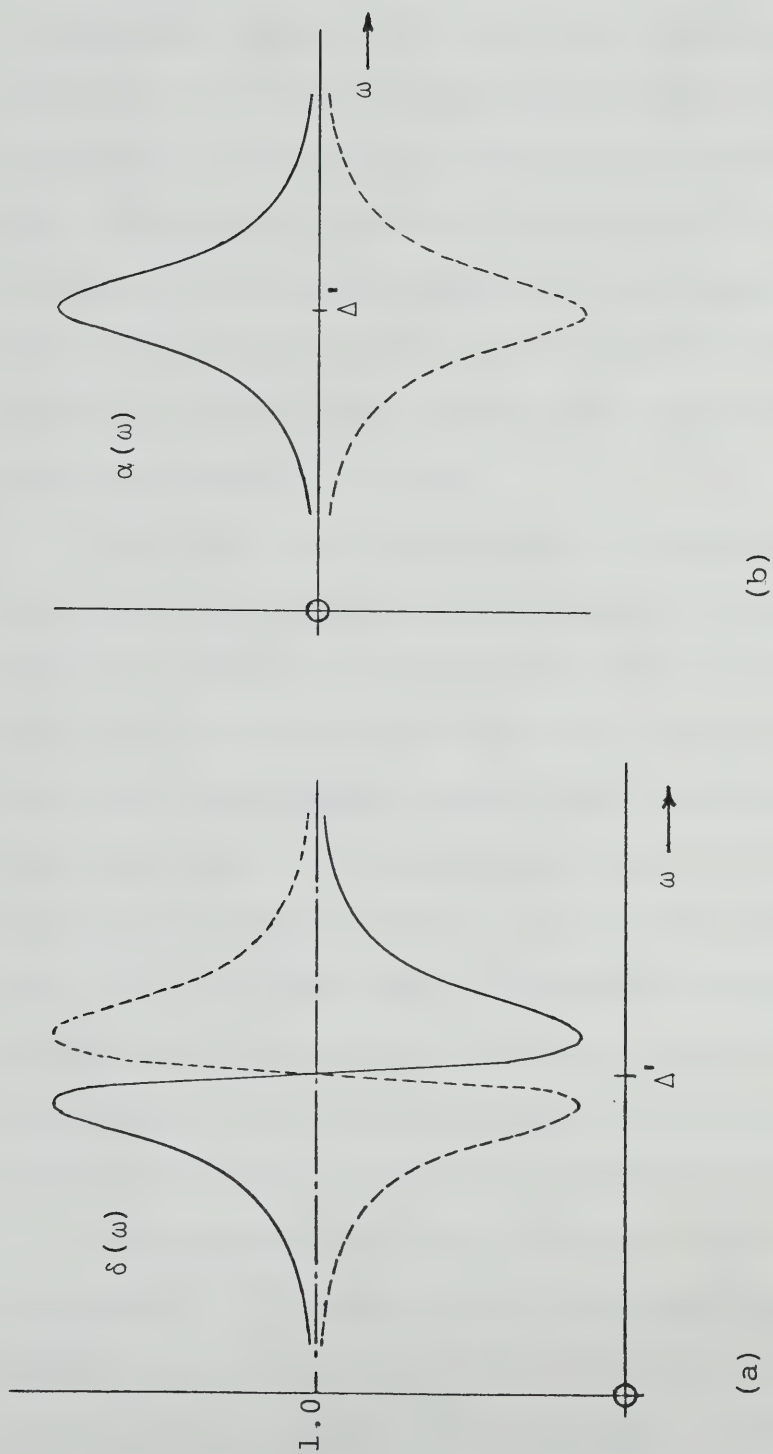


Fig. 1.1 (a) The real part (dispersion), and (b) the imaginary part (absorption) of $c_O/c(\omega)$ as a function of the elastic wave frequency ω ; $\langle S^Z \rangle < 0$ (normal population) solid line, $\langle S^Z \rangle > 0$ (inverted population) dashed line. See text. Taken from Ref. 9.

the phase velocity c_o . This however is in contradiction with a result by Sommerfeld¹⁰ who shows that it is not possible to propagate signals at velocities greater than c_o . Fig. 1.1b shows that for normal populations (solid line) the attenuation $\alpha(\omega)$ of the phonons is a maximum near resonance, whereas for inverted populations (dashed line) there is actually an amplification of the phonons near resonance. This is completely analogous to amplification by stimulated emission in the laser and has been demonstrated experimentally by Tucker¹¹ in 1961.

Thus far the formulation of Jacobsen and Stevens describes the attenuation and dispersion of incoming plane waves by a system of two-level atoms. However it is unclear how to proceed and describe the evolution of the two level atom-phonon system from non-equilibrium conditions because of the anomalous dispersion near resonance for which we cannot define a physically meaningful group velocity. Moreover their formulation supposes that the paramagnetic ions form a regular lattice whereas we are interested in the situation where the ions constitute impurities randomly distributed throughout the crystal.

There are other rate equation models of the phonon bottleneck^{13,18}, but virtually without exception they assume that the emission $f(\nu)$ is rectangular. This is an unrealistic assumption and from Eqs. (1.9)-(1.11) we see that the decay time T_s of the system depends crucially on the lineshape.

1.2 The Phonon Bottleneck in Ruby

In our discussion of the experiments on trapping of optical resonance radiation in gases we mentioned that the experimental results were difficult to interpret because of a variety of effects such as collisions of gas atoms, etc. Many of these effects can be eliminated by studying instead the trapping of resonant phonons by paramagnetic ion impurities in crystals at low temperatures¹²⁻²², because the ions are then not free to move and collide. We will be mainly interested in ruby, which is an Al_2O_3 crystal doped with Cr^{3+} ion impurities, but our discussion is applicable to many other impurity-doped crystals such as sapphire which is Al_2O_3 doped with Ti^{3+} ions.

The relevant part of the electronic energy level diagram for the Cr^{3+} ion in ruby is sketched in Fig. 1.2.¹⁹ The free ion ground state is ^4F with $L=3$ and $S=3/2$. The seven-fold orbital degeneracy is split in a cubic crystalline field into a $^4\text{A}_2$ orbital singlet and the $^4\text{T}_2$ and $^4\text{T}_1$ triplets which are shown cross-hatched and are the main absorption bands of ruby. The famous fluorescent ^2E state arises from the ^2G level and lies below the $^4\text{T}_1$ and $^4\text{T}_2$ levels. The presence of a small trigonal crystalline field in combination with spin-orbit coupling further splits the $^4\text{A}_2$ level by 0.4 cm^{-1} and the ^2E state into two so-called Kramers doublets $2\bar{\text{A}}$ and $\bar{\text{E}}$ separated by approximately 29 cm^{-1} . The $2\bar{\text{A}}$ and $\bar{\text{E}}$ states are metastable against optical transitions to the ground state with lifetimes of approximately

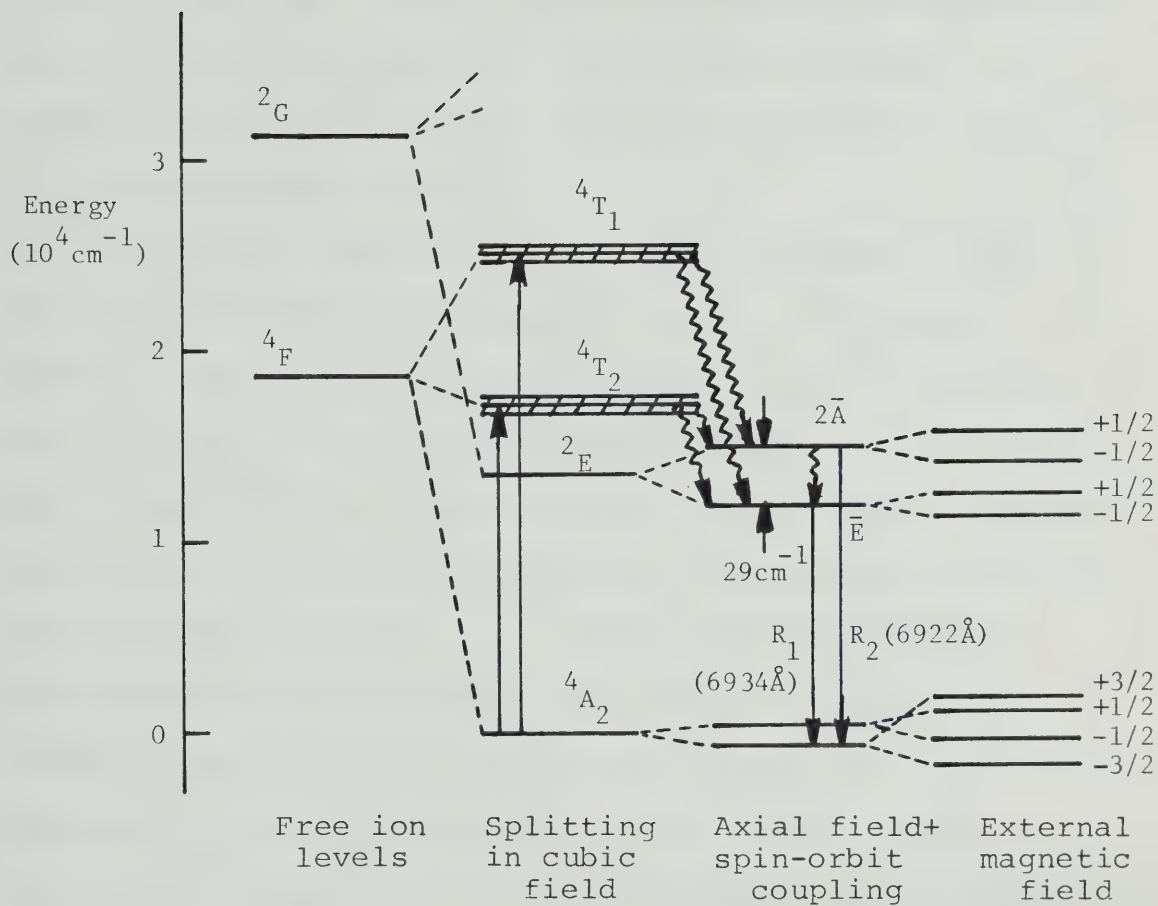


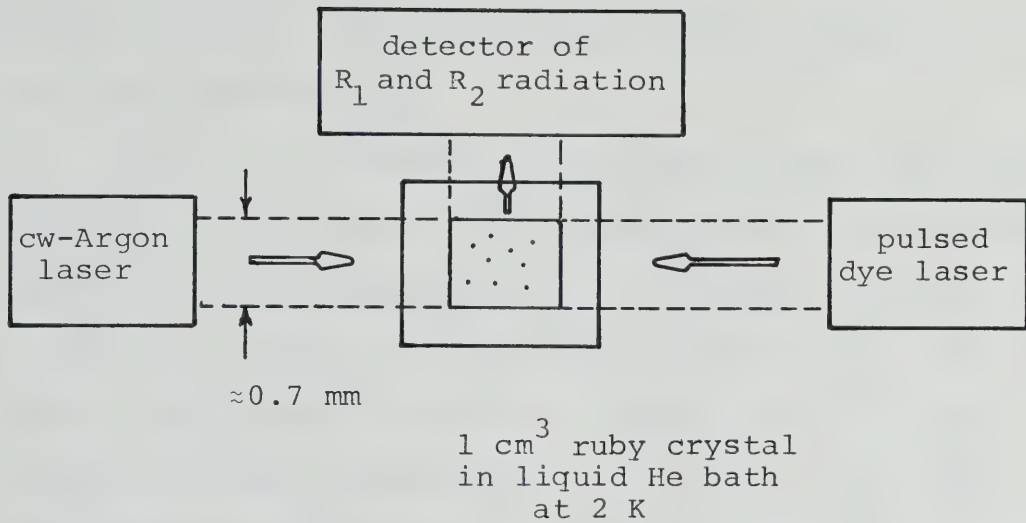
Fig. 1.2. Electronic energy levels of the Cr^{3+} ion in Al_2O_3 . Taken from Reference 19.

4 msec for both. The $2\bar{A}$ state also decays to the \bar{E} state by the emission of a 29 cm^{-1} phonon in a lifetime T_1 of a few nanoseconds. In the phonon bottleneck experiments of interest to us the $2\bar{A}$ and the metastable \bar{E} levels serve as the upper and lower levels of the two level atom system and the 29 cm^{-1} phonons serve as the resonant quanta. In Figure 1.2 we have also shown that each doublet is split in an external magnetic field.

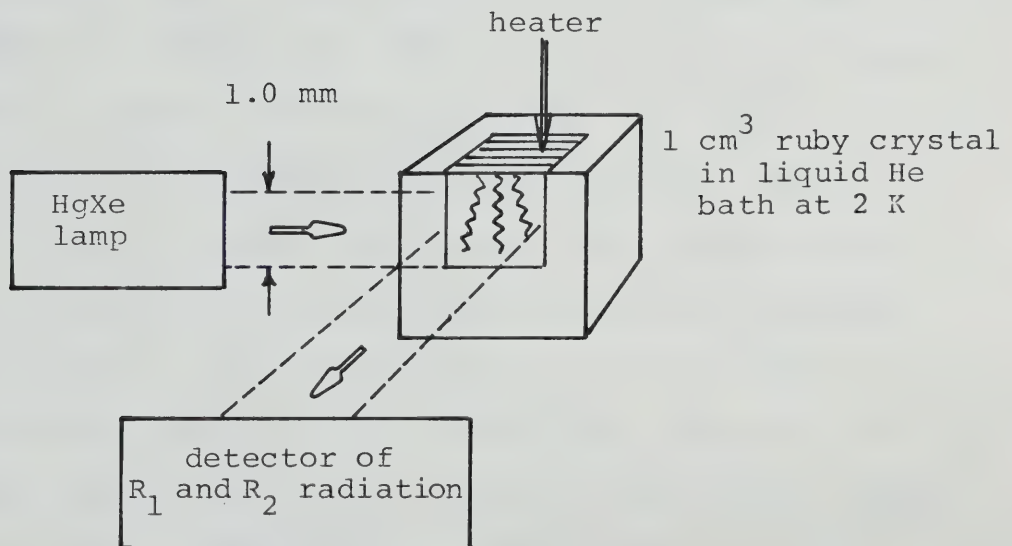
Let us now describe some of the experiments which have studied the bottlenecking of the 29 cm^{-1} phonons resonant between the $2\bar{A}$ and \bar{E} levels of the Cr^{3+} ion in ruby. The most complete experiments were done by K.F. Renk and G. Pauli²⁰⁻²² ca. 1977. In their experiments a cw-Argon laser at 514 nm is used to optically pump a small cylindrical region with diameter $b = .7 \pm 1\text{ mm}$ (full width of the laser beam at half intensity) and 1 cm long (length of crystal) inside a 1 cm^3 ruby crystal (doping .03 wt% Cr^{3+}) immersed in liquid Helium at 2 K. This causes the excitation of Cr^{3+} ions to the 4T_1 and 4T_2 levels, and by radiationless decay, the population of the $2\bar{A}$ and \bar{E} levels in approximately equal numbers. However in the steady state established by the continuous action of the laser nearly all of the excited Cr^{3+} ions are in the \bar{E} state because the lifetime T_1 of the $2\bar{A}$ state is much shorter than the lifetime of the metastable \bar{E} state and the thermal population of the $2\bar{A}$ state is low at low crystal temperature. The emission of R_1 and R_2 radiation (cf Fig. 1.2) can be used

as a weak probe for the measurement of the population of the \bar{E} and $2\bar{A}$ states because the lifetimes of these states against optical transitions to the ground state are nearly equal and so long compared to T_1 . The cylindrical excited volume containing the Cr^{3+} ions in the \bar{E} state is additionally pumped with the radiation of a pulsed dye laser at 580 nm with a pulse length of 2-3 ns, a repetition rate of 30 Hz, and a power of 50 kW. The schematic arrangement of the experiment is shown in Fig. 1.3a. This pulse leads to an initial non-equilibrium population of the $2\bar{A}$ level. It leads as well to a time-dependent population of the \bar{E} level which however is small compared to the permanent population N^* of the \bar{E} level, as evidenced by the fact that the R_1 signal remains more or less unchanged, and that the R_2 signal is small compared to the R_1 signal. The R_1 and R_2 signals are observed with nanosecond time resolution using several time-to-pulse-height converters in parallel. From the ratio of the time dependent R_2 signal to the time independent R_1 signal one can obtain the relative electronic population $N_2(t)/N^* = R_2(t)/R_1$ (where N_2 and N^* are the densities per cm^3 of Cr^{3+} ions in the $2\bar{A}$ and \bar{E} states respectively). It is important to note that the laser pulse is weak enough that the condition $N_2 \ll N^*$ is always satisfied.

In their experiments Pauli and Renk^{20,21} measured the intensity at the R_1 and R_2 lines following the laser pulse for various concentrations N^* (i.e. for various intensities of the cw Argon laser) keeping constant the total initial



(a) Experimental arrangement for high densities $N^* > 10^{16} \text{ cm}^{-3}$.



(b) Experimental arrangement for low densities $N^* < 10^{16} \text{ cm}^{-3}$.

Fig. 1.3. Schematic experimental arrangement used by Pauli and Renk^{20,21} for the study of the phonon bottleneck in ruby. All signals entering and leaving the ruby crystal are transferred via light pipes.

energy injected into the electron-phonon system[†] (i.e. the dye laser pulse energy).

In Fig. 1.4 we show typical decay curves that they found for the R_2 signal. The results shown are the counts accumulated after approximately 10^5 pulses. In the inset we show the initial fast time behavior. We see that after the dye laser pulse reaches the sample, the $2\bar{A}$ levels become populated instantaneously to a peak value R_2^{peak} in the R_2 signal. Phonon emission sets in within the lifetime T_1 of the $2\bar{A}$ state leading to a fast decay of $R_2(t)$ in a time of approximately 3 ns (the duration of the laser pulse). $R_2(t)$ does not vanish but rather falls to a value R_2^{eq} because many of the phonons do not escape but are re-absorbed in resonance by other Cr^{3+} ions in the \bar{E} state. As a result a quasi-stationary state of the coupled electron-phonon system is established, which we will henceforth refer to as the quasi-equilibrium. The electrons and phonons are not in complete equilibrium, but evidently always close to equilibrium as the coupled system slowly decays away. Some of the phonons decay anharmonically or escape from the excitation region and are quickly replenished in $2\bar{A} \rightarrow \bar{E}$ transitions as indicated by the slow decay in the R_2 signal in a time T_s of the order of microseconds.

[†]In this thesis the term 'electron system' refers to the system of Cr^{3+} ions in the \bar{E} state (in the cylindrical excitation region) which can be excited to the $2\bar{A}$ level by absorption of a 29 cm^{-1} phonon.

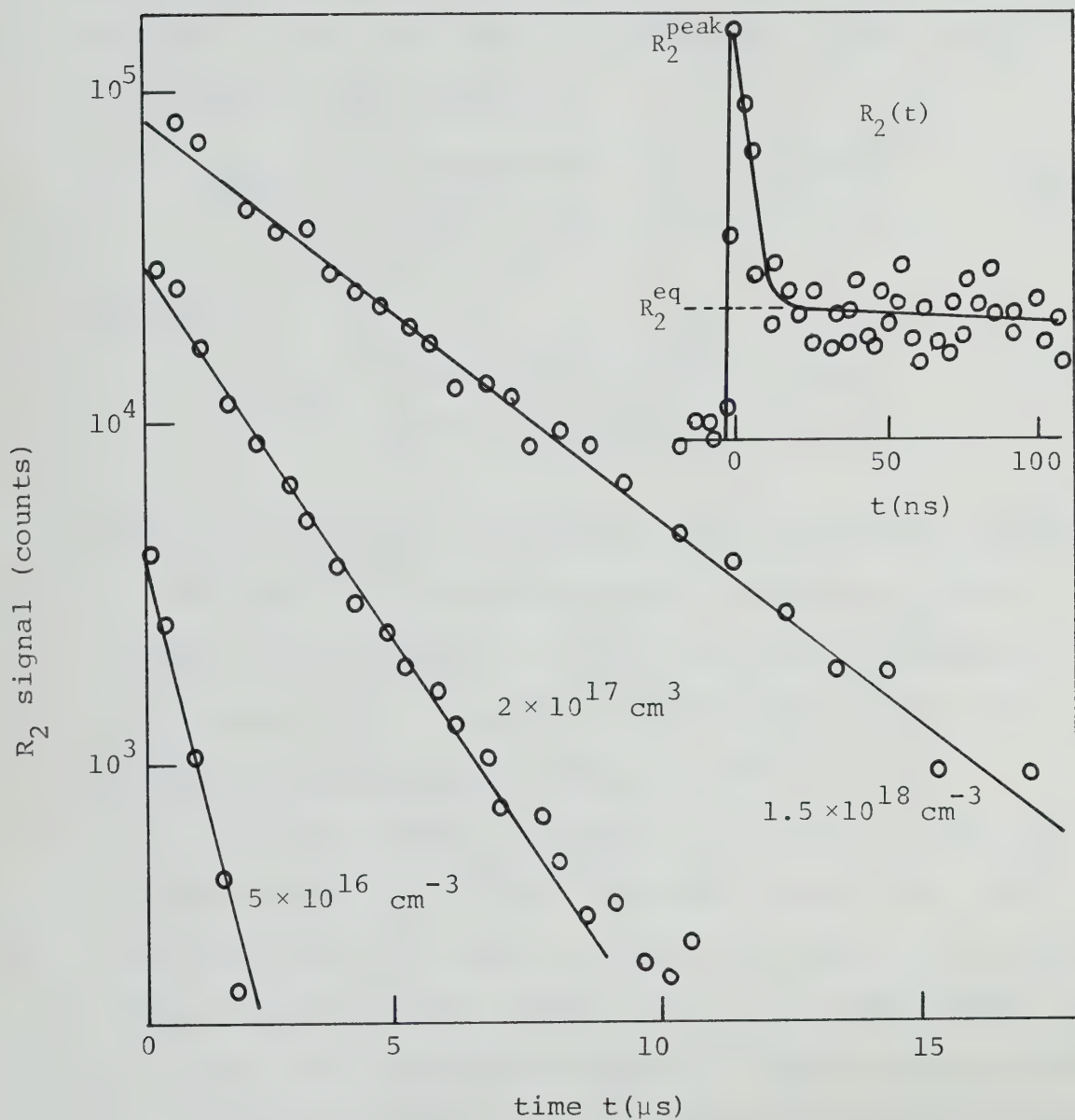


Fig. 1.4. The R_2 signal as a function of time found by Pauli et al.²⁰ at different concentrations N^* of excited Cr^{3+} ions in the \bar{E} state. In the inset, an R_2 signal (at $N^* \approx 5 \times 10^{16} \text{ cm}^{-3}$) is plotted linearly on a nanosecond time scale.

From the R_2 signal one can extract the relative population N_2^{eq}/N^* of the $2\bar{A}$ level after the fast decay and the decay time T_s of the slow decay. These quantities are plotted in Fig. 1.5a and b as functions of the density N^* of \bar{E} levels. One finds that

$$N_2^{\text{eq}}/N^* \sim \begin{cases} \text{constant for } N^* \lesssim 10^{15} \text{ cm}^{-3} \\ N^{*-1/2} & \text{for } N^* \gtrsim 10^{15} \text{ cm}^{-3} \end{cases} ; \quad (1.16)$$

and that

$$T_s \sim \begin{cases} \text{constant for } N^* \lesssim 10^{15} \text{ cm}^{-3} \\ N^{*+1/2} & \text{for } N^* \gtrsim 10^{15} \text{ cm}^{-3} \end{cases} . \quad (1.17)$$

Evidently the phonon bottleneck first appears at a density $N^* \approx 10^{15} \text{ cm}^{-3}$. At lower densities the phonons are not trapped and escape more or less freely with the ballistic flight time while at higher densities the phonons are trapped for increasingly longer periods of time.

For completeness it should be pointed out that for low densities $N^* \lesssim 10^{15} \text{ cm}^{-3}$ Renk and Pauli used a heat pulse to inject the initial energy into the electron-phonon system (see Fig. 1.3b) rather than a dye laser pulse. The heat pulse was produced by passing a 100 ns pulse of electric current through a $1 \times 1 \text{ mm}^2$ film of Constantan evaporated on the surface of the ruby crystal. It was estimated that a Planckian distribution of phonons is produced (with temperature $\approx 20 \text{ K}$), roughly half of which enter the ruby crystal and half of which are lost to the helium bath.

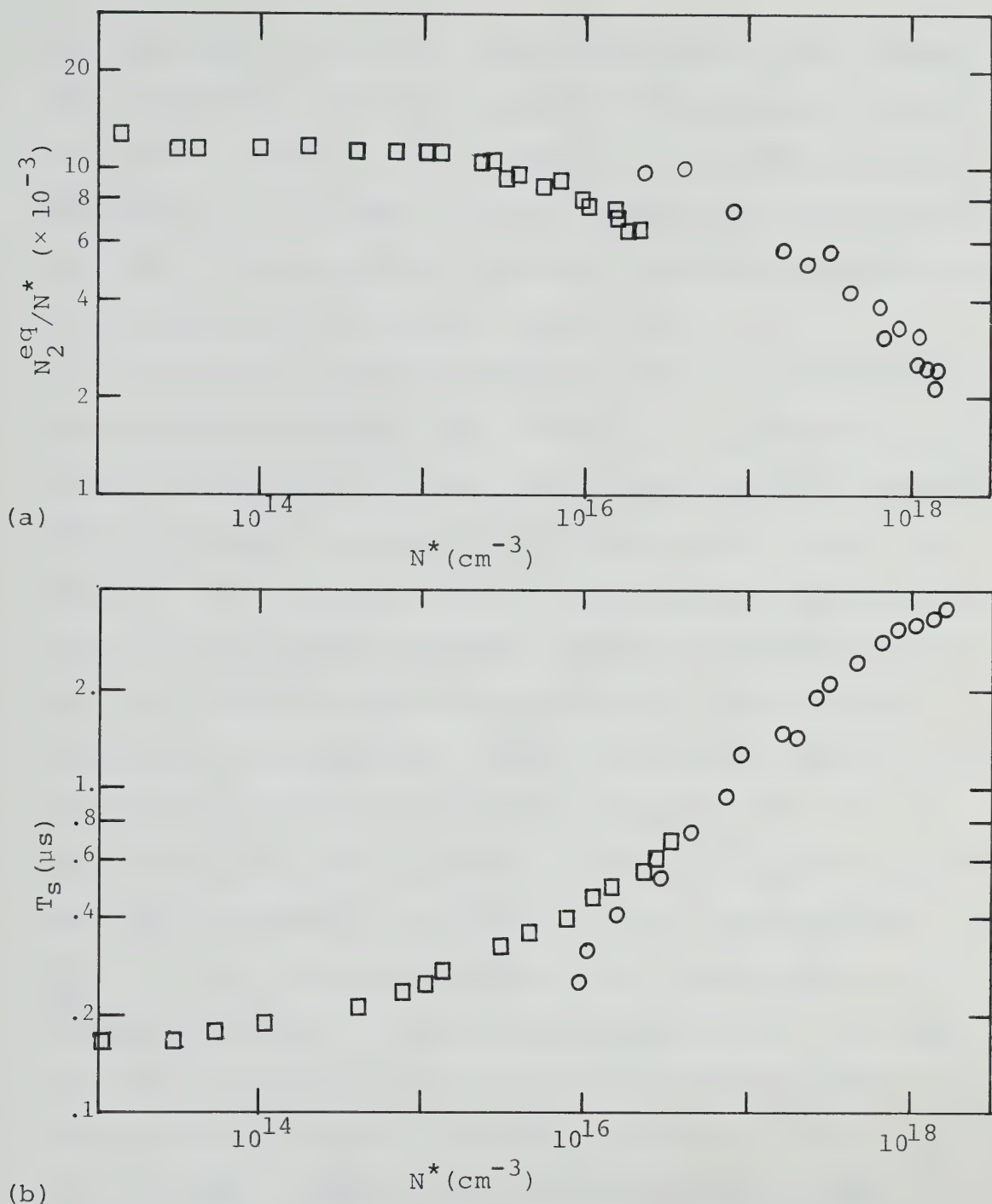


Fig. 1.5 (a) The quasi-equilibrium population N_2^{eq}/N^* , and (b) the slow decay time T_s of the $2\bar{A}$ states as functions of the concentration N^* of Cr^{3+} ions in the \bar{E} state found by Pauli and Renk^{20,21}. The circles were obtained from optical excitation experiments²⁰ and the squares from heat pulse experiments²¹ with excitation region diameters $b = .7$ mm and $b = 1.0$ mm respectively.

The advantage of the heat pulse method is its high repetition rate (10^4 pulses per second vs. 30 pulses per second for the dye laser). It is, however, unsuitable at higher densities $N^* \gtrsim 10^{16} \text{ cm}^{-3}$ because the resonant phonons are not able to penetrate well into the interior of the excitation region due to resonance scattering.

In another similar experiment²² Pauli and Renk utilized a single cw-Argon laser to set up a steady-state population of excited Cr^{3+} ions and phonons and found that N_2^{eq} N_2^{eq}/N^* increased linearly with the excitation region diameter b . This indicates that the phonons escape spatially and not by anharmonic decay as had been previously suggested. In the anharmonic decay hypothesis the resonant phonons are so effectively trapped that they decay in time T_{ph} into two or more non-resonant phonons which can then escape ballistically. Orbach and Vredevoe²³ and Klemens²⁴ have done theoretical calculations which indicate that $T_{\text{ph}} = 30 \text{ ns}$ and 380 ns respectively for longitudinal and transverse phonons. However Kaplyanskii et al.²⁵ in time-of-flight experiments found that the phonons propagated at least 1 cm with little attenuation indicating that $T_{\text{ph}} \gg 1 \text{ } \mu\text{sec}$. Thus we conclude that we may neglect anharmonic decay of phonons in our analysis.

Lengfellner et al.²⁶ studied the lineshape of the $2\bar{A} \rightarrow \bar{E}$ transition by splitting the $2\bar{A}$ and \bar{E} levels in an external magnetic field as shown in Fig. 1.2. In their experiments optical pumping at low crystal temperature

results in the population of the $\bar{E}_{-\frac{1}{2}}$ state. An infrared laser at 29.7 cm^{-1} (slightly greater energy than the difference Δ between the $2\bar{A}$ and \bar{E} states in zero magnetic field) is used to illuminate the crystal. As the external magnetic field is increased from zero, the $2\bar{A}$ and \bar{E} levels are both split (see Fig. 1.2) by increasing amounts and at two values of the magnetic field R_2 radiation is detected indicating that $\bar{E}_{-\frac{1}{2}} \rightarrow 2\bar{A}_{+\frac{1}{2}}$ and then $\bar{E}_{-\frac{1}{2}} \rightarrow 2\bar{A}_{-\frac{1}{2}}$ transitions have taken place. The R_2 signal as a function of the magnetic field has a Lorentz-like lineform for both transitions indicating lifetime broadening of the $2\bar{A}$ level (half width $\Delta\nu_0 = .012 \text{ cm}^{-1}$) and hence a lifetime $T_1 = (2\pi\Delta\nu_0)^{-1} = .44 \text{ ns}$. However Rives and Meltzer¹³ have pointed out that there may be a significant contribution to the linewidth from inhomogeneous broadening[†] implying a longer lifetime.

Geschwind et al.¹⁹ also performed an experiment which measured the lifetime T_1 indirectly by observing the transition $\bar{E}_{+\frac{1}{2}} \rightarrow \bar{E}_{-\frac{1}{2}}$. At low temperatures the direct decay is very slow and the transition takes place in two steps via the

[†]Random local strains in the ruby crystal cause locally different crystalline electric fields and hence locally different splitting between the $2\bar{A}$ and \bar{E} levels. Macroscopically one observes a Gaussian distribution of Lorentzians i.e. a Voigt profile. This smearing is known as inhomogeneous broadening.

so-called Orbach process: $\bar{E}_{+\frac{1}{2}} \rightarrow 2\bar{A}_{\pm\frac{1}{2}}$ and $2\bar{A}_{\pm\frac{1}{2}} \rightarrow \bar{E}_{-\frac{1}{2}}$. (The Raman process, in which the intermediate state is virtual and may lie at any distance above the ground state below the Debye frequency is a second-order process and not important at these low temperatures). A theoretical analysis shows that the relaxation time for the $\bar{E}_{+\frac{1}{2}}$ level is given by

$$T_{\text{Orbach}} = \frac{1}{4} T_1^{\text{flip}} e^{\Delta/kT} \quad (1.18)$$

where $\Delta = 29 \text{ cm}^{-1}$, T is the crystal temperature and T_1^{flip} is the time for the spin-flip transition $2\bar{A}_{+\frac{1}{2}} \rightarrow \bar{E}_{-\frac{1}{2}}$. Comparison with experiment yields $T_1^{\text{flip}} = 15 \text{ ns}$. Theory predicts that the non-flip transition is 50 times faster or $T_1^{\text{non-flip}} = .3 \text{ ns}$ so that the combined decay rate of the $2\bar{A}$ level is $1/T_1 = 1/T_1^{\text{flip}} + 1/T_1^{\text{non-flip}} \approx 1/.3 \text{ ns}$. It should be mentioned that Kurnit et al. in phonon echo experiments²⁷ found that $T_1 = 2.8 \text{ ns}$ and Rives and Meltzer¹³ in time-resolved experiments similar to those of Pauli and Renk^{20,21} previously described found that $T_1 = 1.1 \text{ ns}$. Thus we conclude that there is some uncertainty in the value of the lifetime T_1 of the $2\bar{A}$ state.

To conclude our survey of phonon bottleneck experiments in ruby we briefly mention the results of two other groups. Rives and Meltzer^{12,13}, as already mentioned, performed time-resolved experiments similar to those of Pauli et al. and found qualitatively similar results. However rather than measure the concentration N^* of Cr^{3+} ions in the \bar{E} state they used N^* as an adjustable parameter.

Thus it is difficult to make a quantitative comparison of their experiments with theory. Dijkhuis et al.¹⁴⁻¹⁸ studied the steady state properties of the bottleneck using continuous pumping to populate the \bar{E} and $2\bar{A}$ levels. They found (see Fig. 1.6a) that the intensity R_2 varied quadratically with R_1 indicating strong bottlenecking of the optically generated 29 cm^{-1} phonons. (We shall show later that a linear dependence would indicate no bottlenecking.) Furthermore they found that when an external magnetic field is turned on the R_2 intensity and thus the bottleneck is reduced fourfold as shown in Fig. 1.6b. Evidently this is due to the $2\bar{A} \rightarrow \bar{E}$ transition being gradually split into 4 distinct transitions by the Zeeman effect (see Fig. 1.2). The number of phonon modes to be bottlenecked thereby increases by a factor of 4 and the bottleneck decreases by a factor of 4. From the Gaussian shape of the curves in Fig. 1.6b Dijkhuis et al. conclude that the $2\bar{A} \rightarrow \bar{E}$ transition has a Gaussian lineshape, possibly due to inhomogeneous broadening. Note that the lineshape is the broader the larger R_1 i.e. N^* . This indicates that the phonon spectrum is broadened at large N^* . The inset of Fig. 1.6b gives the external field δH at which $R_2/R_2(H=0) = 0.5$ (this is a measure of the width of the phonon spectrum) vs. R_1 .

This concludes the general introduction and survey of experiments on radiation trapping and the phonon bottleneck in ruby.

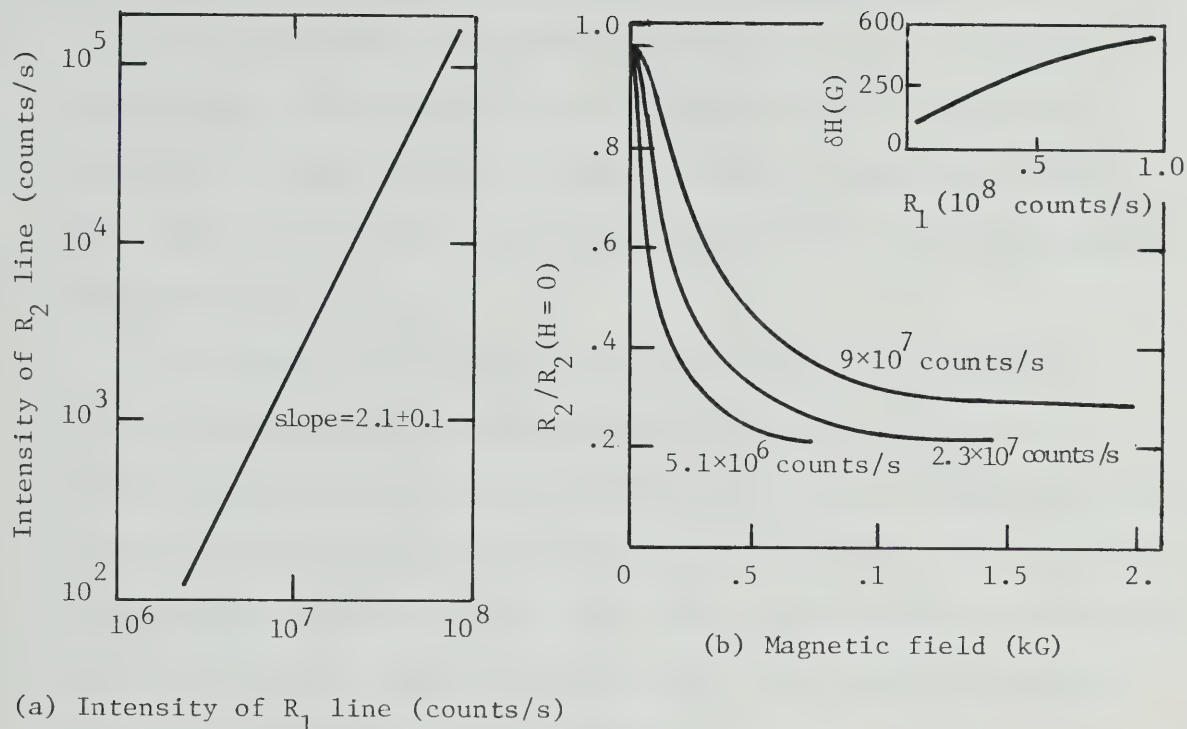


Fig. 1.6 (a) The intensity of the R_2 line vs the intensity of the R_1 line found by Dijkhuis et al.¹⁴ in continuous pumping experiments. The slope of 2 indicates strong bottlenecking of optically generated 29 cm^{-1} phonons. (b) The intensity of the R_2 line, normalized to zero external magnetic field, vs the magnetic field for several excited state populations N^* as measured by the R_1 intensity. The inset gives the field δH at which $R_2/R_2(H=0) = 0.5$ vs R_1 . Both figures taken from Reference 14.

1.3 Aim and Scope of the Present Investigation

The objective of this investigation is to present a theoretical analysis and interpretation of the phonon bottleneck experiments in ruby; notably those done by G. Pauli et al.²⁰⁻²² and Dijkhuis et al.¹⁴⁻¹⁸ which we briefly described in §1.2.

We begin in Chapter 2 by studying the electron-phonon interaction and deriving a field theoretical Hamiltonian describing it. After a survey of the solutions to the interaction problem which have already been studied in various approximations, we close the chapter by deriving a set of linear equations of motion for a set of quantum operators describing the system.

In Chapter 3 we study the simplest case of a single atom interacting with a phonon field. We study in detail the spontaneous decay of the single two-level atom as an example of the decay of an unstable quantum system.

In Chapter 4 we make the transition from quantum field equations to classical rate equations in parallel with W. Pauli's famous derivation of the master equation.

Chapter 5 constitutes the bulk of the thesis in which we solve the rate equations and give a detailed comparison with the results of the bottleneck experiments.

In Chapter 6 we try to improve the rate equations by going back to the quantum equations and extending them and by presenting some exact solutions of them.

CHAPTER 2

FIELD THEORETIC DESCRIPTION OF THE PHONON BOTTLENECK (I)

We wish to present a rigorous theoretical analysis of the phonon bottleneck in ruby, at each step of our argument clearly stating the assumptions and approximations necessary to arrive at our conclusions. Basic to the understanding of the phonon bottleneck is an understanding of the electron (or two-level atom)-phonon interaction, which we now discuss.

2.1 The Electron-Phonon Interaction

Let us begin by deriving a Hamiltonian for our system. As far as the Cr^{3+} ions are concerned we are interested only in electronic transitions between the $2\bar{A}$ and \bar{E} states. Transitions between these levels and the ground state or the absorption bands are used only to monitor or to feed the system and do not affect the dynamics of the bottleneck, so they are ignored. Thus we may approximately describe the Cr^{3+} ion at position \tilde{r} as a two-level system and use the vectors $\begin{pmatrix} 1 \\ 0 \end{pmatrix}_{\tilde{r}}$ and $\begin{pmatrix} 0 \\ 1 \end{pmatrix}_{\tilde{r}}$ to represent the ion in the $2\bar{A}$ and \bar{E} states respectively. Let us introduce the Pauli spin-1/2 operators

$$S_{\tilde{r}}^{+} = \begin{pmatrix} 0 & 1 \\ 0 & 0 \end{pmatrix}_{\tilde{r}}, \quad S_{\tilde{r}}^{-} = \begin{pmatrix} 0 & 0 \\ 1 & 0 \end{pmatrix}_{\tilde{r}}, \quad S_{\tilde{r}}^z = \frac{1}{2} \begin{pmatrix} 1 & 0 \\ 0 & -1 \end{pmatrix}_{\tilde{r}}, \quad (2.1)$$

which we define to act (only) on the \tilde{r}^{th} ion, with commutation relations

$$[S_{\tilde{r}}^-, S_{\tilde{r}}^+,]_- = -2 S_{\tilde{r}}^Z \delta_{\tilde{r}\tilde{r}'} \quad , \quad (2.2)$$

$$[S_{\tilde{r}}^-, S_{\tilde{r}}^Z,]_- = S_{\tilde{r}}^- \delta_{\tilde{r}\tilde{r}'} \quad .$$

Then $S_{\tilde{r}}^+$ represents the excitation transition of the \tilde{r}^{th} ion $\bar{E} \rightarrow 2\bar{A}$, namely

$$S_{\tilde{r}}^+ \begin{pmatrix} 0 \\ 1 \end{pmatrix}_{\tilde{r}} = \begin{pmatrix} 1 \\ 0 \end{pmatrix}_{\tilde{r}} \quad , \quad (2.3)$$

and similarly $S_{\tilde{r}}^-$ represents the decay $2\bar{A} \rightarrow \bar{E}$

$$S_{\tilde{r}}^- \begin{pmatrix} 1 \\ 0 \end{pmatrix}_{\tilde{r}} = \begin{pmatrix} 0 \\ 1 \end{pmatrix}_{\tilde{r}} \quad . \quad (2.4)$$

The levels $2\bar{A}$ and \bar{E} are separated in energy by the amount $\Delta = 29 \text{ cm}^{-1} \equiv h\nu_0$ where $\nu_0 = 874 \text{ GHz}$. If we define the zero of energy to lie halfway between the $2\bar{A}$ and \bar{E} levels then $\Delta S_{\tilde{r}}^Z$ is the energy operator for the \tilde{r}^{th} ion, since

$$\Delta S_{\tilde{r}}^Z \begin{pmatrix} 1 \\ 0 \end{pmatrix}_{\tilde{r}} = \frac{1}{2} \Delta \begin{pmatrix} 1 \\ 0 \end{pmatrix}_{\tilde{r}} \quad , \quad (2.5)$$

and

$$\Delta S_{\tilde{r}}^Z \begin{pmatrix} 0 \\ 1 \end{pmatrix}_{\tilde{r}} = -\frac{1}{2} \Delta \begin{pmatrix} 0 \\ 1 \end{pmatrix}_{\tilde{r}} \quad , \quad (2.6)$$

i.e. the eigenvalues of $\Delta S_{\tilde{r}}^Z$ are the energies of the upper and lower levels. Thus the Hamiltonian for the free Cr^{3+} ions is

$$\mathcal{H}_{\text{ion}} = \sum_{\tilde{r}} \Delta S_{\tilde{r}}^z, \quad (2.7)$$

where the sum is over all excited Cr^{3+} ions in the excitation region.

Let us now turn to the lattice. We wish to analyze the vibrational energy of the lattice in terms of the excitation of phonons. The crystal symmetry of ruby is rhombohedral²⁸ with its unit cell containing two molecules of Al_2O_3 . Thus if we perform the usual normal mode analysis on the lattice vibrations we find dispersion curves $\omega_{\tilde{k}}^{(s)}$ similar to the ones sketched in Fig. 2.1a.

The exact shape of the curves and width of the Brillouin zone will depend on the direction \tilde{k} that we choose. For any given direction \tilde{k} there are $3 \times 10 = 30$ branches due to the 10 atoms per unit cell. Of these, three ($\omega_{\tilde{k}}^{(L)}$, $\omega_{\tilde{k}}^{(T_1)}$, and $\omega_{\tilde{k}}^{(T_2)}$ in Fig. 2.1a denoting the longitudinal and two transverse branches) are acoustic branches linear in \tilde{k} for small \tilde{k} . The rest, denoted $\omega_{\tilde{k}}^{(01)} - \omega_{\tilde{k}}^{(027)}$, are optical branches. We approximate the dispersion curves using the Debye model for the acoustic branches and the Einstein model for the optical branches as shown in Fig. 2.1b. The Brillouin zone is replaced by a sphere of equal volume so that its radius is k_D where

$$\frac{k_D^3}{6\pi^2} = n, \quad (2.8)$$

and n is the density of unit cells per cm^3 in the ruby

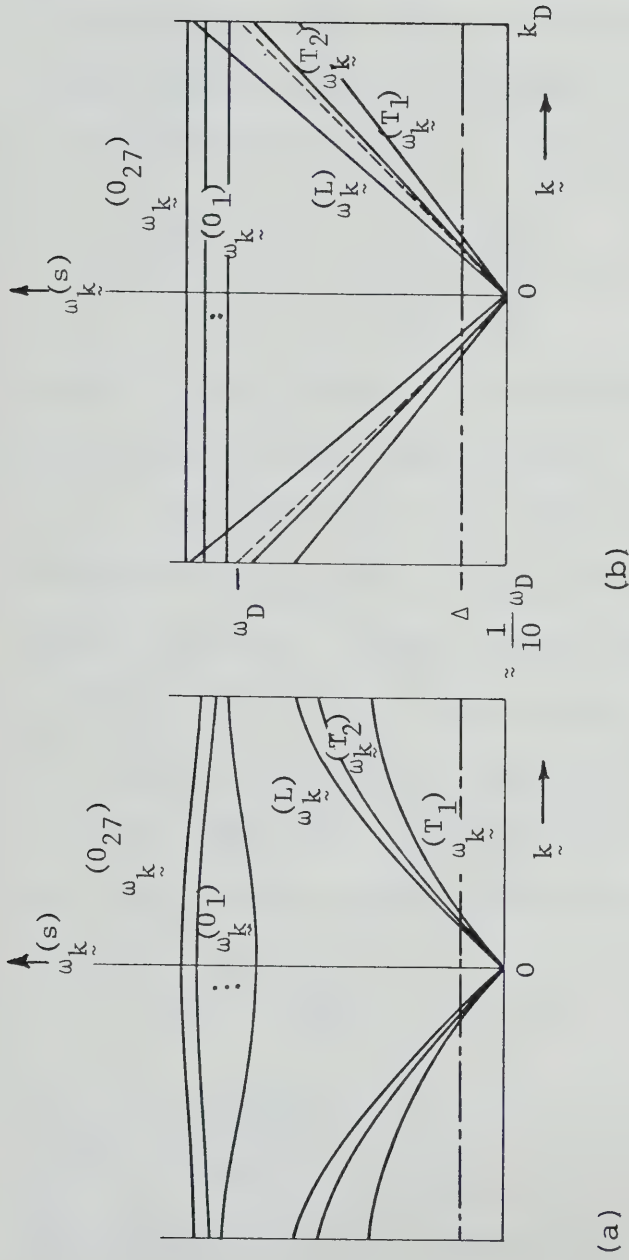


Fig. 2.1.1. Sketch of (a) the true phonon dispersion curves, and (b) the approximate curves along a general direction in \tilde{k} space. The acoustic branches L , T_1 and T_2 are constructed according to the Debye model, and the optical branches according to the Einstein model. Note that the resonance frequency Δ is so small that the optical modes may be ignored and that the Debye approximation for the acoustic modes should be good.

crystal. The acoustic branches are replaced by straight lines with slopes (i.e. longitudinal and transverse sound velocities) c_L , c_{T_1} , and c_{T_2} the same as the original curves near $k=0$, and the optical branches by lines with zero slope (i.e. $\omega_k = \text{constant}$). The average sound velocity c in the Debye model is defined by the relation

$$\frac{3}{c^3} = \frac{1}{c_L^3} + \frac{1}{c_{T_1}^3} + \frac{1}{c_{T_2}^3} \quad (2.9)$$

where c_L , c_{T_1} , and c_{T_2} are averaged over all directions in space because the Debye model is isotropic. For ruby $c \approx 7 \times 10^3$ m/sec and $k_D \approx 10^{10} \text{ m}^{-1}$ so that the Debye cutoff frequency is $\omega_D = ck_D \approx 10 \times \Delta_O$ where $\Delta_O = 2\pi\nu_O$ is the resonance frequency. Since, as we see in Fig. 2.1b, all the optical modes have frequencies $\omega_k \gtrsim \omega_D$, only acoustic and no optical modes can be excited in a $2\bar{A} \rightarrow \bar{E}$ transition. Thus we need only consider the acoustic modes and write the free Hamiltonian for the phonons as

$$\mathcal{H}_{\text{ph}} = \sum_{\tilde{k}, |\tilde{k}| < k_D} \sum_{s=L, T_1, T_2} \omega_{\tilde{k}}^{(s)} b_{\tilde{k}}^{(s)\dagger} b_{\tilde{k}}^{(s)}, \quad (2.10)$$

where $k_i = 2\pi m_i / L$, $i=1,2,3$ with m_i an integer. $b_{\tilde{k}}^{(s)\dagger}$ and $b_{\tilde{k}}^{(s)}$ are the usual phonon creation and annihilation operators satisfying the commutation relations

$$[b_{\tilde{k}}^{(s)}, b_{\tilde{k}'}^{(s')\dagger}]_- = \delta_{\tilde{k}\tilde{k}'} \delta_{ss'} \quad , \quad (2.11)$$

$$[b_{\tilde{k}}^{(s)}, b_{\tilde{k}'}^{(s')}]_- = 0 \quad .$$

Let us now study the Cr^{3+} ion-phonon interaction. In the ruby crystal a small number of Al^{3+} ions are substituted by Cr^{3+} ions. Their nearest neighbors are 6 O^{2-} ions which form a distorted octahedron²⁸ around the Cr^{3+} ion, giving rise to a cubic crystalline electric field and a weaker trigonal field. These static fields, whose potential we denote by V_0 , in conjunction with the spin-orbit coupling give rise to the 29 cm^{-1} splitting of the $2\bar{\text{A}}$ and $\bar{\text{E}}$ levels shown in Fig. 1.2. In addition to this static field, vibrations of the lattice, through the charges of the ligands (the O^{2-} ions), produce a modulating effect on the crystalline field and therefore on the energy levels of the Cr^{3+} ions. This causes electronic transitions in the Cr^{3+} ion. The total crystal field potential can be expressed in powers of the strain as²⁹

$$V_{\text{crystal}} = V_0 + V_1 \epsilon + V_2 \epsilon^2 + \dots \quad (2.12)$$

where V_0 as discussed above is already included in \mathcal{H}_{ion} , $\epsilon = \langle \partial U_i(\underline{x}) / \partial x_j \rangle$ is the direction-averaged strain due to lattice vibrations at the site of the Cr^{3+} ion ($U(\underline{x})$ is the crystal displacement from equilibrium at position \underline{x}) and V_1 and V_2 are coupling parameters which depend on the level of excitation of the Cr^{3+} ion.

Let us consider a simple model of a monatomic one-dimensional lattice with sites indexed by the integer n with a few Cr^{3+} ion impurities at sites $n=r$. Combining (2.7) and (2.10) (specialized to a one-dimensional lattice)

with the first two terms of (2.12) we get the Hamiltonian

$$\mathcal{H} = \mathcal{H}_{\text{ion}} + \mathcal{H}_{\text{ph}} + V_1 \varepsilon \quad , \quad (2.13)$$

where

$$\begin{aligned} \mathcal{H}_{\text{ion}} &= \sum_{\mathbf{r}} \Delta S_{\mathbf{r}}^z \quad , \\ \mathcal{H}_{\text{ph}} &= \sum_{\mathbf{k}} \omega_{\mathbf{k}} b_{\mathbf{k}}^{\dagger} b_{\mathbf{k}} \quad , \end{aligned} \quad (2.14)$$

and

$$V_1 \varepsilon = \gamma \sum_{\mathbf{r}} (U_{\mathbf{r}+1} - U_{\mathbf{r}-1}) V_{1\mathbf{r}} \quad .$$

Here γ is a coupling constant, $U_{\mathbf{r}+1} - U_{\mathbf{r}-1}$ is proportional to the strain at the \mathbf{r}^{th} lattice site and $V_{1\mathbf{r}}$ is for now unspecified. In terms of the one-dimensional phonon annihilation operator

$$b_{\mathbf{k}} = \frac{1}{(2m\omega_{\mathbf{k}}N)^{1/2}} \sum_{\mathbf{n}} e^{-i\mathbf{k}\cdot\mathbf{n}} (P_{\mathbf{n}} - im\omega_{\mathbf{k}} U_{\mathbf{n}}) \quad , \quad (2.15)$$

and its hermitean conjugate $b_{\mathbf{k}}^{\dagger}$ ($P_{\mathbf{n}}$ and $U_{\mathbf{n}}$ are the quantized momentum and displacement of the \mathbf{n}^{th} lattice site), we can write

$$\gamma (U_{\mathbf{r}+1} - U_{\mathbf{r}-1}) = \sum_{\mathbf{k}} g_{\mathbf{k}} (b_{\mathbf{k}}^{\dagger} e^{-i\mathbf{k}\cdot\mathbf{r}} + b_{\mathbf{k}} e^{i\mathbf{k}\cdot\mathbf{r}}) \quad , \quad (2.16)$$

where

$$g_{\mathbf{k}} = -\gamma \sin \mathbf{k} \cdot \left(\frac{1}{2\omega_{\mathbf{k}} m N} \right)^{1/2} \quad . \quad (2.17)$$

The simplest form of $V_{1\mathbf{r}}$ that can cause transitions of the \mathbf{r}^{th} ion and is hermitian is

$$V_{lr} = S_r^+ + S_r^- \equiv S_r^x \quad . \quad (2.18)$$

With this form we finally arrive at the Hamiltonian for the electron-phonon system in one dimension

$$\begin{aligned} \mathcal{H} = & \sum_r \Delta S_r^z + \sum_k \omega_k b_k^\dagger b_k + \sum_r \sum_k g_k (\{S_r^- b_k^\dagger e^{-ikr} + b_k S_r^+ e^{ikr}\} \\ & + \{S_r^- b_k e^{ikr} + b_k^\dagger S_r^+ e^{-ikr}\}) \quad . \end{aligned} \quad (2.19)$$

This Hamiltonian can be trivially extended to the general case of a three-dimensional lattice by including a summation over phonon branches i.e. by everywhere replacing $\sum_k \rightarrow \sum_{\tilde{k}} \sum_s$ and $g_k \rightarrow g_{\tilde{k}}^{(s)}$, $s = L, T_1, T_2$; thus allowing for different coupling to each branch. However since experiment does not give us these couplings we may as well simply choose them all equal.

2.2 Survey of Solutions to the Electron-Phonon Interaction Problem

The Hamiltonian (2.19) is a generalization of a Hamiltonian that was first studied in 1954 by Dicke³⁰ in connection with the spontaneous emission of coherent radiation, i.e. 'superradiance', in a laser. Since then a very large body of literature has appeared³⁰⁻⁴⁵ studying the Hamiltonian under a variety of conditions in various approximations and using various methods.

An approximation that is almost universally made is the so-called rotating approximation in which

the second term in braces in (2.19), the anti-resonance term, proportional to

$$S_r^- b_k e^{ikr} + b_k^\dagger S_r^+ e^{-ikr} \quad (2.20)$$

is dropped. The usual justification is that it does not lead to first order processes that conserve energy (or number of excitations). To see why it is called the anti-resonance term and why it is negligible, we use the interaction picture where

$$i \dot{O}_I(t) = [O_I(t), \mathcal{H}_O]_- ,$$

and (2.21)

$$i |\dot{\psi}_I(t)\rangle = \mathcal{H}' |\psi_I(t)\rangle .$$

where O_I and ψ_I are any operator and state vector in the interaction picture and $\mathcal{H}_O = \mathcal{H}_{\text{ion}} + \mathcal{H}_{\text{phonon}}$ and $\mathcal{H}' = V_1 \epsilon$. According to (2.21) the resonance terms of \mathcal{H}' vary like

$$b_k^\dagger(t) S_r^-(t) = e^{-i(\Delta - \omega_k)t} b_k^\dagger(0) S_r^-(0) , \quad (2.22)$$

$$S_r^+(t) b_k(t) = e^{+i(\Delta - \omega_k)t} S_r^+(0) b_k(0) ;$$

and the anti-resonance terms like

$$S_r^-(t) b_k(t) = e^{-i(\Delta + \omega_k)t} S_r^-(0) b_k(0) , \quad (2.23)$$

$$S_r^+(t) b_k^\dagger(t) = e^{+i(\Delta + \omega_k)t} S_r^+(0) b_k^\dagger(0) .$$

Since Δ and ω_k are both defined positive, for $\omega_k \approx \Delta$ the resonance terms have an approximately stationary phase, whereas the anti-resonance terms have a rapidly varying phase. Thus when we integrate (2.22), for \mathcal{H}' not too strong, we get a strongly resonant denominator for the former ($\psi_I \propto 1/(\omega_k - \Delta)$) and anti-resonant denominator for the latter ($\psi_I \propto 1/(\omega_k + \Delta)$) which we can neglect in comparison except for large times.

Swain³¹ has studied the case of a single two-level atom interacting with a single photon (or phonon) mode of frequency ω_1 with \mathcal{H}' including the anti-resonance term. He found that if initially the atom is excited and there is no phonon present, then the probability $N_\uparrow(t)$ that the atom is excited at time t is given in terms of a continued fraction, namely

$$N_\uparrow(t) = \left| \frac{1}{2\pi i} \oint \frac{d\omega e^{-i\omega t}}{\omega - \Delta - \frac{g^2}{\omega - \omega_1 - \frac{2g^2}{\omega - \Delta - 2\omega_1 - \frac{3g^2}{\omega - 3\omega_1 - \dots}}}} \right|^2. \quad (2.24)$$

Note that with no coupling $g=0$

$$N_\uparrow(t) = \left| \frac{1}{2\pi i} \oint \frac{d\omega e^{-i\omega t}}{\omega - \Delta} \right| = |e^{-i\Delta t}|^2 = 1, \quad (2.25)$$

so that the atom never decays; and that keeping only the first approximant to the continued fraction in (2.24) gives

$$N_{\uparrow}(t) = \left| \frac{1}{2\pi i} \oint \frac{d e^{-i\omega t}}{\omega - \Delta - \frac{g^2}{\omega - \omega_1}} \right|^2, \quad (2.26)$$

which results in a cosinusoidal $N_{\uparrow}(t)$ (as shown in Fig. 3.1 of Chapter 3). We study (2.26) in more detail in Chapter 3 where we find that it is the exact solution to the one atom-one phonon mode problem with no anti-resonance interaction. Let us interpret these results. Eq. (2.25) shows that the uncoupled atom behaves like a harmonic oscillator of frequency Δ . Coupling the atom to another harmonic oscillator of frequency ω_1 (the phonon mode), causes a shift in the frequencies of the two oscillators (determined by the poles of the integrand of (2.26)) and causes the energy of the coupled oscillators to be transferred back and forth cosinusoidally between them at the beat frequency ($\approx g$) as for any pair of coupled classical harmonic oscillators. Finally Eq. (2.24) shows that the inclusion of the anti-resonance term for small times is negligible for small coupling g but that for large times it causes $N_{\uparrow}(t)$ to lose its perfect periodicity because of the infinite number of poles in the integrand of (2.24).

Beyond the almost universally used rotating wave approximation which we just discussed, the approximations that can be made depend on the conditions of the system. For example when applying the Hamiltonian (2.19) to the laser, usually only one radiation mode on resonance is considered. Furthermore if the wavelength of the radiation

is long compared to the dimension of the container of the two-level atoms, when we may also drop the phase factors e^{+ikr} and e^{-ikr} in (2.19) and get the Hamiltonian studied by Dicke³⁰, namely

$$\mathcal{H} = b^\dagger b + \sum_r \Delta S_r^z + g \sum_{r=1}^N (b^\dagger S_r^- + S_r^+ b) \quad . \quad (2.27)$$

Dicke considered all N atoms as a single quantum system and applied to it the rules for the addition of angular momenta. Let us define the operator

$$R^2 = \sum_{i=x,y,z} (R^i)^2 \quad (2.28)$$

where

$$R^i = \sum_r S_r^i \quad (2.29)$$

is the i^{th} component of the 'spin' of the total atom system. Then R^2 has eigenvalues $r(r+1)$ and the operator R^z has eigenvalues m satisfying

$$|m| \leq r \leq \frac{1}{2}N \quad (2.30)$$

r and m are integral or half-integral according to whether N is even or odd. If N_\uparrow and N_\downarrow are the number of excited and unexcited atoms respectively, then

$$N = N_\uparrow + N_\downarrow \quad (2.31)$$

$$m = \frac{1}{2} (N_\uparrow - N_\downarrow) \quad , \quad (2.32)$$

and r is called the coordination number. Note that the energy of the atom system is

$$E_m = \Delta \left(m + \frac{N}{2} \right) . \quad (2.33)$$

A straightforward algorithm using raising and lowering operators can be used to generate the eigenstates $|r, m\rangle$ of R^z and R^2 . Then taking matrix elements of the interaction energy one finds that

$$\langle r, m | \mathcal{H}' | r, m \pm 1 \rangle \propto \sqrt{(r \mp m)(r \pm m + 1)} \quad (2.34)$$

are the only non-vanishing ones. Taking the squares of the matrix elements with the lower sign gives the spontaneous decay probabilities

$$I = I_0 (r + m)(r - m + 1) , \quad (2.35)$$

where I_0 is some constant. These results are conveniently tabulated in Fig. 2.2, where we show the states $|r, m\rangle$, their degeneracies and their energies (the height in the diagram). Let us interpret these results. By setting $N=1$ and $r=m=1/2$ in (2.35), it is evident that I_0 is the radiation rate of a single excited atom. If $r=m=\frac{1}{2}N$, i.e. if all N atoms are initially excited, then

$$I = N I_0 , \quad (2.36)$$

which is just N times the rate for a single atom. The proportionality to N indicates incoherent emission by the atoms. If $r=\frac{1}{2}N$ and $m=0$, i.e. if half the atoms are excited, then

$$I = \frac{1}{2}N \left(\frac{1}{2}N + 1 \right) I_0 \quad (2.37)$$

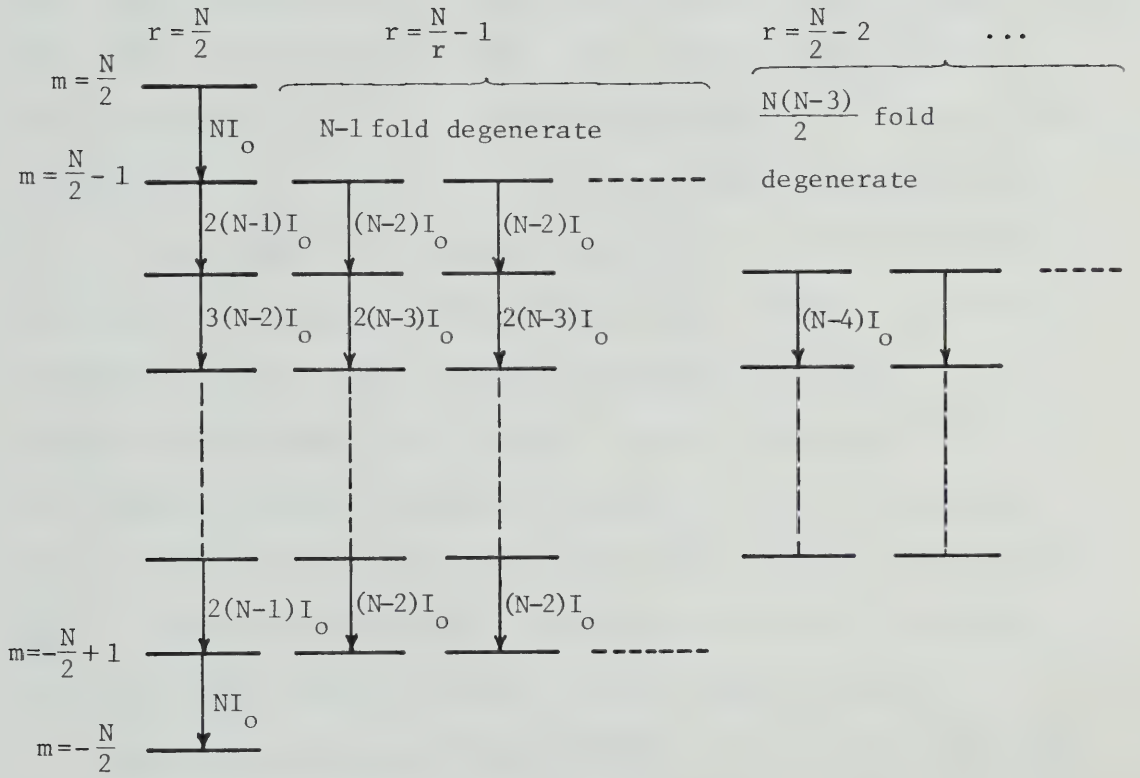


Fig. 2.2. Energy level diagram of an N -atom gas in the Dicke model, each atom having two energy levels separated by energy Δ . Spontaneous radiation rates are indicated. The atom system energy is $E_m = \Delta(m + \frac{N}{2})$. Taken from Reference 30.

which for large N is proportional to N^2 ! This indicates coherent spontaneous emission. Dicke calls this the 'superradiant' state.

Radiation trapping emerges naturally in this formalism. Suppose that exactly one atom of the gas is initially excited. Then the gas radiates initially at the normal incoherent rate but after a short time ceases, with the probability of the photon being emitted being only $1/N$. This follows from Fig. 2.2: The assumed initial state with $m = -\frac{N}{2} + 1$ is an equal superposition of the single state with $r = N/2$ and the $N-1$ degenerate states with $r = \frac{N}{2} - 1$. The latter $N-1$ states cannot decay and thus the probability of radiation trapping is $\frac{N-1}{N}$. (This is exactly analogous to the famous case of helium in which intercombination between the triplet system (orthohelium) and the singlet system (parahelium) is not allowed by the selection rules so that e.g. there is no $2^3S \rightarrow 1^1S$ transition). By field theoretic methods in Chapter 6 we will find that the trapping result just found is exact.

Let us now discuss some other work done on the electron-phonon interaction. Scharf³² studied the Dicke model and found that the mean photon number showed oscillatory behavior given by elliptic functions. Prakash and Chandra³³ wrote the Dicke Hamiltonian in the so-called Boson representation by replacing

$$\begin{aligned}
R^- &\rightarrow a_1^\dagger a_2 \\
R^+ &\rightarrow a_2^\dagger a_1 \\
R^Z &\rightarrow \frac{1}{2}(a_2^\dagger a_2 - a_1^\dagger a_1) \\
|r, m\rangle &\rightarrow |n_1, n_2\rangle
\end{aligned}
\tag{2.38}$$

where $n_1 = r - m$ and $n_2 = r + m$ are the number of excitations, and a_1 and a_2 are boson operators, which annihilate an excitation in the lower and upper levels respectively. Simplifications result if we have a highly excited assembly of atoms because then n_2 is large and the a_2 or upper mode can be treated classically. Similarly if n_1 is large the a_1 mode can be treated classically and if $n_1 \approx n_2 \gg 1$ (superradiative condition) then both modes can be treated classically.

Mallory³⁴ made computer studies of the evolution of the density operator of a system containing a small number of atoms and found oscillations in the photon field similar to those of Scharf³².

Bonifacio et al.^{35,36} also studied various aspects of the Dicke laser model.

All the authors mentioned so far assumed the presence of only a single radiation mode and neglected the spatial dependence of the system. As we know from the results of Holstein (Eqs. (1.9)-(1.11)), the existence of a phonon band and the size of the system is crucial to a quantitative description of the phonon bottleneck. Also, in light

of our discussion after Eq. (2.26), it seems likely that the oscillations in the models of Scharf and Mallory are artifacts of the single mode assumption.

Leonardi and Persico³⁷⁻³⁹ studied the Hamiltonian (1.12) of Jacobsen and Stevens⁹ in connection with the relaxation of an inverted system of paramagnetic spins interacting with a phonon field. However, as we already mentioned in §1.2, this model assumes that there is a spin on each lattice site and therefore is not an appropriate description of the phonon bottleneck in ruby.

Finally we should note that a number of authors have derived and solved macroscopic and kinetic equations describing systems obeying the Dicke Hamiltonian (2.27) or the full Hamiltonian (2.19). For example Walgraef⁴⁰ derived a kinetic equation for the photon density matrix of a monomode laser within the framework of the Prigogine-Résibois theory of non-equilibrium statistical mechanics. Grinberg and Nigmatullin⁴¹ and Bukhbinder et al.⁴² derived kinetic equations for the relaxation of a paramagnetic spin system using Zubarev's method of the nonequilibrium statistical operator. And D'Yakonov and Perel'⁴³, using a Feynmann diagram perturbation method, derived kinetic equations for the time evolution of the density matrix of an excited atom when there is diffusion of resonance radiation. In case the density matrix is diagonal, their equation reduces to that of Holstein (Eq. 1.4).

In this survey we have seen several qualitative features of the phonon bottleneck. Examples were Dicke's radiation trapping due to the selection rule against intercombination of states of different total 'spin' r , and Jacobsen and Steven's anomalous dispersion of phonons near resonance. The only quantitative theory however is that of Holstein and it is only appropriate to photon diffusion. Thus in the next section we begin to derive a quantitative description of the phonon bottleneck from first principles.

2.3 Linear Equations of Motion for the Electron-Phonon System

Let us begin by writing down the Hamiltonian (2.19) (we set $\hbar = 1$), namely

$$\mathcal{H} = \sum_{\tilde{r}} \Delta S_{\tilde{r}}^z + \sum_{\tilde{k}} \omega_{\tilde{k}} b_{\tilde{k}}^{\dagger} b_{\tilde{k}} + \sum_{\tilde{r}} \sum_{\tilde{k}} g_{\tilde{k}} (b_{\tilde{k}}^{\dagger} S_{\tilde{r}}^{-} e^{-i\tilde{k}\tilde{r}} + S_{\tilde{r}}^{+} b_{\tilde{k}} e^{i\tilde{k}\tilde{r}}) . \quad (2.39)$$

In this equation the summation over \tilde{k} implicitly includes a summation over the 3 types of acoustic modes. Using the commutation relations (2.2) and (2.11) we can immediately write down the Heisenberg equations of motion for the operators $b_{\tilde{k}}$, $S_{\tilde{r}}^{-}$, and $S_{\tilde{r}}^z$, namely

$$\begin{aligned} i\dot{b}_{\tilde{k}} &= [b_{\tilde{k}}, \mathcal{H}] = \omega_{\tilde{k}} b_{\tilde{k}} + \sum_{\tilde{r}} g_{\tilde{k}} S_{\tilde{r}}^{-} e^{-i\tilde{k}\tilde{r}} , \\ i\dot{S}_{\tilde{r}}^{-} &= [S_{\tilde{r}}^{-}, \mathcal{H}] = \Delta S_{\tilde{r}}^{-} - 2 \sum_{\tilde{k}} g_{\tilde{k}} S_{\tilde{r}}^z b_{\tilde{k}} e^{i\tilde{k}\tilde{r}} , \\ i\dot{S}_{\tilde{r}}^z &= [S_{\tilde{r}}^z, \mathcal{H}] = \sum_{\tilde{k}} g_{\tilde{k}} (S_{\tilde{r}}^{+} b_{\tilde{k}} e^{i\tilde{k}\tilde{r}} - b_{\tilde{k}}^{\dagger} S_{\tilde{r}}^{-} e^{-i\tilde{k}\tilde{r}}) . \end{aligned} \quad (2.40)$$

It is easy to show that the number of excitations in the system is constant, i.e. $\sum_{\underline{k}} b_{\underline{k}}^{\dagger} b_{\underline{k}} + \sum_{\underline{r}} S_{\underline{r}}^{+} S_{\underline{r}}^{-} = \text{constant}$. Integrating Eqs. (2.40) formally we get

$$\begin{aligned}
 b_{\underline{k}}(t) &= e^{-i\omega_{\underline{k}} t} b_{\underline{k}}(0) - ig_{\underline{k}} \sum_{\underline{r}} e^{-ik \cdot \underline{r}} \int_0^t dt' e^{-i\omega_{\underline{k}}(t-t')} S_{\underline{r}}^{-}(t') , \\
 S_{\underline{r}}^{-}(t) &= e^{-i\Delta t} S_{\underline{r}}^{-}(0) + 2i \sum_{\underline{k}} g_{\underline{k}} e^{ik \cdot \underline{r}} \int_0^t dt' e^{-i\Delta(t-t')} S_{\underline{r}}^z(t') b_{\underline{k}}(t') , \\
 S_{\underline{r}}^z(t) &= S_{\underline{r}}^z(0) - i \sum_{\underline{k}} g_{\underline{k}} (e^{ik \cdot \underline{r}} \int_0^t dt' S_{\underline{r}}^{+}(t') b_{\underline{k}}(t') \\
 &\quad - e^{-ik \cdot \underline{r}} \int_0^t dt' b_{\underline{k}}^{\dagger}(t') S_{\underline{r}}^{-}(t')) . \quad (2.41)
 \end{aligned}$$

These equations can be solved by iteration.

Let us first find the solution in first order perturbation theory. Keeping terms up to order g^2 we find that

$$\begin{aligned}
 S_{\underline{r}}^{-}(t) &= A^{(1)}(\underline{r}, t) S_{\underline{r}}^{-} + \sum_{\underline{k}} g_{\underline{k}} A_{\underline{k}}^{(2)}(\underline{r}, t) S_{\underline{r}}^z b_{\underline{k}} + \sum_{\underline{k}, \underline{k}'} g_{\underline{k}} g_{\underline{k}'} A_{\underline{k}, \underline{k}'}^{(3)}(\underline{r}, t) \\
 &\quad \times b_{\underline{k}}^{\dagger} b_{\underline{k}'} S_{\underline{r}}^{-} + \sum_{\underline{k}, \underline{r}'} g_{\underline{k}}^2 A_{\underline{k}, \underline{r}'}^{(4)}(\underline{r}, t) S_{\underline{r}}^z S_{\underline{r}'}^{-} + \sum_{\underline{k}, \underline{k}'} g_{\underline{k}} g_{\underline{k}'} A_{\underline{k}, \underline{k}'}^{(5)}(\underline{r}, t) S_{\underline{r}}^{+} b_{\underline{k}} b_{\underline{k}'} , \quad (2.42)
 \end{aligned}$$

where all operators on the right hand side are evaluated at time $t=0$ and $A^{(i)}(\underline{r}, t)$, $i=1, \dots, 5$ are some functions of time. The probability $N_{\underline{r}}^{\uparrow}(t)$ that the $\underline{r}^{\text{th}}$ atom is excited at time t is given by

$$N_{\tilde{r}}^{\uparrow}(t) = \langle i | S_{\tilde{r}}^+(t) S_{\tilde{r}}^-(t) | i \rangle , \quad (2.43)$$

where $|i\rangle$ is the state of the system at time $t=0$. After some algebra we find that to order g^2

$$N_{\tilde{r}}^{\uparrow}(t) = N_{\tilde{r}}^{\uparrow}(0) + \sum_{\tilde{k}} g_{\tilde{k}}^2 F_{\tilde{k}}(t) \{ N_{\tilde{r}}^{\downarrow}(0) n_{\tilde{k}}^{\text{ph}}(0) - N_{\tilde{r}}^{\uparrow}(0) (1 + n_{\tilde{k}}^{\text{ph}}(0)) \} , \quad (2.44)$$

where

$$n_{\tilde{k}}^{\text{ph}}(t) = \langle i | b_{\tilde{k}}^{\dagger}(t) b_{\tilde{k}}(t) | i \rangle \quad (2.45)$$

is the number of phonons in mode k at time t and

$$F_{\tilde{k}}(t) \equiv \frac{\sin^2\left(\frac{\Delta - \omega_{\tilde{k}}}{2} t\right)}{\left(\frac{\Delta - \omega_{\tilde{k}}}{2}\right)^2} . \quad (2.46)$$

We wish to point out several features of the perturbation solution. For small times $\lim_{t \rightarrow 0} F_{\tilde{k}}(t) = t^2$ so that if there are no phonons initially present, the excited atom decays like

$$N_{\tilde{r}}^{\uparrow}(t) = N_{\tilde{r}}^{\uparrow}(t=0) (1 - \sum_{\tilde{k}} g_{\tilde{k}}^2 t^2) . \quad (2.47)$$

We note that initially the atom does not decay exponentially; rather it begins with zero slope. Indeed in the case of a single phonon mode the factor $1 - g^2 t^2$ is the beginning of the series expansion for the cosinusoidal evolution of the excited atom found by Swain³¹. Notice also that $F_{\tilde{k}}(t=0) = t^2$ is independent of \tilde{k} i.e. any phonon regardless of its energy can be emitted by the atom initially in accord with the energy-time uncertainty relation $\Delta E \Delta t \gtrsim \hbar$. However as time progresses $F_{\tilde{k}}(t)$

becomes more peaked around $\omega_{\tilde{k}} = \Delta$. Let us now assume that the phonon modes form a continuum so that we can replace

$$\frac{1}{\Omega} \sum_{\tilde{k}} \rightarrow \int D(\omega) d\omega , \quad (2.48)$$

where $D(\omega) d\omega$ is the density of phonon modes per cm^3 in the frequency interval $d\omega$ about ω and Ω is the volume of the crystal. Then in the limit of very large times

$$\lim_{t \rightarrow \infty} \frac{1}{t} F_{\tilde{k}}(t) = 2\pi \delta(\omega_{\tilde{k}} - \Delta) , \quad (2.49)$$

expressing the fact that for large times energy is conserved. Plugging (2.48, 49) into (2.44) we find that the probability that the atom is excited at time t is

$$N_{\tilde{r}}^{\uparrow}(t) = N_{\tilde{r}}^{\uparrow}(0) + \Gamma t \{ N_{\tilde{r}}^{\downarrow}(0) n_{\Delta}^{\text{ph}}(0) - N_{\tilde{r}}^{\uparrow}(0) (1 + n_{\Delta}^{\text{ph}}(0)) \} , \quad (2.50)$$

where

$$\Gamma = 2\pi g_{\Delta}^2 D(\Delta) \Omega \quad (2.51)$$

is the spontaneous decay rate in agreement with Fermi's golden rule. The three terms in braces represent the excitation by initially present phonons of the atom in the lower level, spontaneous decay, and stimulated decay by phonons of the atom in the upper level respectively.

It is interesting to note that in thermal equilibrium where all occupation numbers must be constant, Eq. (2.50) yields

$$N_{\tilde{r}}^{\downarrow} n_{\Delta}^{\text{ph}} = N_{\tilde{r}}^{\uparrow} (1 + n_{\Delta}^{\text{ph}}) . \quad (2.52)$$

Combining this with the fact that at temperature T , the number of atoms in the \uparrow and \downarrow states are given by $N_{\uparrow} = \exp(-E_{\uparrow}/kT)$ and $N_{\downarrow} = \exp(-E_{\downarrow}/kT)$, with $E_{\uparrow} - E_{\downarrow} = \Delta$, we get the Planck distribution for the phonons, namely

$$n_{\Delta}^{\text{ph}} = \frac{1}{e^{\Delta/kT} - 1} . \quad (2.53)$$

Perturbation theory has the shortcoming that, although it gives the decay rate of an excited atom, it does not give directly the spectrum of phonons that is emitted. For example, Eq. (2.50) claims that only a phonon of energy exactly $\omega_k = \Delta$ can interact with a two-level atom. But we know from the uncertainty relation that actually a band of phonons of width $\Delta\omega \approx \frac{1}{T_1} = 2\pi g^2 D(\Delta)\Omega$ can interact with the atom. For this reason we wish to iterate Eqs. (2.41) to all orders. To facilitate this we represent the equations pictorially. For now, forget the phase factors, summations and time integrations, and focus attention on the power of the coupling g and the order of the non-commuting operators. We write symbollically

$$\begin{aligned} b(t) &\sim b(0) + gS^{-}(t') \\ S^{-}(t) &\sim S^{-}(0) + gS^Z(t')b(t') \\ S^Z(t) &\sim S^Z(0) + g(S^{+}(t')b(t') + b^{\dagger}(t')S^{-}(t')) , \end{aligned} \quad (2.54)$$

which we represent pictorially as

$$b(t) \equiv \begin{array}{c} \bullet^b \\ | \\ \circ^{s^-} \end{array} \quad , \quad (2.55a)$$

$$s^-(t) \equiv \begin{array}{c} \bullet^{s^-} \\ | \\ \text{---} \circ^{s^z} \text{---} \circ^b \text{---} \end{array} \quad , \quad (2.55b)$$

and

$$s^z(t) \equiv \begin{array}{c} \bullet^{s^z} \\ / \quad \backslash \\ \text{---} \circ^{s^+} \text{---} \circ^b \quad \circ^{b^+} \text{---} \circ^{s^-} \text{---} \end{array} \quad . \quad (2.55c)$$

Here the dots represent operators at time $t=0$ e.g.

$$\bullet^b \equiv b(t=0), \quad (2.56)$$

open circles represent operators at finite times e.g.

$$\circ^b \equiv b(t') \quad , \quad (2.57)$$

vertical lines represent addition, e.g.

$$\begin{array}{c} \text{---} \\ | \\ \square \end{array} \text{---} \equiv +g \times \square \quad , \quad (2.58)$$

and horizontal lines represent multiplication, e.g.

$$\square^1 \text{---} \square^2 \equiv \square^1 \times \square^2 \quad . \quad (2.59)$$

The diagrams are read from top to bottom (in ascending powers of g). The order from left to right is important since the operators in general do not commute. To iterate Eqs. (2.41) pictorially we simply plug the diagram for operator q into \odot^q . For example iterating $S^-(t)$ several times we get the perturbation tree shown in Fig. 2.3.

The open circles at the ends of the branches indicate that we have to iterate ad infinitum. To regain the first order perturbation result we cut off the 'tree' at the g^2 level and multiply out the branches to get

$$S^-(t) \Big|_{\text{to order } g^2} \hookrightarrow S^- + g S^z b + g^2 (S^+ b b + b^\dagger S^- b + S^z S^-) . \quad (2.60)$$

Re-inserting all the summations and time dependencies we again get exactly Eq. (2.42).

Linearizing Approximation

Let us now make the important assumption that there are very few excitations present in the system, i.e.

$$\sum_k \langle b_k^\dagger b_k \rangle + \sum_r \langle S_r^+ S_r^- \rangle \ll \sum_r \langle S_r^- S_r^+ \rangle \approx \sum_r 1 \quad (2.61)$$

where $\langle \dots \rangle \equiv \langle i | \dots | i \rangle$. Indeed, let us assume that there is just a single excitation initially present in the system. Then it is easy to see that we may replace the perturbation tree, Fig. 2.3, by the tree

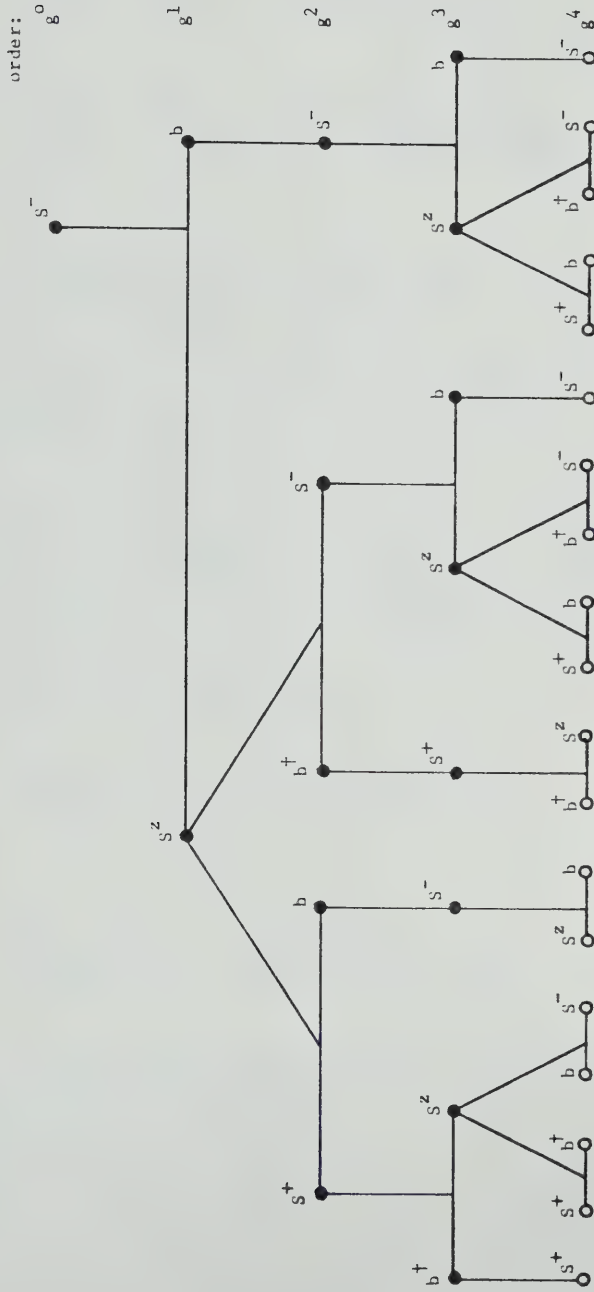


Fig. 2.3 Perturbation tree for $s^-(t)$.

$$S_r^-(t) \sim \begin{array}{c} S^- \\ | \\ S^Z \quad b \\ | \\ S^- \\ | \\ S^Z \quad b \\ | \\ S^- \\ | \\ S^Z \quad b \\ | \\ S^- \\ \vdots \end{array} \quad (2.62)$$

i.e. we everywhere replace $S^Z(t) \rightarrow S^Z(0)$, because from the other terms of $S^Z(t)$ (see Eq. (2.55c)) there will come contributions to $S_r^-(t)|i\rangle$ with at least two annihilation operators acting on a state $|i\rangle$ (with only one excitation present), and these will vanish. Furthermore any term of the series for $S_r^-(t)$ represented by (2.62) acting on state $|i\rangle$ has the form

$$S_{\tilde{r}_1}^Z(0) \dots S_{\tilde{r}_n}^Z(0) b_{\tilde{k}}(0) |i\rangle$$

or (2.63)

$$S_{\tilde{r}_1}^Z(0) \dots S_{\tilde{r}_n}^Z(0) S_{\tilde{r}'}^-(0) |i\rangle$$

which either have the value $(-1/2)^n |0\rangle$ or vanish depending on whether or not state $|i\rangle$ has a phonon present in mode k or the r^{th} atom excited. We may summarize this by saying that if the state $|i\rangle$ has just a single excitation present, then we may everywhere replace $S^Z(t) \rightarrow -1/2$. We expect this to be approximately valid also for a small number of excitations present. With this replacement, Eqs. (2.40) become

$$i\dot{b}_{\tilde{k}} = \omega_{\tilde{k}} b_{\tilde{k}} + \sum_{\tilde{r}} g_{\tilde{k}} S_{\tilde{r}}^{-} e^{-ik \cdot \tilde{r}} \quad (2.64)$$

$$i\dot{S}_{\tilde{r}}^{-} = \Delta S_{\tilde{r}}^{-} + \sum_{\tilde{k}} g_{\tilde{k}} b_{\tilde{k}} e^{+ik \cdot \tilde{r}} \quad .$$

Whereas Eqs. (2.40) were non-linear in the number of operators, these equations are linear and thus exclude processes such as stimulated emission.

CHAPTER 3

SPONTANEOUS DECAY OF A SINGLE TWO-LEVEL ATOM AND THE GENERAL THEORY OF THE DECAY OF UNSTABLE QUANTUM SYSTEMS

Let us first study the simple case of the interaction of a single atom with a phonon field. In this case Eqs. (2.64) reduce to

$$\begin{aligned} i\dot{b}_{\tilde{k}} &= \omega_{\tilde{k}} b_{\tilde{k}} + g_{\tilde{k}} S^{-} \quad , \\ i\dot{S}^{-} &= \Delta S^{-} + \sum_{\tilde{k}} g_{\tilde{k}} b_{\tilde{k}} \quad ; \end{aligned} \tag{3.1}$$

where the operators S^{+} and S^{-} refer to the single atom. These equations can be uncoupled by the use of (one-sided) Fourier transforms. Define the Fourier transforms of $S^{-}(t)$ and $b_{\tilde{k}}(t)$ to be

$$\mathcal{S}^{-}(x) \equiv \mathcal{F}[S^{-}(t)] \equiv \int_0^{\infty} dt S^{-}(t) e^{ixt} \quad ,$$

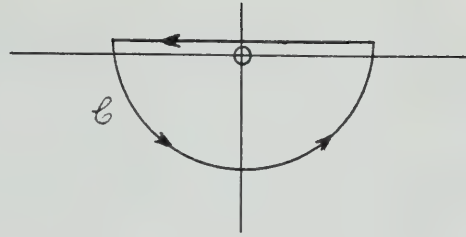
and (3.2)

$$B_{\tilde{k}}(x) \equiv \mathcal{F}[b_{\tilde{k}}(t)] \equiv \int_0^{\infty} dt b_{\tilde{k}}(t) e^{ixt} \quad ;$$

with inverse transforms

$$\begin{aligned} S^{-}(t) &\equiv \mathcal{F}^{-1}[\mathcal{S}^{-}(x)] \equiv -\frac{1}{2\pi} \oint_{\mathcal{C}} dx \mathcal{S}^{-}(x) e^{-ixt} \quad , \\ b_{\tilde{k}}(t) &\equiv \mathcal{F}^{-1}[B_{\tilde{k}}(x)] \equiv -\frac{1}{2\pi} \oint_{\mathcal{C}} dx B_{\tilde{k}}(x) e^{-ixt} \quad ; \end{aligned} \tag{3.3}$$

where the integration contour \mathcal{C} encloses the lower half-plane as shown:



$$(3.3)$$

The Fourier transforms of Eqs. (3.1) are

$$B_{\tilde{k}}(x) = \frac{i}{x - \omega_{\tilde{k}}} b_{\tilde{k}}(0) + \frac{g_{\tilde{k}}}{x - \omega_{\tilde{k}}} \mathcal{J}^-(x) , \quad (3.4a)$$

$$\mathcal{J}^-(x) = \frac{i}{x - \Delta} S^-(0) + \sum_{\tilde{k}} \frac{g_{\tilde{k}}}{x - \Delta} B_{\tilde{k}}(x) . \quad (3.4b)$$

Using (3.4a), $\mathcal{J}^-(x)$ can be written in closed form as

$$\mathcal{J}^-(x) = \frac{1}{x - \Delta - \sum_{\tilde{k}} \frac{g_{\tilde{k}}^2}{x - \omega_{\tilde{k}}}} \left\{ i S^-(0) + \sum_{\tilde{k}} g_{\tilde{k}} \frac{i b_{\tilde{k}}(0)}{x - \omega_{\tilde{k}}} \right\} . \quad (3.5)$$

Expanding the denominator in a binomial series about $x - \Delta$ gives the same series that would result from the simple iteration of Eqs. (3.4a,b). The atom-phonon system may be viewed as a single oscillator of frequency Δ (the atom) coupled to a set of N harmonic oscillators of frequencies $\omega_{\tilde{k}}$ (the phonons). The coupling shifts these $N+1$ frequencies slightly to new values given by the positions of the poles of $\mathcal{J}^-(x)$. There are two quite different cases depending on whether the phonon modes are discrete or form a continuum.

3.1 Decay of a Two-Level Atom in a Finite Crystal

In a crystal of finite extent it is well known that there are a finite number of discrete phonon modes. It is

easy to show in this case that $S^-(t)$ and hence the probability $N_\uparrow(t)$ of the atom being excited at time t has some sort of periodic behavior. To be specific assume that at time $t=0$ the atom is excited and there are no phonons present. Dropping therefore the second term in braces, we can write (3.5) as

$$S^-(x) = \frac{i S^-(0)}{x - \Delta - \sum_k \frac{g_k^2}{x - \omega_k}} = \frac{i \prod_k (x - \omega_k) S^-(0)}{\det(x\hat{1} - \hat{M})}, \quad (3.6)$$

where $\hat{1}$ is the identity matrix, and \hat{M} is the matrix

$$\hat{M} = \left(\begin{array}{c|ccc} \Delta & g_1 & \dots & g_N \\ \hline g_1 & \omega_1 & & 0 \\ \vdots & & \ddots & \\ g_N & 0 & & \omega_N \end{array} \right) \quad (3.7)$$

It is well known that the $N+1$ eigenvalues of the symmetric matrix M , which we denote $\omega'_1, \omega'_2, \dots, \omega'_{N+1}$ are real. Thus inverting the Fourier transform we find that the probability $N_\uparrow(t)$ that the atom is excited at time t is given by

$$N_\uparrow(t) = |S^-(t)|^2 = \left| \sum_{k=1}^{N+1} A_k e^{-i\omega'_k t} \right|^2, \quad (3.8)$$

which is obviously periodic ($A_k, k=1,2,\dots,N+1$ are some time independent coefficients).

Let us look in detail at the case of coupling to a single phonon mode whose frequency we denote ω_1 . In this

case the poles of

$$\phi^-(x) = \frac{i\phi^-(0)}{x - \Delta - \frac{g^2}{x - \omega_1}} \quad (3.9)$$

are shifted to positions

$$x_{\pm} = \frac{\Delta + \omega_1}{2} \pm \sqrt{\left(\frac{\Delta - \omega_1}{2}\right)^2 + g^2} \quad (3.10)$$

We find that the probability $N_{\uparrow}(t)$ that the atom is excited at time t is given by

$$N_{\uparrow}(t) = 1 - \frac{g^2}{\left(\frac{\Delta - \omega_1}{2}\right)^2 + g^2} \sin^2 \sqrt{\left(\frac{\Delta - \omega_1}{2}\right)^2 + g^2} t \quad (3.11)$$

which is sketched in Fig. 3.1 for various values of ω_1 .

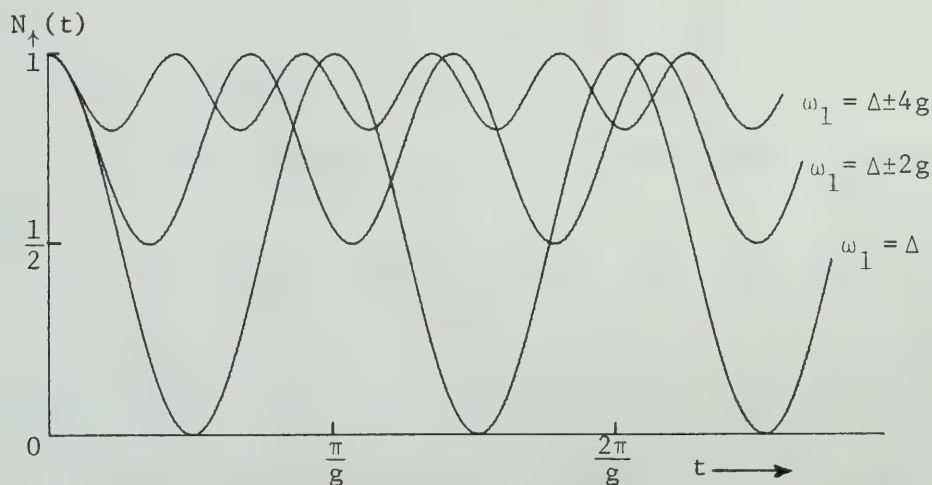


Fig. 3.1 The probability $N_{\uparrow}(t)$ that a two-level atom, coupled with strength g to a single phonon mode of frequency ω_1 , is excited at time t ; for various values of ω_1 .

We note several features:

- (1) The time evolution of the excited atom is periodic and similar to the behavior of a pair of classical coupled pendulums. Recall that Swain³¹, Scharf³², and Mallory³⁴ also found similar periodic time evolution in the case of coupling to a single mode.
- (2) According to Eq. (3.10), if $\omega_1 \approx \Delta$, the coupling splits the degenerate frequencies of the two oscillators by an amount $\approx g$.
- (3) As shown in Fig. 3.1 only modes within a distance $\Delta\omega \approx g$ of Δ interact strongly with the atom.
- (4) The atom 'decays' in time $T_1 \approx 1/g$. Thus we have an 'uncertainty' relation $\Delta\omega \cdot T_1 \approx 1$.
- (5) Expanding (3.11) in a power series for small times we find

$$N(t) = 1 - g^2 t^2 + \dots, \quad (3.12)$$

which is just the result (2.47) of first order perturbation theory.

With this experience let us now consider the case of coupling of the two-level atom to a finite but large number of phonon modes. This case can be solved exactly if we assume a perfect one-dimensional N lattice-site crystal with constant coupling $g_k = g$ for all k . Then the N phonon modes have frequencies given by $\omega_k = c|k|$ where $k = 2\pi n/Na$ is the wavenumber, a is the interatomic spacing and n is an integer in the range $-N/2 \leq n \leq N/2$. Since $\omega_k = \omega_{-k}$ we have

$N/2$ distinct evenly spaced phonon energy levels in the interval $0 \leq \omega_k \leq \omega_D$, where $\omega_D = c\pi/a$ is the Debye cutoff frequency. Thus in this case, with no phonons initially present, the amplitude $\delta^-(x)$ is given by

$$\delta^-(x) = \frac{iS^-(0)}{x - \Delta + \frac{g^2 N}{\omega_D} I_{N/2}(x)} , \quad (3.13)$$

where

$$I_{N/2}(x) = \sum_{k=1}^{N/2} \frac{1}{n - \frac{Nx}{2\omega_D}} . \quad (3.14)$$

The series $I_{N/2}(x)$ can be represented in terms of the digamma or ψ -function⁴⁶, which satisfies the following relations⁴⁷:

$$\begin{aligned} \psi(x) &= \frac{d}{dx} \ln \Gamma(x) , \\ \psi(x+N) - \psi(x) &= \sum_{k=0}^{N-1} \frac{1}{x+k} , \end{aligned} \quad (3.15)$$

$$\psi(1-x) = \psi(x) + \pi \cot \pi x ,$$

$$\lim_{N \rightarrow \infty} (\psi(x+N) - \ln N) = 0 .$$

Using these formulas we can write the series $I_{N/2}(x)$ as

$$\begin{aligned} I_{N/2}(x) &= \psi\left(\frac{N}{2} + 1 - \frac{Nx}{2\omega_D}\right) - \psi\left(1 - \frac{Nx}{2\omega_D}\right) \\ &\approx \begin{cases} \ln \frac{x - \omega_D}{x} , & \text{for } x < 0 \text{ or } x > \omega_D \\ \ln \frac{\omega_D - x}{x} - \cot \frac{\pi Nx}{2\omega_D} , & \text{for } 0 < x < \omega_D \end{cases} \quad (3.16) \end{aligned}$$

The approximation in (3.16) becomes exact as the number of phonon modes $N \rightarrow \infty$. From the discussion after (3.7) we know that for any finite number N of phonon modes the poles of $\epsilon^-(x)$ are real. We find the poles graphically by looking for the points of intersection of the functions $f_1(x) = x - \Delta$ and $f_2(x) = \frac{-g^2 N}{\omega_D} I_{N/2}(x)$ with x real as shown in Fig. 3.2. Notice that the $N/2$ distinct phonon frequencies and the one atom frequency have been shifted in such a way that $N/2 - 1$ of the poles (denoted $\omega'_1, \omega'_2, \dots, \omega'_{N/2-1}$) occupy interstitial positions that interlace the 'old' uncoupled system phonon poles and the two remaining endpoint poles (denoted $\omega'_0, \omega'_{N/2}$) have been shifted out of the phonon spectrum $0 \leq x \leq \omega_D$. The poles to the left/right of frequency Δ have been shifted to the left/right, with the poles near Δ being shifted the most, indicating maximal coupling to those modes. The positions of the poles can be expressed as

$$\omega'_n = \omega_D \left(\frac{2n}{N} + \frac{2}{N\pi} \sigma_n \right), \quad n = 1, 2, \dots, \frac{N}{2} - 1 \quad (3.17)$$

where the amount of shift σ_n of the n^{th} pole is given by

$$\sigma_n = \cot^{-1} \left[\frac{\omega_D \frac{2n}{N} - \Delta + \frac{g^2 N}{\omega_D} \ln \left(\frac{1 - \frac{2n}{N}}{\frac{2n}{N}} \right)}{\frac{g^2 N}{\pi \omega_D}} \right] \quad (3.18)$$

as can be seen in Fig. 3.2 from the fact that the n^{th} cotangent curve is raised/lowered towards the right/left by the amount

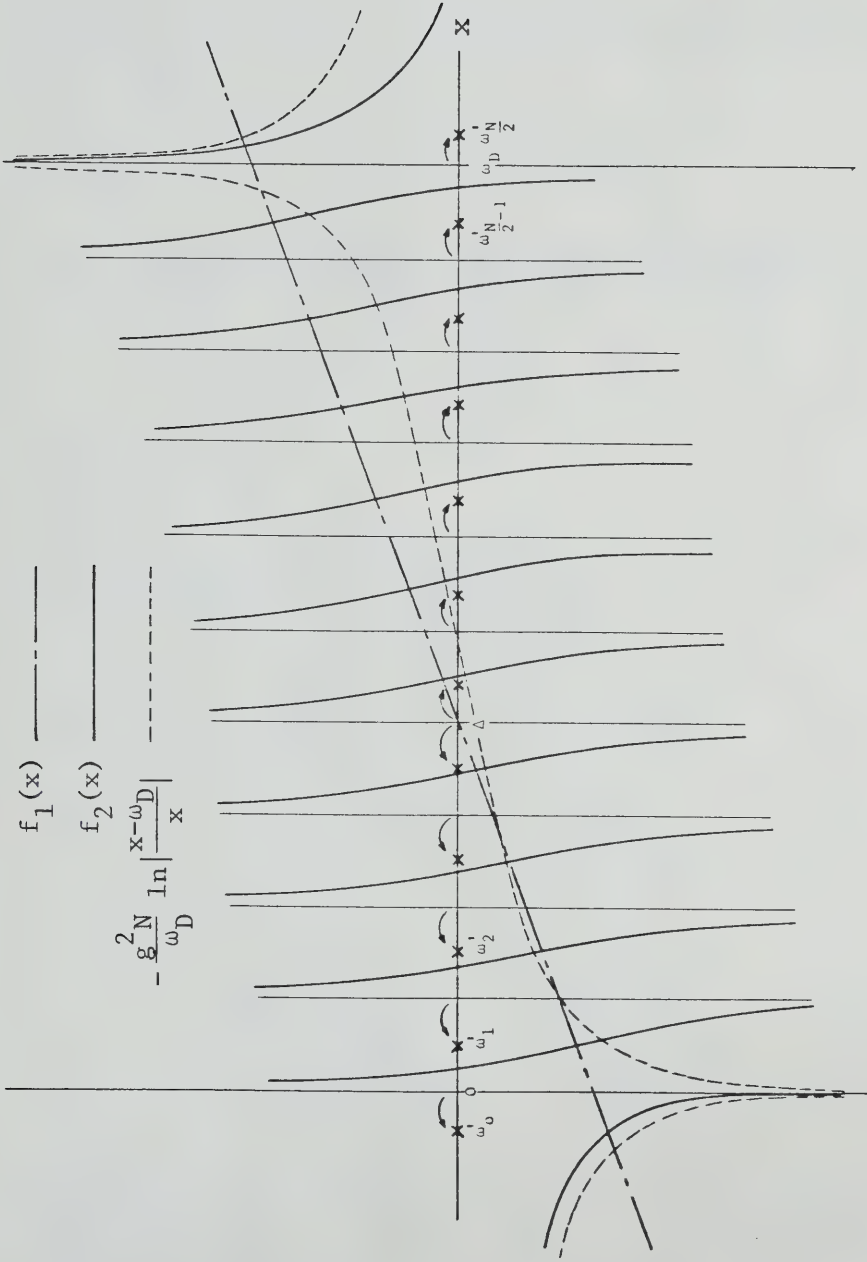
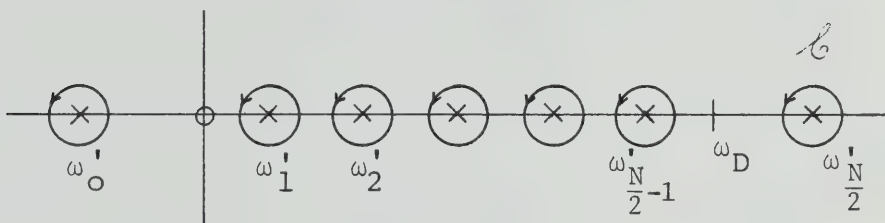


Fig. 3.2 Graphical solution of the poles of $f_2^-(x)$. Poles are denoted by crosses. Arrows indicate the movement of the poles when the coupling is switched on. The dashed curve is proportional to the function $\ln|(x - \omega_D)/x|$. Inside the region $0 \leq x \leq \omega_D$ the cotangent curves are lifted by this amount. Outside this region, $f_2(x)$ approaches this function as $N \rightarrow \infty$.

$$\frac{-g_N^2}{\omega_D} \ln \frac{1 - \frac{2n}{N}}{\frac{2n}{N}} \quad . \quad (3.19)$$

Now that we have found the positions of the poles we can invert the Fourier transform using the following integration contour



and find that

$$\begin{aligned} S^-(t) &= \frac{1}{2\pi i} \oint \frac{dx e^{-ixt} S^-(0)}{x - \Delta + \frac{g_N^2}{\omega_D} I_{N/2}(x)} \\ &= S^-(0) \left\{ \sum_{k=1}^{\frac{N}{2}-1} \frac{e^{-i\omega'_k t}}{1 + \frac{g_N^2}{\omega_D} \left[\frac{\pi^2 N}{2 \sin^2(\frac{\pi N \omega'_k}{2\omega_D})} - \frac{\omega_D^2}{\omega'_k (\omega_D - \omega'_k)} \right]} \right. \\ &\quad \left. + \frac{e^{-i\omega'_0 t}}{1 + \frac{g_N^2}{\omega'_0 (\omega_D - \omega'_0)}} + \frac{e^{-i\omega'_{N/2} t}}{1 + \frac{g_N^2}{\omega'_{N/2} (\omega_D - \omega'_{N/2})}} \right\} . \quad (3.20) \end{aligned}$$

Plugging (3.17) and (3.18) into (3.20), taking N large, and using the fact that

$$\sin^2 \cot^{-1} x = \frac{1}{1+x^2} \quad , \quad (3.21)$$

we can write $S^-(t)$ as

$$S^-(t) = S^-(0) \left\{ \sum_{k=1}^{\frac{N}{2}-1} e^{-i \frac{2n\omega_D}{N} t} \mathcal{L}_n + \frac{e^{-i\omega'_0 t}}{1 + \frac{g^2_N}{\omega'_0(\omega_D - \omega'_0)}} + \frac{e^{-i\omega'_{N/2} t}}{1 + \frac{g^2_N}{\omega'_{N/2}(\omega_D - \omega'_{N/2})}} \right\}, \quad (3.22)$$

where

$$\mathcal{L}_n = \frac{2g^2}{\left[\frac{2n}{N} \omega_D - \Delta + \frac{g^2_N}{\omega_D} \ln\left(\frac{\frac{N}{2}-n}{n}\right) \right]^2 + \left(\frac{\pi g^2_N}{\omega_D} \right)^2}. \quad (3.23)$$

Notice the following features of (3.22) and (3.23).

(1) In the exponent of (3.22) the shift σ_n of the poles for large N is negligible and has been dropped because of the way the 'new' poles interlace the 'old' poles (see Fig. 3.2).

(2) The coefficient \mathcal{L}_n generally is approximately a Lorentzian of width $2\pi g^2_N/\omega_D$ centered about frequency

$$\Delta' = \Delta - \frac{g^2_N}{\omega_D} \ln\left(\frac{\frac{N}{2}-n}{n}\right) \Big|_{n = \frac{N\Delta}{2\omega_D}}.$$

It is not a perfect Lorentzian because of the logarithm term but if the coupling g is small then this term should not be too important.

(3) Conversely, the last two terms of (3.22), i.e. the contributions to $S^-(t)$ from the outlying poles ω'_0 and $\omega'_{N/2}$ will shortly be shown to be important only when \mathcal{L}_n is not

approximately a Lorentzian.

Let us illustrate Eq. (3.22) with an example where \mathcal{L}_n is a Lorentzian and the outlying poles give a negligible contribution, namely suppose that

$$\mathcal{L}_n = \frac{2g^2}{\left(\frac{2n\omega_D}{N} - \Delta'\right)^2 + \left(\frac{\pi g^2 N}{\omega_D}\right)^2} \quad .$$

In Fig. 3.3 we have sketched \mathcal{L}_n and the corresponding probability $N_\uparrow(t) = |S^-(t)|^2$ that the atom is excited at time t .

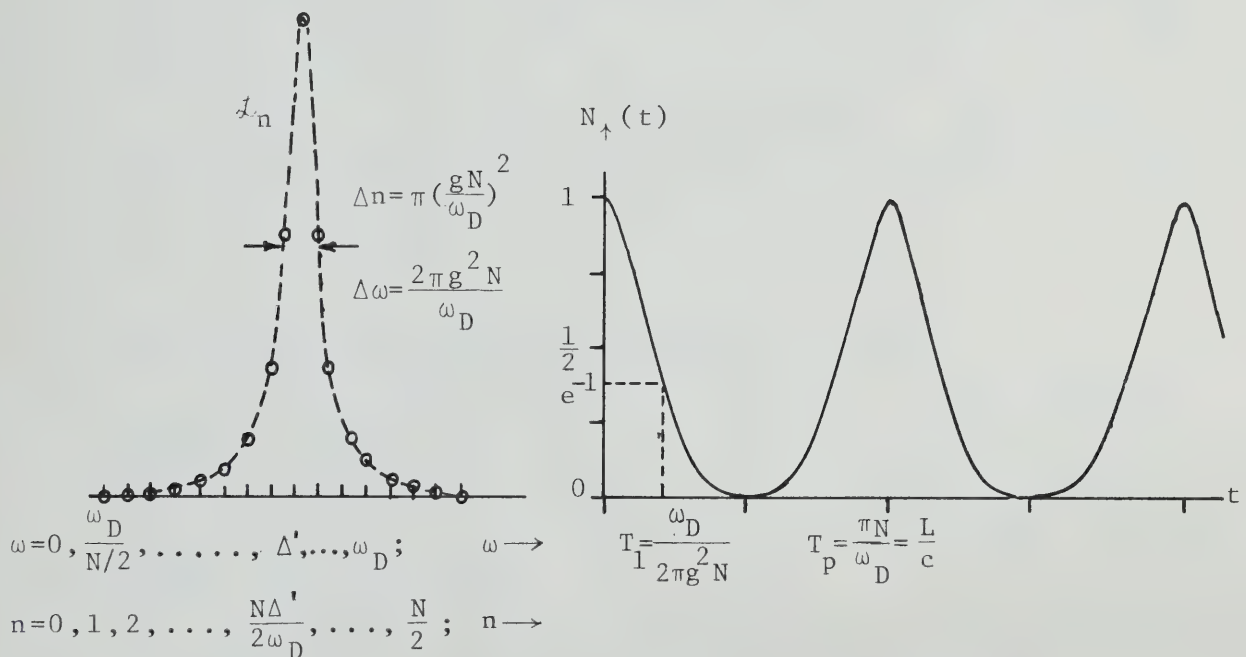


Fig. 3.3. (a) The lineshape \mathcal{L}_n , and (b) the corresponding probability $N_\uparrow(t)$ that the atom is excited at time t . Notice that $N_\uparrow(t)$ is periodic with period $T_p = L/c$ where L is the length of the crystal and c is the speed of sound.

Notice that $N_{\uparrow}(t)$ decays in a time $T_1 = \omega_D / (2\pi g^2 N)$, which is just the inverse of the halfwidth $\Delta\omega$ of the lineshape \mathcal{L}_n . Thus T_1 and $\Delta\omega$ obey the uncertainty relation $T_1 \Delta\omega = 1$. Notice also that $N_{\uparrow}(t)$ is periodic with period L/c , where L is the size of the crystal and c is the speed of sound. This period is just the time that it takes a phonon to traverse the crystal and re-excite the atom. Mathematically the system is periodic because $S^-(t)$ (Eq. (3.22)) is given by a discrete Fourier series rather than a continuous Fourier transform. (Notice that the perfect periodicity of $N_{\uparrow}(t)$ is due to the approximation that the poles are unshifted and uniformly spaced. In reality due to the shifts σ_n we expect $N_{\uparrow}(t)$ to be 'almost periodic'.) In the next section we show that as the size of the crystal $L \rightarrow \infty$ the atom simply decays and is never re-excited.

3.2 Decay of an Atom in an Infinite Crystal

To solve this problem we can either simply let the number of phonon modes N go to infinity in the finite crystal result (3.22) or consider the crystal to be of infinite extent from the outset.

In the former case the series in (3.22) can then be replaced by an integral, so that the amplitude $S^-(t)$ becomes

$$\begin{aligned}
S^-(t) = S^-(0) & \left\{ \int_0^{\omega_D} d\omega e^{-i\omega t} \frac{\Gamma/2\pi}{(\omega - \Delta + \frac{\Gamma}{2\pi} \ln \frac{\omega_D - \omega}{\omega})^2 + (\frac{\Gamma}{2})^2} \right. \\
& + \frac{e^{-i\omega'_0 t}}{1 + \frac{\Gamma\omega_D}{2\pi\omega'_0(\omega_D - \omega'_0)}} + \frac{e^{-i\omega'_{N/2} t}}{1 + \frac{\Gamma\omega_D}{2\pi\omega'_{N/2}(\omega_D - \omega'_{N/2})}} \left. \right\}, \quad (3.24)
\end{aligned}$$

where

$$\Gamma = \frac{2\pi g^2_N}{\omega_D} \quad (3.25)$$

now defines the strength of the coupling.

The other route is to replace (3.13) and (3.14) by the amplitude

$$\mathcal{J}^-(x) = \frac{iS^-(0)}{x - \Delta + \frac{\Gamma}{2\pi} \int_0^{\omega_D} \frac{d\omega}{\omega - x}}, \quad (3.26)$$

where the phonon modes are assumed from the outset to be continuous so that

$$S^-(t) = \frac{1}{2\pi i} \oint_{\mathcal{C}} dx e^{-ixt} \frac{S^-(0)}{x - \Delta + \frac{\Gamma}{2\pi} \int_0^{\omega_D} \frac{d\omega}{\omega - x}}. \quad (3.27)$$

The integral in the denominator of (3.27) results in branch points at $x=0$ and $x=\omega_D$ which we can connect by a branch cut. This branch cut evidently replaces the discrete set of phonon poles ω_n , $0 \leq \omega_n \leq \omega_D$ of the finite case. It is easy to show that the two outlying poles remain.

Thus to integrate (3.27) we may use the contour

$$(3.28)$$

On \mathcal{C}_1 we let $x \rightarrow x + i\varepsilon$ and on \mathcal{C}_2 we let $x \rightarrow x - i\varepsilon$ where $\varepsilon \rightarrow 0^+$ and x is now a real number. Then using the fact that

$$\lim_{\varepsilon \rightarrow 0^+} \frac{1}{x \pm i\varepsilon} = \mathcal{P} \frac{1}{x} \mp i\pi\delta(x) , \quad (3.29)$$

where \mathcal{P} represents the principal value, we find that

$$\begin{aligned} \lim_{\varepsilon \rightarrow 0^+} \int_0^{\omega_D} \frac{d\omega}{\omega - x \pm i\varepsilon} &= \left[\int_0^{x-\delta} + \int_{x+\delta}^{\omega_D} \right] \frac{d\omega}{\omega - x} \mp i\pi\delta(\omega - x) \\ &= \begin{cases} \ln \frac{x - \omega_D}{x} & \text{for } x > \omega_D \text{ or } x < 0 \\ \ln \frac{\omega_D - x}{x} \mp i\pi & \text{for } 0 < x < \omega_D \end{cases} \end{aligned} \quad (3.30)$$

Combining the contributions from \mathcal{C}_1 and \mathcal{C}_2 into a single integral and evaluating \mathcal{C}_3 and \mathcal{C}_4 for the outlying poles as in the finite case we get just the result (3.24).

Eq. (3.24) is the exact amplitude that an initially excited two-level atom is still excited at time t , when the atom is coupled arbitrarily strongly but equally to all phonon modes of a perfect infinite monatomic one-dimensional lattice obeying the dispersion relation $\omega_k = c|k|$. Let us study (3.24) in detail.

The lineshape

$$\mathcal{L}(\omega) = \frac{\Gamma/2\pi}{(\omega - \Delta + \frac{\Gamma}{2\pi} \ln \frac{\omega_D - \omega}{\omega})^2 + (\frac{\Gamma}{2})^2} \quad (3.31)$$

is to a first approximation a Lorentzian of width Γ centered about frequency $\omega = \Delta$. This is a good approximation as long as the lineshape is narrow and well within the phonon band $0 < \omega < \omega_D$. This is clear because the factor

$$\ln \frac{\omega_D - \omega}{\omega}$$

which makes $\mathcal{L}(\omega)$ non-Lorentzian becomes large only when $\omega \approx 0$ or $\omega \approx \omega_D$. If the lineshape has already fallen off at these frequencies then this term is negligible and $\mathcal{L}(\omega)$ is approximately Lorentzian. Fig. 3.4a shows an example where $\mathcal{L}(\omega)$ is almost Lorentzian and hence leads to almost exponential decay. If the coupling Γ is large, then the lineshape is broad and the outlying modes ω'_0 and $\omega'_{N/2}$ also become excited to some extent. An example of this is shown in Fig. 3.4b. To understand the time evolution in this case we must use some results from Fourier integral theory: If we Fourier transform some given lineshape $\mathcal{L}(\omega)$, then the interior of that lineshape gives contributions which decay in time faster than any power of t . The endpoints $\omega_{\text{e.p.}}$ of the lineshape give contributions that decay like $\frac{d}{d\omega} \mathcal{L}(\omega_{\text{e.p.}}) e^{-i\omega_{\text{e.p.}}t} / t$. And simple poles, of course, give non-decaying contributions.

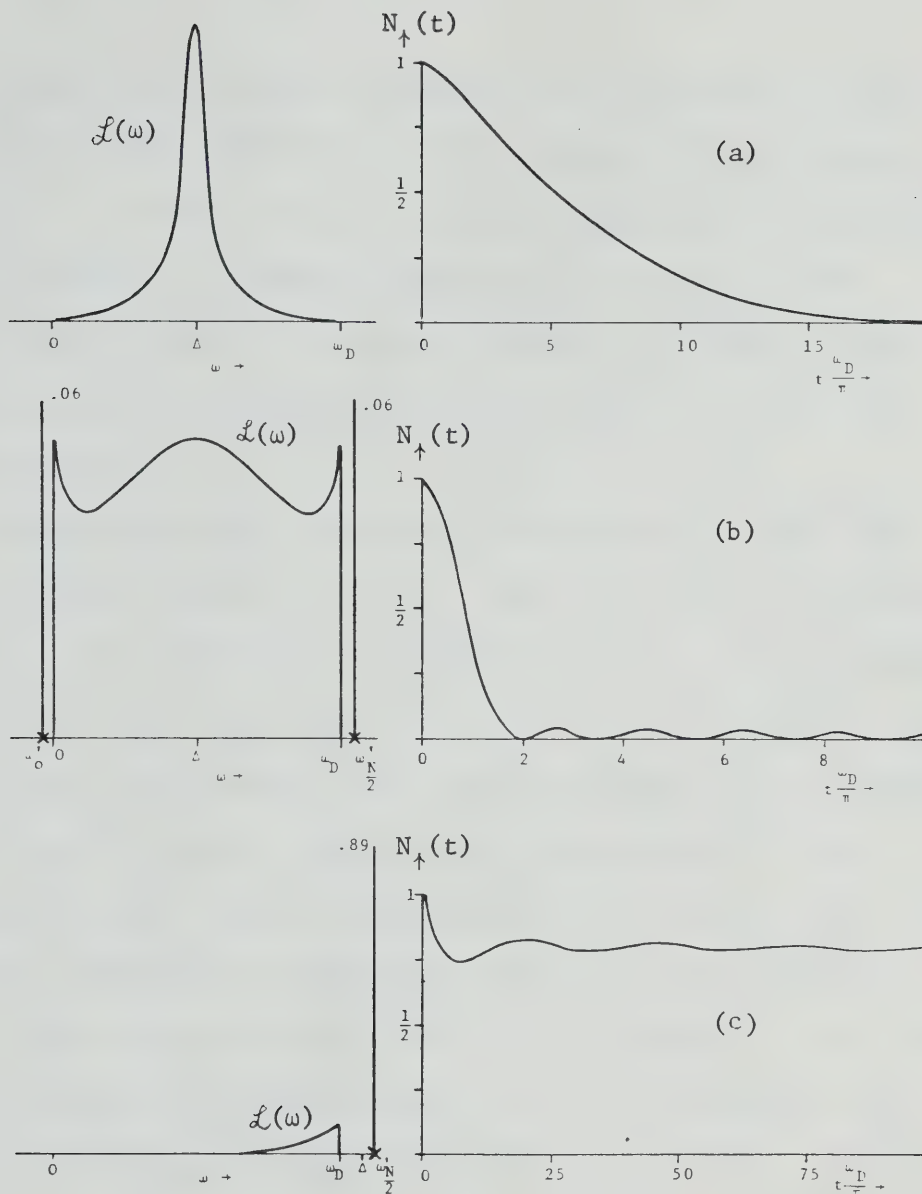


Fig. 3.4 The lineshapes and corresponding decays of an excited two-level atom under various conditions: (a) $\Gamma = .06\omega_D$, $\Delta = .5\omega_D$; lineshape is narrow and well within phonon band $0 < \omega < \omega_D$. (b) $\Gamma = .6\omega_D$, $\Delta = .5\omega_D$; lineshape is so wide that both outlying modes ω'_0 and $\omega'_{N/2}$, also become excited. (c) $\Gamma = .06\omega_D$, $\Delta = 1.05\omega_D$; The two-level atom frequency Δ lies above the phonon band so only $\omega'_{N/2}$ mode and upper edge of the phonon band become excited. (The number above the outlying pole is the amplitude of that mode.)

Thus in Fig. 3.4b there are three types of decay: (1) an exponential type decay due to the interior of the line-shape, (2) a slower power-law decay with oscillations due to the frequency ω'_0 beating against ω_D and $\omega'_{N/2}$, and frequencies ω'_0 and $\omega = 0$ beating against ω_D , and (3) beating of the outlying modes ω'_0 and $\omega'_{N/2}$ against each other with no decay.

A third possible situation occurs when Δ lies outside the phonon band $0 < \omega < \omega_D$. Then the atom is unlikely to decay if the coupling Γ is not too strong. An example is shown in Fig. 3.4c where $\Delta = 1.05 \omega_D$ is just above the phonon band. We see that the isolated mode $\omega'_{N/2}$ is highly excited and the upper edge of the phonon band is only slightly excited. The contribution to $N_\uparrow(t)$ from the outlying pole gives the probability that the atom does not decay. The slight oscillation in $N_\uparrow(t)$ is due to the beating of the mode ω_D (which decays like $1/t$) against the isolated mode $\omega'_{N/2}$ at beat frequency $\omega_{\text{beat}} = (\omega'_{N/2} - \omega_D)/2 = \omega_D/25$.

Let us discuss the significance of the outlying poles at ω'_0 and $\omega'_{N/2}$. We have seen that these poles allow for the possibility that the atom does not decay when the atom frequency Δ lies outside the phonon band. To be specific assume that $\Delta > \omega_D$. Then from Fig. 3.2 we see that $\omega'_0 \approx 0$, and $\omega'_{N/2}$ is given by the solution of the equation

$$\omega'_{N/2} = \Delta - \frac{\Gamma}{2\pi} \ln\left(\frac{\omega'_{N/2} - \omega_D}{\omega'_{N/2}}\right) \approx \Delta - \frac{\Gamma}{2\pi} \ln\left(\frac{\Delta - \omega_D}{\Delta}\right) \quad (3.22)$$

Thus the mode $\omega'_{N/2}$ can be identified with the uncoupled atom mode Δ but shifted slightly. Because the frequency $\omega'_{N/2}$ lies outside the phonon band, its corresponding wave-number is imaginary, so $\omega'_{N/2}$ represents a mode localized in space. In field theory language the two-level atom surrounds itself with a local cloud of virtual phonons which shift slightly the atom's energy Δ . Because $\omega'_{N/2}$ is a single isolated mode outside the phonon band, it does not decay.

When Δ lies inside the phonon band $0 < \omega < \omega_D$, then as we see in Fig. 3.2, the two outlying poles move very close to the endpoints of the phonon band and lose their significance as non-decaying modes. Eq. (3.24) also shows that their amplitude then becomes small. A band of phonon modes near frequency Δ' becomes excited with a Lorentzian-like amplitude

$$\mathcal{L}(\omega) = \frac{\Gamma/2\pi}{(\omega - \Delta')^2 + (\frac{\Gamma}{2})^2} \quad , \quad (3.33)$$

where

$$\Delta' = \Delta - \frac{\Gamma}{2\pi} \ln \frac{\omega_D - \Delta}{\Delta} \quad , \quad (3.34)$$

(Here in the argument of the logarithm we have replaced $\omega \rightarrow \Delta$.) and the energy of the excited atom goes irreversibly and completely into the infinite number of degrees of freedom of the phonon continuum.

Three Dimensional Crystal

For completeness let us study the case of a general 3-dimensional crystal. Although the analysis for a finite 3-D crystal cannot be done analytically, the analysis for an infinite 3-D crystal follows that for an infinite 1-D crystal with the only change being that the phonon density of states is different. Thus the Fourier transform of $S^-(t)$, namely

$$\mathcal{S}^-(x) = \frac{iS^-(0)}{x - \Delta - \sum_{\vec{k}} \frac{g^2}{x - \omega_{\vec{k}}}} , \quad (3.35)$$

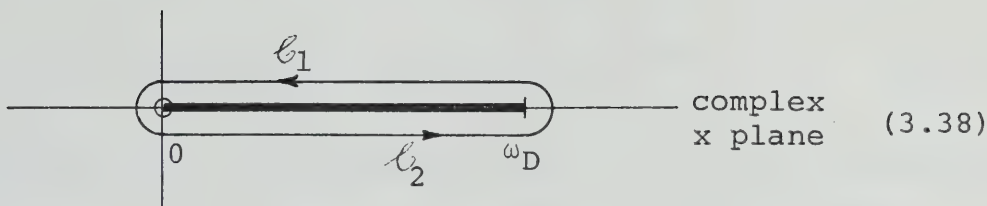
becomes

$$\mathcal{S}^-(x) = \frac{iS^-(0)}{x - \Delta + g^2 \Omega \int_0^{\omega_D} \frac{D(\omega) d\omega}{\omega - x}} , \quad (3.36)$$

where we have replaced

$$\frac{1}{\Omega} \sum_{\vec{k}} \rightarrow \int_0^{\omega_D} D(\omega) d\omega . \quad (3.37)$$

$D(\omega) d\omega$ is the (for now unspecified) phonon density of states per unit volume, and Ω is the volume of the crystal. As in the 1-D case $\mathcal{S}^-(x)$ has branch points at $x=0$ and $x=\omega_D$. (We ignore any isolated outlying poles which it may have under the assumption that Δ lies well inside the phonon band.) Thus we may Fourier transform $\mathcal{S}^-(x)$ using the contour shown:



Along this contour we decompose the integrand in the denominator of (3.36) into principal and imaginary parts according to Eq. (3.29). Combining the contributions from ℓ_1 and ℓ_2 into a single integral we get

$$S^-(t) = -\frac{1}{2\pi} \int_0^{\omega_D} dx e^{-ixt} \{-\mathcal{J}^-(x+i\epsilon) + \mathcal{J}^-(x-i\epsilon)\}, \quad (3.39)$$

where

$$\mathcal{J}^-(x \pm i\epsilon) = \frac{iS^-(0)}{x - \Delta'(x) \pm \frac{i}{2} \Gamma(x)}, \quad (3.40)$$

with

$$\Delta'(x) = \Delta - g^2 \mathcal{P} \int_0^{\omega_D} \frac{d\omega D(\omega) \Omega}{\omega - x}, \quad (3.41)$$

and

$$\Gamma(x) = 2\pi g^2 D(x) \Omega. \quad (3.42)$$

Since only a narrow range of frequencies near $x = \Delta$ (which we assume is inside the phonon band) is important in (3.39) we may to a first approximation replace $\Delta'(x) \rightarrow \Delta'(\Delta) \equiv \Delta'$ and $\Gamma(x) \rightarrow \Gamma(\Delta) \equiv \Gamma$ and extend the limits of integration from $-\infty$ to ∞ . Thus we get

$$S^-(t) = \frac{\Gamma}{2\pi} S^-(0) \int_{-\infty}^{\infty} \frac{dx e^{-ixt}}{(x - \Delta')^2 + (\frac{\Gamma}{2})^2} = S^-(0) e^{-i\Delta' t} e^{-\frac{\Gamma}{2} t} \quad (3.43)$$

so that

$$N_{\uparrow}(t) = \langle i | S^+(t) S^-(t) | i \rangle = N_{\uparrow}(0) e^{-\Gamma t} \quad (3.44)$$

i.e. the excited atom decays at rate $\Gamma = 2\pi g^2 D(\Delta) \Omega$ which is the same rate (2.51) found by first order perturbation theory.

3.3 Notes on the General Theory of Decay of Unstable Quantum Systems

We wish to present a short summary of the results that we found in §§3.1 and 3.2 on the decay of an excited ion in the context of the theory of dissipation in quantum mechanics. At some time $t < 0$ we prepare the electron-phonon system in a stationary eigenstate of the uncoupled Hamiltonian $\mathcal{H}_0 = \mathcal{H}_{\text{ion}} + \mathcal{H}_{\text{ph}}$, namely with an ion in the upper level and no phonons present. At time $t = 0$ we switch on the electron-phonon interaction (Hamiltonian \mathcal{H}'). Since the initial state is no longer an eigenstate of the total Hamiltonian $\mathcal{H} = \mathcal{H}_0 + \mathcal{H}'$ the system evolves according to the total Hamiltonian to some new state. We are interested in the probability that the system remains in the initial state, i.e. that the atom is still excited.

We found that there were many analogies with the classical theory of coupled harmonic oscillators. For example in the case of an initially excited two-level atom coupled to a finite number of discrete phonon modes, we found that the energy of the decaying atom is transferred to the finite number of phonon modes and, in a finite time,

is transferred back to the atom. This time is just the time it takes for a phonon to transit the crystal.

Phenomena similar to this have been observed in spin flip experiments⁴⁸. In the case of a continuum of phonon modes (infinite crystal) the excited atom simply decays and is never re-excited because in this case the energy is transferred to an infinite number of degrees of freedom.

The decay of the two-level atom is for the most part exponential (assuming that Δ is well inside the phonon continuum). This is indicative of a system that does not depend on its previous history, i.e. with no memory. However, via perturbation theory, we found the result (for finite and infinite crystals) that the excited atom decays initially like

$$N_{\uparrow}(t) = N_{\uparrow}(0) \left(1 - \sum_k g_k^2 t^2\right),$$

i.e. with zero slope. This is a very general result⁴⁹ in quantum mechanics and assumes only that the energy in the initial state is finite. On the other hand for very large times $N_{\uparrow}(t)$ must always exhibit a power law decay $\propto 1/t$ due to the sharp cutoff of the Lorentzian by the finite extent of the phonon band as explained after Eq. (3.31).

In the rest of the thesis we will ignore these deviations from exponential decay and assume that $S^-(t)$ can be approximated by (3.43).

We would like to point out that our theory and results are very similar to those of Weisskopf and Wigner⁴⁴ on the theory of spontaneous decay. For atomic and nuclear systems Razavy and Henley⁵⁰ have similarly obtained exact solutions for the γ decay of spinless bound particles. Also, Senitzky⁴⁵ has studied various models for the decay of harmonic oscillators or two-level atoms due to generalized loss mechanisms.

CHAPTER 4

DERIVATION OF PHENOMENOLOGICAL RATE EQUATIONS FOR THE PHONON BOTTLENECK

4.1 Derivation

Now that we have studied the interaction of the phonon field with a single two-level atom, let us proceed to the general case of the interaction of the field with many atoms. We begin by rewriting the linearized, coupled equations of motion (2.64) for the phonons and atoms, namely

$$i\dot{b}_{\tilde{k}} = \omega_{\tilde{k}} b_{\tilde{k}} + \sum_{\tilde{r}} g_{\tilde{k}} S_{\tilde{r}}^{-} e^{-i\tilde{k} \cdot \tilde{r}}, \quad (4.1a)$$

$$i\dot{S}_{\tilde{r}}^{-} = \Delta S_{\tilde{r}}^{-} + \sum_{\tilde{k}} g_{\tilde{k}} b_{\tilde{k}} e^{+i\tilde{k} \cdot \tilde{r}}. \quad (4.1b)$$

To recapitulate $b_{\tilde{k}}$ is the annihilation operator for a phonon of momentum \tilde{k} and $S_{\tilde{r}}^{-}$ is the lowering operator for the atom at site \tilde{r} . We are interested in evaluating quantities such as the probability that the \tilde{r}^{th} atom is excited at time t , namely

$$N_{\tilde{r}}^{\uparrow}(t) = \langle i | S_{\tilde{r}}^{+}(t) S_{\tilde{r}}^{-}(t) | i \rangle, \quad (4.2)$$

and the number of phonons in mode \tilde{k} at time t , namely

$$n_{\tilde{k}}^{\text{ph}}(t) = \langle i | b_{\tilde{k}}^{\dagger}(t) b_{\tilde{k}}(t) | i \rangle. \quad (4.3)$$

$|i\rangle$ denotes the initial state of the system at time $t=0$. To solve Eqs. (4.1) we again use the method of Fourier

transforms. We define the Fourier transforms of $b_{\tilde{k}}(t)$ and $S_{\tilde{r}}^-(t)$ as

$$\begin{aligned} B_{\tilde{k}}(x) &\equiv \mathcal{F}[b_{\tilde{k}}(t)] \quad , \\ \mathcal{J}_{\tilde{r}}^-(x) &\equiv \mathcal{F}[S_{\tilde{r}}^-(t)] \quad , \end{aligned} \quad (4.4)$$

respectively (see Eqs. (3.2,3) for details), and Fourier transform Eqs. (4.1) to get

$$B_{\tilde{k}}(x) = \frac{ib_{\tilde{k}}(0)}{x - \omega_{\tilde{k}}} + \frac{g}{x - \omega_{\tilde{k}}} \sum_{\tilde{r}'} e^{-ik \cdot \tilde{r}'} \mathcal{J}_{\tilde{r}'}^-(x) \quad , \quad (4.5a)$$

$$\mathcal{J}_{\tilde{r}}^-(x) = \frac{iS_{\tilde{r}}^-(0)}{x - \Delta} + \frac{g}{x - \Delta} \sum_{\tilde{k}} e^{ik \cdot \tilde{r}} B_{\tilde{k}}(x) \quad . \quad (4.5b)$$

We have dropped the subscript k on the coupling g_k assuming that the coupling is approximately constant over the range of frequencies of importance near resonance. We eliminate $B_{\tilde{k}}(x)$ from Eq. (4.5b) for $\mathcal{J}_{\tilde{r}}^-(x)$ by breaking the summation over \tilde{r}' in (4.5a) into two parts, namely

$$\sum_{\tilde{r}'} e^{-ik \cdot \tilde{r}'} \mathcal{J}_{\tilde{r}'}^-(x) = e^{-ik \cdot \tilde{r}} \mathcal{J}_{\tilde{r}}^-(x) + \sum_{\tilde{r}' \neq \tilde{r}} e^{-ik \cdot \tilde{r}'} \mathcal{J}_{\tilde{r}'}^-(x) \quad , \quad (4.6)$$

and plugging (4.5a) into (4.5b). Thus Eq. (4.5b) is replaced by

$$\begin{aligned} \mathcal{J}_{\tilde{r}}^-(x) &= \frac{iS_{\tilde{r}}^-(0)}{x - \Delta - \sum_{\tilde{k}} \frac{g^2}{x - \omega_{\tilde{k}}}} + \frac{g}{x - \Delta - \sum_{\tilde{k}'} \frac{g^2}{x - \omega_{\tilde{k}'}}} \sum_{\tilde{k}} e^{ik \cdot \tilde{r}} \frac{ib_{\tilde{k}}(0)}{x - \omega_{\tilde{k}}} \\ &+ \sum_{\tilde{r}' \neq \tilde{r}} \frac{g^2}{x - \Delta - \sum_{\tilde{k}'} \frac{g^2}{x - \omega_{\tilde{k}'}}} \sum_{\tilde{k}} \frac{e^{ik \cdot (\tilde{r} - \tilde{r}')}}{x - \omega_{\tilde{k}}} \mathcal{J}_{\tilde{r}'}^-(x) \quad . \end{aligned} \quad (4.7)$$

Let us discuss this equation. Notice that the first term on the right hand side of (4.7) depends only on the \tilde{r}^{th} atom and the third term depends on all atoms but the \tilde{r}^{th} atom. From our studies of Chapter 3 we know that the first term on the right hand side of (4.7) describes the spontaneous decay of the \tilde{r}^{th} atom (if it is initially excited). Similarly, the second term on the right hand side depends on the initially present phonons, and it evidently describes the excitation of the (unexcited) \tilde{r}^{th} atom by these phonons. Finally, by iterating (4.7) we see that the third term describes the indirect excitation of atom \tilde{r} by phonons coming from other atoms \tilde{r}' (which either were themselves originally excited at time $t=0$ or became excited by yet other atoms). The implicit 'integral' equation (4.7) is of course very difficult to solve exactly except in special cases. We shall consider these cases in Chapter 6.

For now we simply derive from Eqs. (4.5a) and (4.7) a set of rate equations describing the number of excited atoms and the number of phonons present in the coupled system. To do this we imagine that at some instant of time, call it $t=0$, the system is in some eigenstate $|i\rangle$ of the uncoupled Hamiltonian, with several specified excited atoms and phonons present. We solve Eqs. (4.5a) and (4.7) and find the state of the system a short time Δt later. Since the time $t=0$ is arbitrary, we can now repeat the argument with $t=\Delta t$. Continuing in a stepwise

manner we can find the complete time evolution of the system.

From our work of Chapter 3, we actually know how to find the time evolution of the \tilde{r}^{th} atom due to the first term on the right hand side of (4.7) (the spontaneous decay term) for all times, not just a short time Δt . We shall see shortly that this is also true for the second (excitation by phonons) term. The trouble comes from the third term because it makes Eq. (4.7) non-local in space and time: It says that what happens to the \tilde{r}^{th} atom at time t depends on what happened to the other atoms at points \tilde{r}' of the system at all previous times. However if we choose the time-step Δt for the rate equations shorter than the time $t = |\mathbf{r}-\mathbf{r}'|/c$ that it takes for a phonon to travel from atom \tilde{r}' to atom \tilde{r} then this term cannot contribute to $\mathcal{J}_{\tilde{r}}^{-}(\mathbf{x})$ at time Δt and we may drop it. Thus we may replace (4.7) by the equation

$$\mathcal{J}_{\tilde{r}}^{-}(\mathbf{x}+i\varepsilon) = \frac{iS_{\tilde{r}}^{-}(0)}{\mathbf{x} - \Delta' + \frac{i}{2T_1}} + \frac{g}{\mathbf{x} - \Delta' + \frac{i}{2T_1}} \sum_{\tilde{k}} e^{i\tilde{k} \cdot \tilde{r}} \frac{ib_{\tilde{k}}(0)}{\mathbf{x} - \omega_{\tilde{k}}} . \quad (4.8)$$

In Eq. (4.8) we have used the simpler expression (3.40) with $\Delta'(\mathbf{x}) \rightarrow \Delta'$ and $\Gamma(\mathbf{x}) \rightarrow \Gamma$ for the 'propagator' $\mathcal{J}_{\tilde{r}}^{-}(\mathbf{x})$ of a single atom in a phonon field. ($T_1 = 1/\Gamma$ is the lifetime of a single atom.) Eq. (4.8) is now a local equation. It says that the probability amplitude for the \tilde{r}^{th} atom being excited depends only on whether or not the \tilde{r}^{th} atom

was initially excited and on what phonons were initially present near that atom. Thus it cannot describe the diffusion of excitations. (We will remedy this shortcoming presently.) In keeping with this restriction we assume for now that the system is spatially uniform.

We proceed and derive first the rate equation for the phonons. Plugging Eq. (4.8) for $\mathcal{J}_{\vec{r}}^-(x)$ into Eq. (4.5a) for $B_{\vec{k}}(x)$ and Fourier transforming we find that

$$b_{\vec{k}}(t) = e^{-i\omega_{\vec{k}}t} \left\{ b_{\vec{k}}(0) + g \sum_{\vec{r}} e^{-i\vec{k} \cdot \vec{r}} S_{\vec{r}}^-(0) \frac{1 - e^{\frac{i(\omega_{\vec{k}} - \Delta')t}{2T_1}}}{\omega_{\vec{k}} - \Delta' + \frac{i}{2T_1}} - g^2 \sum_{\vec{r}} b_{\vec{k}}(0) \left[\frac{1 - e^{\frac{i(\omega_{\vec{k}} - \Delta')t}{2T_1}}}{(\omega_{\vec{k}} - \Delta' + \frac{i}{2T_1})^2} + \frac{it}{\omega_{\vec{k}} - \Delta' + \frac{i}{2T_1}} \right] \right\} \quad (4.9)$$

Let us define the following quantities:

$\Omega \equiv$ volume of the optically excited region containing the two-level atoms,

$N^* \equiv \frac{1}{\Omega} \sum_{\vec{r}} 1$ is the total density per cm^3 of two-level atoms,

$N_2(t) \equiv \frac{1}{\Omega} \sum_{\vec{r}} \langle i | S_{\vec{r}}^+(t) S_{\vec{r}}^-(t) | i \rangle$ is the density per cm^3 of excited atoms,

$D(\omega) d\omega$ is the density of phonon modes per cm^3 in frequency interval $d\omega$ (recall that $\frac{1}{\Omega} \sum_{\vec{k}} \rightarrow \int D(\omega_{\vec{k}}) d\omega_{\vec{k}}$). We shall henceforth assume that $D(\omega) \approx D(\Delta')$ for all frequencies near resonance.

$n_{ph}(\omega_k) d\omega_k \equiv \langle i | b_k^\dagger(t) b_k(t) | i \rangle D(\omega_k) d\omega_k$ is the density of phonons per cm^3 in frequency interval $d\omega_k$,

$$f(\omega) d\omega \equiv \frac{g^2 D(\Delta) \Omega}{(\omega - \Delta')^2 + (\frac{1}{2T_1})^2} d\omega \quad \text{is the Lorentzian}$$

emission spectrum of an atom, normalized to unity, i.e.

$$\int_{-\infty}^{\infty} f(\omega) d\omega = 1.$$

Using these definitions we can derive from Eq. (4.9) the rate of change of the density of phonons per cm^3 in frequency interval $d\omega$ at time t , namely

$$\begin{aligned} \frac{d}{dt} n_{ph}(\omega, t) d\omega = & f(\omega) d\omega N_2(0) \Gamma_1(\omega, t) - f(\omega) d\omega \frac{N^*}{D(\Delta')} n_{ph}(\omega, 0) \\ & \times \Gamma_2(\omega, t) \end{aligned} \quad (4.10)$$

where

$$\Gamma_1(\omega, t) = \frac{d}{dt} (1 + e^{-t/T_1} - 2e^{-t/2T_1} \cos(\omega - \Delta')t), \quad (4.11)$$

and

$$\Gamma_2(\omega, t) = \frac{d}{dt} \left\{ \frac{t}{T_1} + \left[\frac{\omega - \Delta' + \frac{i}{2T_1}}{\omega - \Delta' - \frac{i}{2T_1}} (1 - e^{i(\omega - \Delta')t} e^{-t/2T_1}) + c.c. \right] \right\} \quad (4.12)$$

are rates having the units sec^{-1} . The first term on the right hand side of (4.10) represents the production of a spectrum of phonons due to the decay of initially excited atoms. The second term represents the resonance absorption of the phonons initially present.

Note that the emission and absorption rates of the phonons are actually time- as well as frequency-dependent.

For example at time $t \approx 0$ the phonon production rate due to decaying atoms is

$$\frac{d}{dt} n_{ph}(\omega, t) = N_2(0) 2t g^2 D(\Delta') , \quad (4.13)$$

which is frequency independent because the frequency dependence of $\Gamma_1(\omega, t)$ exactly cancels that of the Lorentzian $f(\omega)$. Thus phonons of all frequencies are produced at the same rate for time $t \approx 0$ in accordance with Heisenberg's uncertainty relation $\Delta E \cdot \Delta t \gtrsim \hbar$. Notice also that the rate actually vanishes at $t=0$.

For finite times $t > 0$ $\Gamma_1(\omega, t)$ is a rapidly varying function of frequency. Experimentally this variation is on too fine a scale to be observable, and one sees only $\Gamma_1(\omega, t)$ averaged over the entire emission spectrum. If we perform this average we find that

$$\begin{aligned} \langle \Gamma_1(\omega, t) \rangle &\equiv \frac{\int f(\omega) \Gamma_1(\omega, t) d\omega}{\int f(\omega) d\omega} = \frac{d}{dt} (1 - e^{-t/T_1}) \\ &= \frac{1}{T_1} e^{-t/T_1} . \end{aligned} \quad (4.14)$$

For small times this gives the observed rate $1/T_1$ for spontaneous decay. For larger times $\langle \Gamma_1(\omega, t) \rangle$ vanishes simply because the supply of excited atoms is used up as the decay proceeds. To avoid the latter, we replace in the rate equation

$$\Gamma_1(\omega, t) \rightarrow 1/T_1 \quad (4.15)$$

for times $t \gtrsim T_1$.

Similar arguments show that this holds also for $\Gamma_2(\omega, t)$, namely

$$\langle \Gamma_2(\omega, t) \rangle \rightarrow 1/T_1 \quad (4.16)$$

for times $t \gtrsim T_1$. Thus we find that over the coarse-grained time scale of order T_1 the rate of change of the phonon density at time $t=0$ is given by

$$\frac{d}{dt} n_{ph}(\omega, t=0) = f(\omega) d\omega \frac{N_2(t=0)}{T_1} - f(\omega) d\omega \frac{N^*}{D(\Delta')} \cdot \frac{n_{ph}(\omega, t=0)}{T_1} . \quad (4.17)$$

To derive the rate equation for the density of excited atoms we simply use the fact that the system Hamiltonian conserves the number of excitations

$$\sum_r S_r^+(t) S_r^-(t) + \sum_k b_k^\dagger(t) b_k(t) = \text{constant} ; \quad (4.18)$$

or differentiating,

$$\frac{d}{dt} N_2 + \frac{d}{dt} \int d\omega n_{ph}(\omega) = 0 . \quad (4.19)$$

With Eq. (4.17) this implies that

$$\frac{d}{dt} N_2(t=0) = -\frac{N_2(t=0)}{T_1} + \int d\omega (f(\omega) \frac{N^*}{D(\Delta') T_1}) n_{ph}(\omega, t=0) . \quad (4.20)$$

To this point we have tacitly assumed spatial uniformity. The phonons were non-local plane waves extending over the crystal and we replaced $\frac{1}{\Omega} \sum_r \langle S_r^+ S_r^- \rangle$ by the average density N_2 . Let us now assume that phonons are absorbed or emitted locally at the position of the

atom where the interaction takes place and allow a small amount of spatial non-uniformity in the quantities n_{ph} and N_2 . Then Eqs. (4.17) and (4.20) are still locally valid.

With the following modification they are valid everywhere:

We add a phenomenological diffusion term $\mathcal{D}(\omega) \nabla^2 n_{ph}(\underline{r}, \omega, t)$ to the right hand side of the phonon equation because the phonons tend to diffuse from regions of high to regions of low phonon density. For the frequency dependent diffusion constant $\mathcal{D}(\omega)$ we choose the classical expression

$$\mathcal{D}(\omega) = \frac{\Lambda(\omega) c}{3} = \frac{c}{3\alpha(\omega)} \quad (4.21)$$

where $\Lambda(\omega)$ is the mean-free-path,

$$\alpha(\omega) \equiv \frac{1}{\Lambda(\omega)} = \frac{N^*}{D(\Delta) c T_1} f(\omega) \quad (4.22)$$

is the absorption coefficient per cm of phonons of angular frequency ω , and c is the average speed of sound.

If we now assume that these equations are valid for all times we get the equations in the final form

$$\left\{ \begin{aligned} \frac{\partial}{\partial t} n_{ph}(\underline{r}, \omega, t) d\omega &= f(\omega) d\omega \frac{N_2(\underline{r}, t)}{T_1} - n_{ph}(\underline{r}, \omega, t) d\omega \alpha(\omega) c \\ &\quad + \mathcal{D}(\omega) \nabla^2 n_{ph}(\underline{r}, \omega, t) d\omega , \\ \frac{\partial}{\partial t} N_2(\underline{r}, t) &= - \frac{N_2(\underline{r}, t)}{T_1} + \int d\omega n_{ph}(\underline{r}, \omega, t) \alpha(\omega) c . \end{aligned} \right. \quad (4.23)$$

4.2 Comparison with Pauli's Derivation of the Master Equation

It is instructive to compare the assumptions that went into our derivation of the rate equations (4.17) and (4.20) with those that went into the derivation of Pauli's master equation or Boltzmann's equation^{51,52}.

In all cases an important assumption is the existence of distinguishable time scales, an idea first introduced by Bogoliubov⁵³. The first characteristic time T_1 is the order of the duration of the interaction of a phonon with a Cr^{3+} ion. For times $t < T_1$ we saw that in our rate equations the rates $\Gamma_1(\omega, t)$ and $\Gamma_2(\omega, t)$ change very rapidly and a detailed quantum description of the system is needed. In the kinetic regime, i.e. for times $t > T_1$ the rapid variations of $\Gamma_1(\omega, t)$ and $\Gamma_2(\omega, t)$ can be averaged out leading to the kinetic Eqs. (4.17) and (4.20). The second characteristic time is the mean-free-time

$$T_2 = \Lambda(\omega_0)/c = \frac{1}{\alpha(\omega_0)c} \quad (4.24)$$

between interactions of the resonant phonons with Cr^{3+} ions. For times $t \gg T_2$ the resonant phonons will have interacted with the Cr^{3+} ions several times and reached a local equilibrium. Thus in this hydrodynamic regime Eqs. (4.17) and (4.20) are locally valid, and it is sufficient to add a hydrodynamic diffusion term to get a set of equations (4.23) which are globally valid.

In the case of the Boltzmann equation, the assumption that $T_1 \ll T_2$ means that it is restricted to the description of a dilute gas. In our case, using Eq.(4.24), we see that it means that the density of Cr^{3+} ions in the \bar{E} state must be less than the density of phonon modes on resonance, i.e.:

$$N^* < D(\Delta) \Delta\omega_0 \quad (4.25)$$

where $\Delta\omega_0 = 1/T_1$ is the halfwidth of the resonance. This restricts us to rather low densities $N^* < 10^{16} \text{ cm}^{-3}$. However since the Boltzmann equation works well at much higher densities than one would suspect, we hope the same holds for our rate equations.

To derive the Boltzmann equation a second assumption is required, namely the Stosszahlansatz, i.e. the assumption that each collision destroys the correlations that have built up between the two colliding particles during the time since the last collision. This allows a dynamical description of the system in terms of the one-particle distribution function f_1 alone, which introduces irreversibility. In our case and in the case of Pauli's master equation the Stosszahlansatz allows a description of the system in steps of time Δt where $T_1 < \Delta t < T_2$. In each time step the system begins in an eigenstate of the uncoupled Hamiltonian without any correlations (e.g. in our system only the number of excited atoms and phonons is specified.

This is a frequent criticism of Pauli's derivation of the master equation.) In the case of the master equation, the choice $T_1 < \Delta t < T_2$ allows one to find the transition rates using first order perturbation theory. In our case it allows us to drop the non-local term in (4.7). In both cases the result is a set of first order differential equations which describe the irreversible evolution of the system.

These parallels between the master equation and the bottleneck equations are summarized in Table 4.1.

In conclusion we emphasize that the bottleneck equations (4.23) are valid for densities N^* low enough that the condition $T_1 < T_2(N^*)$ holds. At higher densities where $T_2(N^*) < T_1$ we expect that we must include the non-local term of (4.7) in the rate equations, yielding a new effective lifetime T_1 of a local cooperative group of two-level atoms.

(Schrodinger picture)

(Heisenberg picture)

Construct the Hamiltonian for the system in the form:

$$\mathcal{H} = \mathcal{H}_O + v \quad \mathcal{H} = \{\mathcal{H}_O = \mathcal{H}_{ion} + \mathcal{H}_{ph}\} + \left\{ \begin{matrix} \text{interaction} \\ \text{energy term} \end{matrix} \right\}$$

Specify some initial state of the uncoupled system at time $t = 0$

Statevector $|j\rangle$

Operators $S_I^-(t=0), b_k(t=0),$ etc.

given the time evolution of the uncoupled system:

$$e^{-i\mathcal{H}_O t} |j\rangle = e^{-i\epsilon_j t} |j\rangle \quad i\mathcal{H}_O t \left\{ S_I^-(t=0) \right\} e^{-i\mathcal{H}_O t} = \left\{ S_I^-(t=0) e^{-i\Delta t} \right\} e^{-i\omega_k t} = \left\{ b_k(t=0) e^{-i\omega_k t} \right\}$$

Find the time evolution of the coupled system:

$$e^{-i\mathcal{H} t} |j\rangle = \sum_i \gamma_{ij}(t) e^{-i\epsilon_i t} |i\rangle \quad S_I^-(t) = e^{i\mathcal{H} t} S_I^-(0) e^{-i\mathcal{H} t} = S_I^-(0) e^{-i\Delta' t} e^{-t/2T_1} + \dots$$

Find the probability that the system has evolved to some state:

$$\begin{aligned} \text{e.g. State } i: & \Rightarrow \text{rate } \underbrace{W_{ij}}_{\substack{\text{e.g. State with } i^{\text{th}} \text{ atom excited:} \\ S_I^+(t) S_I^-(t) = S_I^+(0) S_I^-(0) e^{-t/T_1} \Rightarrow \text{rate } 1/T_1}} \\ P_i(t) = |\gamma_{ij}(t)|^2 &= \frac{2\pi}{\hbar} |\langle i|V|j\rangle|^2 \delta(\epsilon_i - \epsilon_j) t \end{aligned}$$

We have used 1st order perturbation theory and the Fermi Golden Rule formula for the long time limit. Differentiating, evaluating at time $t=0$, and considering evolution from all initial states gives the equations:

$$\frac{dP_i}{dt} = \sum_j (W_{ij} P_j - W_{ji} P_i)$$

supplemental condition: $\sum_i P_i = 1$

We have dropped the non-local terms and have used rates valid for times $t \geq T_1$.

Differentiating, evaluating at time $t=0$, and considering evolution from all initial states gives the equations:

$$\left\{ \begin{aligned} \frac{d}{dt} N_2 &= \int d\omega (\alpha(\omega)c) n_{ph}(\omega) - \frac{N_2}{T_1} \\ \frac{d}{dt} n_{ph}(\omega) &= \frac{f(\omega)}{T_1} N_2 - (\alpha(\omega)c) n_{ph}(\omega) \end{aligned} \right.$$

supplemental condition: $N_2 + \int d\omega n_{ph}(\omega) = \text{constant}$

At this stage the equations hold only for small times. Using a repeated random phase approximation or Stosszahlansatz implies that they hold for all times.

Table 4.1 Comparison of Pauli's master equation with phonon bottleneck equations.

CHAPTER 5

SOLUTIONS OF THE RATE EQUATIONS

5.1 The Solution and Comparison with Experiment

In this chapter we solve the rate equations (4.23) describing the time evolution of the coupled system of phonons and atomic two-level states of excited Cr^{3+} ions. We begin by rewriting Eqs. (4.23) in a notation more in line with previous works on the phonon bottleneck, namely

$$\left\{ \begin{aligned} \frac{\partial}{\partial t} n_{\text{ph}}(\underline{r}, \nu, t) d\nu &= f(\nu) d\nu \frac{N_2(\underline{r}, t)}{T_1} - n_{\text{ph}}(\underline{r}, \nu, t) d\nu \alpha(\nu) c \\ &+ \mathcal{Q}(\nu) \nabla^2 n_{\text{ph}}(\underline{r}, \nu, t) d\nu , \end{aligned} \right. \quad (5.1a)$$

$$\left\{ \begin{aligned} \frac{\partial}{\partial t} N_2(\underline{r}, t) &= -\frac{N_2(\underline{r}, t)}{T_1} + \int d\nu n_{\text{ph}}(\underline{r}, \nu, t) \alpha(\nu) c . \end{aligned} \right. \quad (5.1b)$$

$n_{\text{ph}}(\underline{r}, \nu, t) d\nu$ is the density of phonons per cm^3 in frequency interval $d\nu$ about $\nu = \omega/2\pi$ and at position \underline{r} , and $N_2(\underline{r}, t)$ is the density of Cr^{3+} ions per cm^3 in the $2\bar{A}$ state at position \underline{r} . The first term on the right hand side of (5.1a) describes the increase in the phonon density at position \underline{r} and frequency ν due to decays of Cr^{3+} ions in the $2\bar{A}$ state at position \underline{r} occurring at the rate $1/T_1$. Due to these decays a spectrum $f(\nu)$ of phonons is produced. We assume (for now) that this spectrum is a Lorentzian

$$f(\nu) = \frac{\frac{2}{\pi \Delta \nu_0}}{1 + \left(\frac{\nu - \nu_0}{\Delta \nu_0 / 2} \right)^2} , \quad (5.2)$$

with full-width-at-half-maximum $\Delta\nu_0$ centered about the resonance frequency $\nu_0 = \Delta/2\pi$ and normalized to unity. The lifetime T_1 of the Cr^{3+} ion against phonon emission is $T_1 = (2\pi\Delta\nu_0)^{-1}$. We regard T_1 as the single adjustable parameter of the theory.

The second term describes the absorption of phonons by atoms in the \bar{E} state. The frequency-dependent absorption rate $\alpha(\nu)c$ per second is peaked at the resonance frequency. We assume that the absorption coefficient $\alpha(\nu)$ per cm is proportional to the emission spectrum and given by²⁹

$$\alpha(\nu) = \frac{N^*}{D(\nu) c T_1} f(\nu) = \frac{N^*}{D_0 c T_1} \cdot \frac{1}{1 + \frac{(\nu - \nu_0)^2}{(\Delta\nu_0/2)^2}} \quad (5.3)$$

Here $D(\nu)d\nu$ is the density of phonon modes per cm^3 in the ruby crystal in frequency interval $d\nu$ which we assume to be the Debye spectrum

$$D(\nu)d\nu = 4\pi\nu^2 d\nu \left(\frac{2}{c_t^3} + \frac{1}{c_\ell^3} \right) \equiv \frac{12\pi\nu^2 d\nu}{c^3} \quad (5.4)$$

$c_t = 6.4 \times 10^5$ cm/sec, $c_\ell = 11.3 \times 10^5$ cm/sec and $c = 7.1 \times 10^5$ cm/sec are the transverse, longitudinal and average sound velocities respectively of ruby¹⁸. Our use of the Debye spectrum is justified because $\nu_0 \ll \nu_D$. The quantity $D_0 \equiv D(\nu) \frac{\pi}{2} \Delta\nu_0 \approx D(\nu_0) \frac{\pi}{2} \Delta\nu_0$ is a measure of the density of phonon modes per cm^3 "on speaking terms" with the decaying atom. $(\Delta\nu_0 \frac{\pi}{2})$ is the width of a rectangular spectrum

with the same area and height as the Lorentzian (5.2). The prefactor in (5.3) is fixed by the condition that²⁹

$$\int_{-\infty}^{\infty} \alpha(\nu) d\nu = \frac{N^*}{D(\nu_0) c T_1} \quad . \quad (5.5)$$

We can understand the expression for $\alpha(\nu)$ as follows:

According to equipartition of energy a quantum of energy $h\nu_0$ added to the atom-phonon system is as likely to excite one of the N^* atoms as one of the D_0 phonons that are all at approximately the same energy $h\nu_0$ and are all approximately equally coupled to the N^* atoms. Thus if the lifetime of an excited atom is T_1 seconds then the lifetime of a phonon of frequency ν_0 must be $T_1 \times (D_0/N^*)$ seconds.

Since this phonon travels with velocity c , its mean-free-path is $\Lambda(\nu_0) = 1/\alpha(\nu_0) = D_0 c T_1 / N^*$. The absorption $\alpha(\nu)$ per cm of a phonon of any frequency ν is reduced from $\alpha(\nu_0)$ by just the Lorentz factor

$$\frac{1}{1 + \frac{\nu - \nu_0}{\Delta\nu_0/2}} \quad .$$

Hence we get Eq. (5.3). For ruby we have $D(\nu_0) = 7.9 \times 10^7$ sec/cm³.

The third term describes the decrease in density of phonons at position r by diffusion of phonons away from position \underline{r} and eventually out of the excitation region. The frequency dependent diffusion coefficient $\mathcal{D}(\nu)$ is a minimum on resonance and increases as $|\nu - \nu_0|$ increases.

We take $\mathcal{D}(\nu)$ to be given by the standard kinetic theory expression

$$\mathcal{D}(\nu) = \frac{1}{3} \Lambda(\nu) c = \frac{c}{3\alpha(\nu)} \quad (5.6)$$

where $\Lambda(\nu)$ is the mean-free-path and c is the average phonon velocity. Eqs. (5.1a,b) together implicitly take into account the fact that the time taken to traverse a mean-free-path is the sum of the time between collisions and the time T_1 of the collision itself. (Note that $\mathcal{D}(\nu)$ actually increases without bound as $|\nu - \nu_0| \rightarrow \infty$ but this pathology will be remedied shortly.)

Finally we impose the restriction that $N_2(t) \ll N^*$ for all times so that we can neglect reductions in N^* due to excitations as well as neglect stimulated emission. Also we neglect the continuous, slow generation and loss of ions in the $2\bar{A}$ and \bar{E} states due to optical pumping and R_1 and R_2 radiation. Noting that the lifetime of a longitudinal phonon against anharmonic decay is $\sim 2 \mu\text{s}$ and that of a transverse phonon even longer by orders of magnitude^{18,21}, we neglect anharmonic phonon decay. We defer until §5.2 the possibility that the spectrum $f(\nu)$ may be replaced by an inhomogeneously broadened Voigt profile.

Spatial Dependence of Solutions

Eqs. (5.1a,b) are coupled, first order, linear, homogeneous differential equations and can be solved as follows. We group together the phonon source and sink terms as

$$S(\underline{r}, \nu, t) d\nu = f(\nu) d\nu \frac{N_2(\underline{r}, t)}{T_1} - n_{ph}(\underline{r}, \nu, t) d\nu \alpha(\nu) c , \quad (5.7)$$

and write Eq. (5.1a) as

$$\frac{\partial}{\partial t} n_{ph}(\underline{r}, \nu, t) d\nu = S(\underline{r}, \nu, t) + \mathcal{D}(\nu) \nabla^2 n_{ph}(\underline{r}, \nu, t) d\nu . \quad (5.8)$$

We try a separation of variables solution of Eq. (5.8) of the form

$$n_{ph}(\underline{r}, \nu, t) d\nu \equiv n_{ph}(\nu, t) d\nu R(\underline{r}) , \quad (5.9a)$$

and

$$N_2(\underline{r}, t) \equiv N_2(t) R(\underline{r}) , \quad (5.9b)$$

so that

$$S(\underline{r}, \nu, t) d\nu \equiv S(\nu, t) R(\underline{r}) . \quad (5.9c)$$

That n_{ph} and N_2 must have the same spatial dependence can be seen from Eq. (5.1b) and is essentially due to the homogeneity of Eqs. (5.1a) and (5.1b).

Substituting Eqs. (5.9) into Eq. (5.8) gives us the two equations

$$\left\{ \begin{array}{l} \frac{d}{dt} n_{ph}(\nu, t) d\nu = -\kappa^2(\nu) n_{ph}(\nu, t) d\nu + S(\nu, t) , \\ \nabla^2 R(\underline{r}) + \kappa^2 R(\underline{r}) = 0 , \end{array} \right. \quad (5.10a)$$

$$(5.10b)$$

where κ^2 is the separation constant. If we assume that the excitation region (defined by the pumping laser beam) is an infinite cylinder of radius $r=b/2$ (and that we therefore have cylindrical symmetry) then the solutions of

Eq. (5.10b) are the zeroth order Bessel functions $R(r) = J_0(\kappa \cdot r)$. The boundary condition that N_2 (and therefore[†] n_{ph}) vanish at the edge of the cylinder $r=b/2$ requires that the separation constant κ takes on only the values⁵⁴:

$$\kappa = \left(\frac{4.8}{b}\right), \left(\frac{11.04}{b}\right), \dots, \left(\frac{x_i}{b/2}\right), \dots \quad (5.11)$$

Here x_i is the i^{th} zero of $J_0(x)$. The general solution of Eq. (5.8) is then

$$n_{ph}(r, v, t) dv = \sum_{i=1}^{\infty} C_i J_0(\kappa_i \cdot r) n_{ph}^{\kappa_i}(v, t) dv \quad (5.12)$$

where the C_i 's are constants prescribed by the initial conditions and $n_{ph}^{\kappa_i}(v, t) dv$ is the solution of Eq. (5.10a) with $\kappa = \kappa_i$. The mode $n_{ph}^{\kappa_1}$ is the only mode excited to any appreciable extent if the initial condition of a spatially uniform laser pulse obtains. Furthermore, by inspection of Eq. (5.10a) we can see that $n_{ph}^{\kappa_1}$ is the mode with the slowest decay rate and therefore the one of primary concern to us. It is interesting to note that κ_1 is rather insensitive to the precise geometry of the excitation region.

[†]Of course there are phonons outside the excitation region but they can no longer be scattered back into the region to participate in the electron-phonon interaction. Therefore we can take $n_{ph} = 0$ for $r > b/2$.

For instance if the region is a cube of edge b then $\kappa_1 = \sqrt{3} \frac{\pi}{b}$.

Time Dependence of Solutions

Let us now obtain the time dependent factors of the densities, namely $n_{ph}^{\kappa_1}(\nu, t) d\nu$ (henceforth we omit the κ_1 superscript) and $N_2(t)$. They are the solutions of the coupled differential equations

$$\begin{aligned} \frac{d}{dt} n_{ph}(\nu, t) d\nu = f(\nu) d\nu \frac{N_2(t)}{T_1} - n_{ph}(\nu, t) d\nu \alpha(\nu) c \\ - \frac{1}{t_d(\nu)} n_{ph}(\nu, t) d\nu \end{aligned} \quad (5.13a)$$

$$\frac{d}{dt} N_2(t) = - \frac{N_2(t)}{T_1} + \int d\nu n_{ph}(\nu, t) \alpha(\nu) c \quad (5.13b)$$

where

$$t_d(\nu) = \left\{ \left(\frac{4.8}{b} \right)^2 \mathcal{Q}(\nu) \right\}^{-1} \quad (5.14)$$

is the diffusion time of phonons of frequency ν . We have noted already that (5.14) must break down for $|\nu - \nu_0|$ large enough that the mean-free-path is longer than b , because then $\mathcal{Q}(\nu) \gg bc$ and $t_d(\nu) \gg b/c$. This is unacceptable because the minimum time required for a phonon of any frequency to leave the excitation region is the ballistic

escape time $t_b = b/c^\dagger$. Thus we replace (5.14) by the generalized escape time

$$t_e(v) = t_b + t_d(v) = \frac{b}{c} + \frac{1}{\mathcal{Q}(v)} \left(\frac{b}{4.8}\right)^2. \quad (5.15)$$

Then for $\mathcal{Q}(v) \gg bc$ we have $t_e \approx t_b = b/c$ and for $\mathcal{Q}(v) \ll bc$ we have $t_e \approx t_d$. Solving Eqs. (5.13) by the method of Laplace transforms we find that

$$n_{ph}(v, t) = \frac{1}{2\pi i} \oint_{\mathcal{C}} ds e^{st} n_{ph}(v, s), \quad (5.16a)$$

and

$$N_2(t) = \frac{1}{2\pi i} \oint_{\mathcal{C}} ds e^{st} N_2(s), \quad (5.16b)$$

where $n_{ph}(v, s)$ and $N_2(s)$, given by the Laplace transforms of Eq. (5.13), are

$$n_{ph}(v, s) = \frac{\{n_{ph}(v, t=0) + \frac{f(v)}{T_1} N_2(s)\}}{s + \alpha(v)c + \frac{1}{t_e(v)}}, \quad (5.17a)$$

with

$$N_2(s) = \frac{\{N_2(t=0) + \int_{-\infty}^{\infty} dv n_{ph}(v, t=0) \frac{\alpha(v)c}{s + \alpha(v)c + 1/t_e(v)}\}}{s + \frac{\sum(s)}{T_1}} \quad (5.17b)$$

[†]The average ballistic path length $\langle \ell \rangle$ inside a cylinder of radius r and length $L \gg r$ is approximately $\langle \ell \rangle = r \frac{2}{\pi} (\ln \frac{2L}{r} - 1)$. In our case $r \approx .35$ mm and $L = 10$ mm so that $\langle \ell \rangle \approx 2r \approx b$.

where

$$\sum(s) = \int_{-\infty}^{\infty} dv f(v) \frac{s + \frac{1}{t_e(v)}}{s + \alpha(v)c + \frac{1}{t_e(v)}} . \quad (5.17c)$$

General Features of Solutions

The contour \mathcal{C} encloses the various poles and branch cuts of $n_{ph}(v, s)$ and $N_2(s)$ which are located in the half-plane $\text{Re}\{s\} < 0$. Let us begin by studying the singularities of $N_2(s)$ in the simplest case when there are no phonons initially present. If we replace the integration over v in $\sum(s)$ in the denominator of $N_2(s)$ by a summation over the phonon modes, we can locate the singularities graphically by finding the values of s for which $-T_1 s = \sum(s)$. As we see in Fig. 5.1, $\sum(s)$ has a pole due to each phonon mode included in the sum, and the poles lie spaced in the range $s_R \leq s \leq -c/b$ where

$$s_R = -\frac{c}{b} \left[\alpha(v_0)b + \frac{1}{1 + \frac{1}{(4.8)^2} \alpha(v_0)b} \right] . \quad (5.18)$$

The pole at $s = s_R$ is due to the resonance phonons which are the quickest to disappear due mainly to resonant absorption. The pole at $s = -c/b$ is due to phonons far-from-resonance which disappear relatively slowly via ballistic flight. Coupling the atom-phonon system causes these poles to shift to new positions determined by the roots of the equation $-T_1 s = \sum(s)$. The graphical solution shows that all but two of the roots are located in the interval

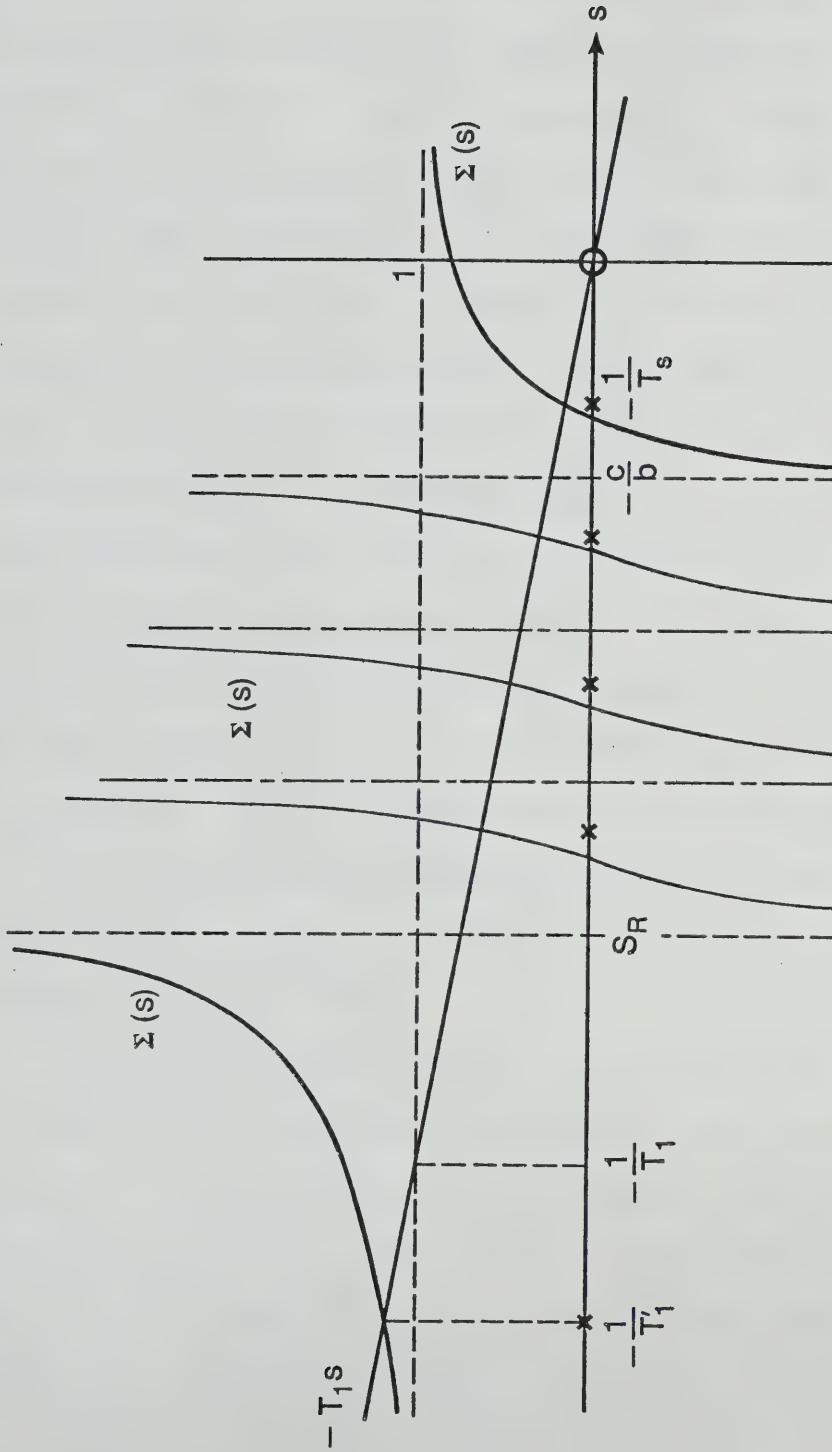


Fig. 5.1. Graphical solution of the equation $-T_1 s = \Sigma(s)$, see (5.23). Solutions are denoted by crosses on the s -axis. In the continuum limit the dense set of poles of $\Sigma(s)$ in the interval $s_R < s < -c/b$ is replaced by a branch cut.

$s_R \leq s \leq -c/b$ and are shifted only a small amount. One pole, whose position we have labelled $s = (-T_1')^{-1}$, has been shifted to the left of $-T_1^{-1}$ and when inserted into Eq. (5.16b) yields the initial fast decay in time $T_1' \leq T_1$ of the coupled atom-phonon system. The other pole whose position we have labelled $s = -T_s^{-1}$, has been shifted into the interval $-c/b < s < 0$ and represents the final slow decay in time T_s of the coupled system. The poles in the interval $s_R \leq s < -c/b$, when inserted into Eq. (5.16b) yield the intermediate decay. We should point out that Fig. 5.1 as drawn describes the situation for densities $N^* \approx 10^{14} - 10^{15} \text{ cm}^{-3}$ for ruby. As noted in the introduction, at lower densities the phonons escape ballistically, $\alpha(v_0)b \ll 1$ and the interval $s_R \leq s \leq -c/b$ becomes narrower than Fig. 5.1 suggests. On the other hand for densities $N^* \geq D_0 \approx 10^{15} \text{ cm}^{-3}$, the resonant phonon lifetime is less than the $2\bar{A}$ state lifetime T_1 , and $-T_1^{-1}$ actually lies inside the interval $s_R \leq s \leq -c/b$.

Let us now go back to the continuum limit of $\sum(s)$ and replace the summation over phonon modes by the original integral. A detailed calculation shows that the two poles located at $s = (-T_1')^{-1}$ and $s = -T_s^{-1}$ remain but the set of poles in the interval $s_R \leq s < -c/b$ is replaced by a branch cut connecting branch points at $s = s_R$ and $s = -c/b$.

Thus the only change in the above description is the rather minor change that a discrete set of intermediate

decay rates is replaced by a continuous one. Indeed we find that the time evolution of the density N_2 of atoms in the $2\bar{A}$ state, with no phonons initially present, using Eq. (5.16b), is given by

$$\frac{N_2(t)}{N_2(t=0)} = R_1 e^{-t/T_1'} + \int_{s_R}^{-c/b} ds e^{st} \mathcal{L}(s) + R_s e^{-t/T_s} \quad (5.19)$$

where $\mathcal{L}(s)$ is the discontinuity across the branch cut,

$$\mathcal{L}(s) = \lim_{\epsilon \rightarrow 0+} \frac{1}{2\pi i} \left\{ \frac{-1}{s + \frac{1}{T_1'} \int (s + i\epsilon)} + \frac{1}{s + \frac{1}{T_1} \int (s - i\epsilon)} \right\}, \quad (5.20)$$

and R_1, R_s are the residues of $N_2(s)/N_2(t=0)$ at the poles $s = -1/T_1', s = -1/T_s$ respectively, i.e.

$$R_1, R_s = \frac{1}{1 + \frac{1}{T_1} \frac{d}{ds} \int (s)} \bigg|_{s = -\frac{1}{T_1'}, s = -\frac{1}{T_s}}. \quad (5.21)$$

These quantities of course obey the normalization condition

$$R_1 + R_s + \int_{s_R}^{-c/b} \mathcal{L}(s) ds = 1. \quad (5.22)$$

Solutions of the Rate Equations

Fig. 5.2 shows a typical example of the time evolution of the excited atom density $N_2(t)$, given by Eq.(5.19), showing the fast initial, intermediate, and slow final decay. Also shown are the total phonon density $N_{ph}(t) =$

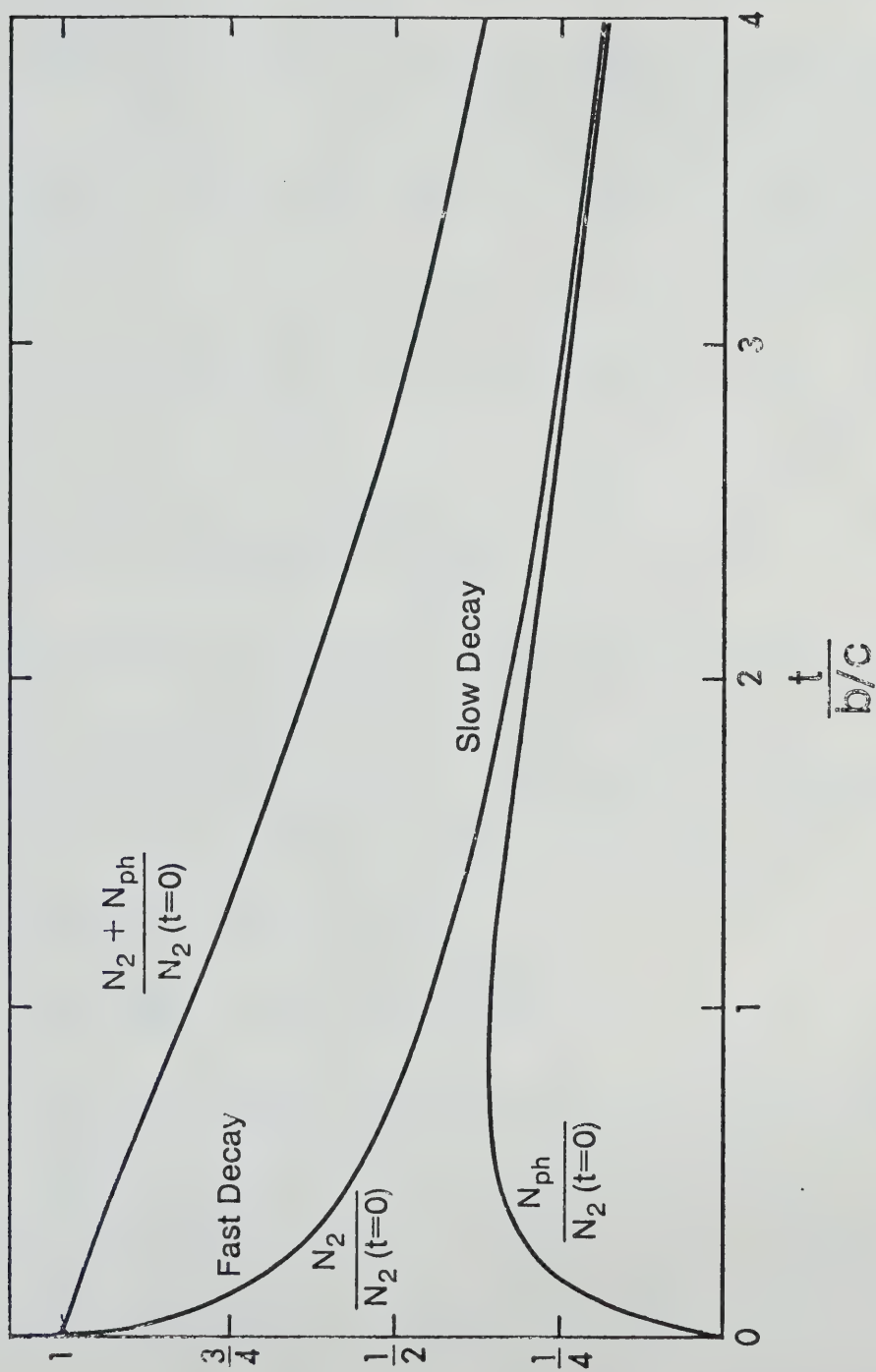


Fig. 5.2. Typical example of the time evolution of the density of atoms in the $2\bar{A}$ state (N_2), the total density of phonons (N_{ph}), and their sum; for $N^*/D_0 = 4$ and $T_1 c/b = 1/3$.

$\int_{-\infty}^{\infty} d\nu n_{\text{ph}}(\nu, t)$, and the total density of excitations $N_2(t) + N_{\text{ph}}(t)$ in the region.

Let us now look at the final slow decay of the system in detail. We recall that its decay time is $T_s = -1/s$ where s lies in the interval $-c/b < s < 0$ and satisfies the equation

$$-T_1 s = \chi(s) = \int_{-\infty}^{\infty} d\nu f(\nu) \{1 - P_s(\nu)\} , \quad (5.23)$$

where

$$P_s(\nu) = \frac{\alpha(\nu)c}{s + \alpha(\nu)c + \frac{1}{t_e(\nu)}} . \quad (5.24)$$

In general Eq. (5.23) must be solved numerically and these results are shown in Fig. 5.3. Here we plot T_s vs N^*/D_0 for various values of $T_1 c/b$. Note that D_0 , and thus the horizontal scale, depends on the time T_1 of a particular curve because of the relation

$$D_0 = \frac{D(\nu)}{4T_1} = \frac{2.0 \times 10^7 \text{ sec/cm}^3}{T_1} .$$

Fig. 5.3 clearly shows that there are two density regimes with quite different physical processes governing the decay of the system in each. As we will see in detail below, for low densities the system decays in time $T_s \approx b/c (1 + \alpha(\nu_0)b)$, which is the ballistic or free-flight time plus the resonant phonon diffusion time. Because for large $\alpha(\nu_0)b$ (i.e. large probability of phonon scattering)

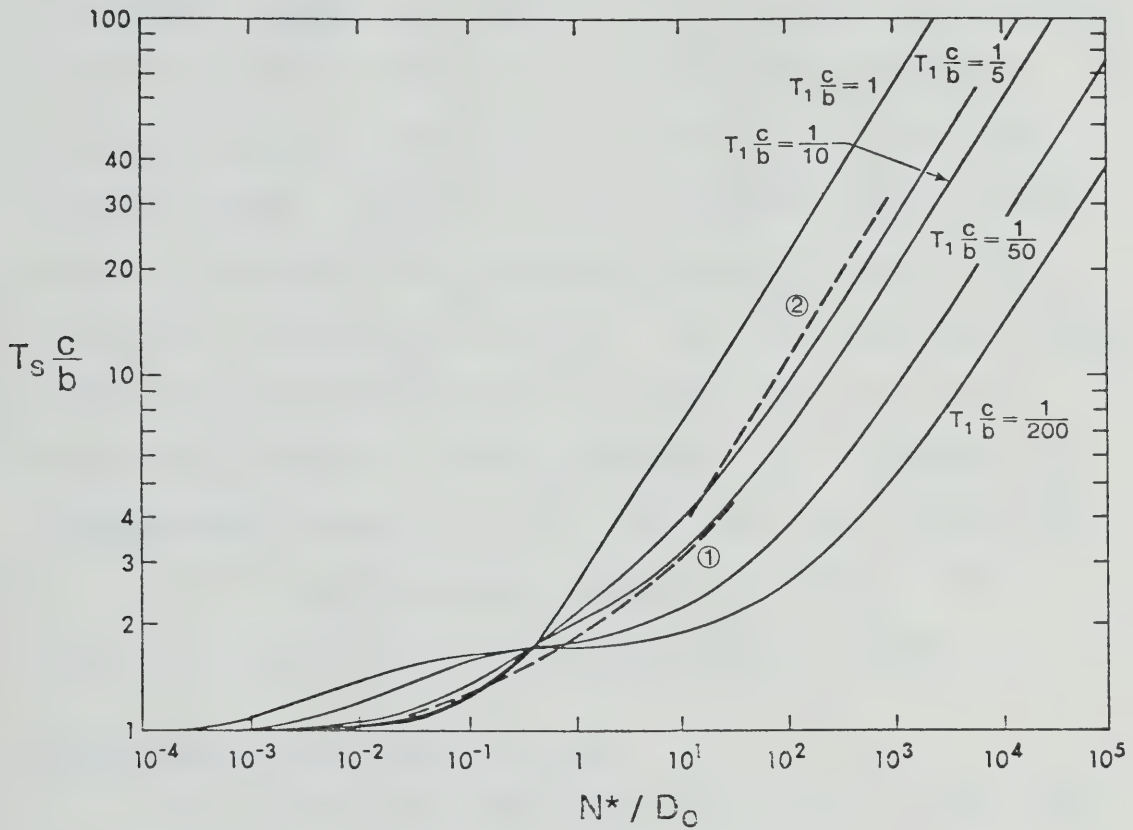


Fig. 5.3. Solid lines: Theoretical final slow decay time T_s as a function of the density N^*/D_0 for various values of $T_1 c/b$, from Eq. (5.23). Note that the order of lines is reversed at low densities. Dashed line: Experimental results from Refs. 20 and 21 (see also Fig. 1.5) plotted assuming $D_0 = 10^{15} \text{ cm}^{-3}$. Curve ① $b/c = 150 \text{ ns}$; Curve ② $b/c = 100 \text{ ns}$.

this would suggest that $T_s \propto b^2$, we may call this the spatially diffusive regime. However the figure shows that beginning already when $\alpha(\nu_0)b \approx 1$, T_s hardly increases as we increase N^* by orders of magnitude, indicating a process competing with spatial diffusion. In the high density regime $\alpha(\nu_0)b \gg 1$ this process, which we call spectral diffusion and for which we will find that $T_s \approx T_1 \sqrt{\alpha(\nu_0)b}$, completely dominates. We also show the decay times found by Pauli et al^{20,21} (see Fig. 1.5) for two different excitation region diameters b . For these two experimental curves $D_0 \approx 10^{15} \text{ cm}^{-3}$ was found to give the best fit to the theoretical curves so that $T_1 \approx 20 \text{ ns}$. We shall say more about this rather large lifetime in §5.3.

Decay Time T_s in Case $N^* \ll D_0$

For the limiting case $N^* \ll D_0$ we can actually find T_s analytically as follows. We assume that the absorption probability $\alpha(\nu_0)b \equiv \frac{N^*b}{D_0 c T_1} \ll 1$ and that the diameter b of the excitation region is so large that $T_1 \ll b/c$. In this ballistic regime we cannot speak of true diffusion and we replace the diffusion time (5.14) by

$$t_d(\nu) = \frac{b}{c} \times \alpha(\nu)b \quad (5.25)$$

which is the ballistic time multiplied by the (small) probability of the phonon being absorbed and scattered in this time. Keeping the first three terms of the binomial expansion of the reciprocal escape time

$$\frac{1}{t_e(v)} = \left(\frac{b}{c} (1 + \alpha(v)b) \right)^{-1}, \quad (5.26)$$

Eq. (5.24) becomes

$$P_s(v) = \frac{\frac{\alpha(v_o)b}{s \frac{b}{c} + 1}}{\left(\frac{v - v_o}{\Delta v_o/2} \right)^2 + \left\{ 1 + \frac{(\alpha(v_o)b)^2}{(s \frac{b}{c} + 1) \left(1 + \left(\frac{v - v_o}{\Delta v_o/2} \right)^2 \right)} \right\}}, \quad (5.27)$$

and the integrand of Eq. (5.23) can be written as a sum of powers of Lorentzians. These can be integrated exactly so that Eq. (5.23) becomes

$$-T_1 s = 1 - \frac{\alpha(v_o)b}{2(s \frac{b}{c} + 1)} + \frac{5}{4} \cdot \frac{(\alpha(v_o)b)^3}{4(s \frac{b}{c} + 1)^2} + \dots \quad (5.28)$$

Since the right hand side of Eq. (5.28) varies very rapidly for $s = -c/b$ (see Fig. 5.1) and the left hand side is relatively constant, we replace the left hand side by $-T_1 s \approx T_1 c/b$ and find the solution of Eq. (5.28) to be

$$s = -\frac{c}{b} \left(1 - \frac{\alpha(v_o)b}{2(1 - T_1 \frac{c}{b})} + \dots \right). \quad (5.29)$$

The final slow decay time T_s for $N^*/D_o \ll 1$ is therefore

$$T_s = -\frac{1}{s} = \frac{b}{c} \left(1 + \frac{\alpha(v_o)b}{2(1 - T_1 \frac{c}{b})} + \dots \right). \quad (5.30)$$

Thus we get the reasonable result that the system decays in a time $T_s \approx t_b + \frac{1}{2} t_d(v_o)$, which is the time an "average"

phonon, namely a phonon a half-width from resonance would escape in.

Decay Time T_s in Case $N^* \gg D_0$

In this more interesting case we assume that the absorption probability $\alpha(v_0)b \gg 1$, so we are well within the diffusive regime. Since $1/t_e(v) \ll c/b$ and we demand that $|s| < c/b$, we can approximate (5.24) by

$$P_s(v) = \begin{cases} 1 & \text{when } \alpha(v)c > \frac{c}{b} \leftrightarrow \left| \frac{v - v_0}{\Delta v_0/2} \right| < \sqrt{\alpha(v_0)b} , \\ 0 & \text{when } \alpha(v)c < \frac{c}{b} \leftrightarrow \left| \frac{v - v_0}{\Delta v_0/2} \right| > \sqrt{\alpha(v_0)b} . \end{cases} \quad (5.31)$$

Substituting (5.31) into Eq. (5.23) we get

$$-T_1 s = \frac{2}{\pi} \int_{\sqrt{\alpha(v_0)b}}^{\infty} \frac{dx}{1+x^2} \approx \frac{2}{\pi} \cdot \frac{1}{\sqrt{\alpha(v_0)b}} \quad (5.32)$$

where

$$x \equiv \frac{v - v_0}{\Delta v_0/2} ,$$

or

$$T_s = -\frac{1}{s} = \frac{\pi}{2} T_1 \sqrt{\alpha(v_0)b} . \quad (5.33)$$

This is just the decay time found by Holstein⁶ and Veklenko⁷ by rather more complicated arguments. Eq. (5.33) is a very interesting result. It says that the final slow decay has absolutely nothing to do with spatial diffusion.

Indeed approximation (5.31) requires only that the absorption probability $\alpha(\nu_0)b \gg 1$ and would have held just as well had we chosen the diffusion time $t_d(\nu) = 0$. (Of course we must still have the total escape time $t_e(\nu) \geq b/c$.) In other words when $\alpha(\nu_0)b \gg 1$ spatial diffusion is so slow and ineffective as an escape mechanism that, as we shall see in detail below, the phonons use a shortcut - namely spectral diffusion. By this we mean the following process.

Excited atoms in the excitation region decay in time T_1 emitting a Lorentzian spectrum of phonons. Those phonons in the wings of the Lorentzian satisfying $\alpha(\nu)b < 1$ (i.e. a fraction $f = 2/(\pi\sqrt{\alpha(\nu_0)b})$) escape unhindered. The rest are absorbed in times $t \ll T_1$ and subsequently re-emitted again in a Lorentzian spectrum. The process repeats itself again and again until all the phonons have escaped "through the wings" of the spectrum. From this simple argument Eq. (5.33) follows immediately. Although some spatial diffusion obviously takes place concurrently, we see that it plays a secondary role.

Phonon Spectrum

To prove these assertions let us now look at the time evolution of the phonons. We recall that $n_{ph}(\nu, t)d\nu$ is given by (5.16a) with (5.17). In general these equations must be solved numerically and some typical results are shown in Fig. 5.4 where we assume that there are no

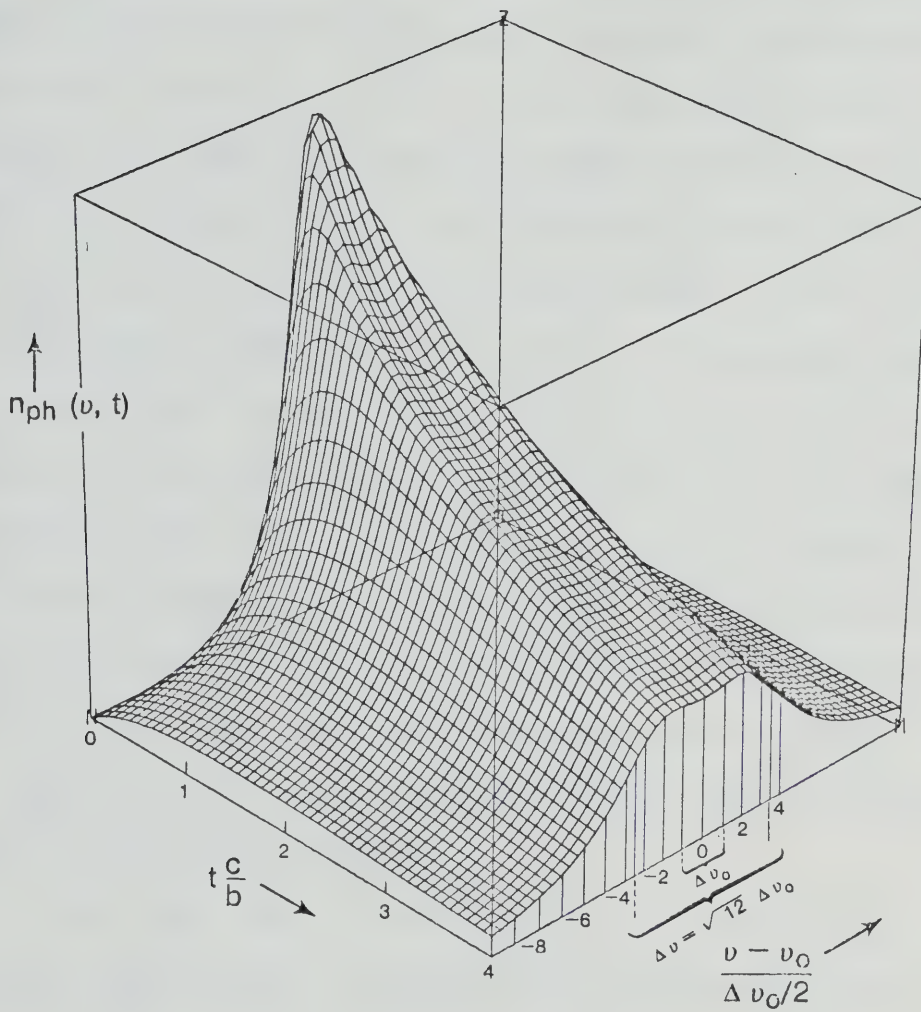


Fig. 5.4. Time evolution of the phonon spectrum $n_{ph}(v, t)$ for case $N^*/D_0 = 4$ and $b/(cT_1) = 3$. Note that as $t \rightarrow \infty$ the spectrum is approximately rectangular with width $\Delta v = \sqrt{\alpha(v_0)b} \Delta v_0$.

phonons initially present and that the absorption probability $\alpha(\nu_0)b$ is large. We see that for very small times some of the excited atoms decay and emit a Lorentzian spectrum of phonons. Soon the resonant phonons are absorbed by other atoms causing self-reversal of the spectrum. Since only the off-resonant phonons exist for an appreciable amount of time before they too are absorbed, the spectrum broadens and flattens. The spectrum continues to broaden until time $t=b/c$. By this time the far-from-resonance phonons are escaping ballistically and those now-empty modes can be re-occupied by other phonons whose excitation energy comes from phonons lost from the middle of the spectrum. Thus a steady state is established with a phonon spectrum which is continually losing energy from the center to the wings and which decays away uniformly with a single decay time T_s .

This slow decay of the phonon spectrum can be derived analytically. From Eq. (5.17a) we have that

$$n_{ph}(\nu, s)d\nu = D(\nu)d\nu \cdot \frac{\alpha(\nu)c}{s + \alpha(\nu)c + \frac{1}{t_e(\nu)}} \cdot \frac{N_2(s)}{N^*} . \quad (5.34)$$

The factor $(s + \alpha(\nu)c + \frac{1}{t_e(\nu)})^{-1}$ has a pole which lies in the interval $s_R < s < -c/b$ (see discussion before Eq. (5.18)) and the factor $N_2(s)$ of course has poles at $s = -1/T_1'$ and $s = -1/T_s$ and a branch cut in the interval $s_R < s < -c/b$. The final slow decay therefore is given by the residue of

$n_{\text{ph}}(\nu, s) d\nu$ at the "slow-pole" $s = -1/T_s$. We find that

$$\lim_{t \rightarrow \infty} n_{\text{ph}}(\nu, t) d\nu = D(\nu_0) d\nu \cdot P_{-1/T_s}(\nu) \cdot \frac{N_2(t=0)}{N^*} R_{-1/T_s} e^{-t/T_s}. \quad (5.35)$$

Thus the final broadened phonon spectrum, $P_{-1/T_s}(\nu) d\nu$, does not change shape but decays uniformly in time T_s as we asserted.

Recall that for large densities $N^* \gg D_0$ the spectral shape $P_{-1/T_s}(\nu)$ is given by the approximation (5.31), i.e. it is quite flat and has breadth $\Delta\nu = \sqrt{\alpha(\nu_0)b} \Delta\nu_0$. The slight self-reversal is due to the negative term $s = -1/T_s$ in (5.24) which is relatively important near the "shoulders" of the spectrum.

For low densities $N^* \ll D_0$ Eqs. (5.27) and (5.29) give the phonon spectrum

$$P_{-1/T_s}(\nu) = \frac{2(1 - T_1 \frac{c}{b})}{\frac{\nu - \nu_0}{(\Delta\nu_0/2)} + \left\{ 1 + \frac{2\alpha(\nu_0)b(1 - T_1 \frac{c}{b})}{1 + \frac{\nu - \nu_0}{(\Delta\nu_0/2)}} \right\}} \quad (5.36)$$

whose half-width appears to be increased from the intrinsic Lorentzian emission spectrum by a factor $\approx (1 + \frac{3}{2}\alpha(\nu_0)b)$, but which is equal to the original Lorentzian in the far wings.

Quasi-Equilibrium Populations

Finally let us look at the quasi-equilibrium populations of the two-level states and the phonons. We now generalize and assume that the initial laser pulse excites both phonons and Cr^{3+} ions in the $2\bar{A}$ state. Then Eqs. (5.16) and (5.17) become for the final slow decay

$$\frac{N_2(t)}{N^*} = \frac{N_2(\text{eq})}{N^*} \cdot e^{-t/T_S} \quad (5.37a)$$

where

$$\frac{N_2(\text{eq})}{N^*} = \left\{ \frac{N_2(t=0) + \int_{-\infty}^{\infty} d\nu P_{-1/T_S}(\nu) n_{\text{ph}}(\nu, t=0)}{N^* + \int_{-\infty}^{\infty} d\nu P_{-1/T_S}^2(\nu) D(\nu)} \right\}, \quad (5.37b)$$

and

$$\frac{n_{\text{ph}}(\nu, t) d\nu}{D(\nu) d\nu} = P_{-1/T_S}(\nu) \cdot \frac{N_2(t)}{N^*}. \quad (5.37c)$$

Evaluating the relative $2\bar{A}$ state population in the limit $N^* \ll D_0$ we get

$$\frac{N_2(\text{eq})}{N^*} = \frac{N_2(t=0) + 2n_0^{\text{ph}}(1 - T_1 \frac{c}{b} - \frac{3}{4} \alpha(\nu_0) b + \dots)}{N^* + 2D_0(1 - 2T_1 \frac{c}{b} - \frac{5}{2} \alpha(\nu_0) b + \dots)} \quad (5.38a)$$

where

$$n_0^{\text{ph}} \equiv \Delta\nu_0 \frac{\pi}{2} n_{\text{ph}}(\nu_0, t=0) \quad (5.38b)$$

is the density of initially injected phonons in the frequency interval $\Delta\nu_0 \frac{\pi}{2}$.

Summing over phonons in (5.37c) we get the total phonon density

$$N_{\text{ph}}(t) \equiv \int_{-\infty}^{\infty} n_{\text{ph}}(\nu, t) d\nu = 2D_0 \left(1 - T_1 \frac{c}{b} - \frac{3}{4} \alpha(\nu_0)b + \dots\right) \cdot \frac{N_2(t)}{N^*} . \quad (5.38c)$$

The factor of 2 in front of n_0^{ph} and D_0 in (5.38a) and (5.38c) is due to the following fact: If a Cr^{3+} ion absorbs a phonon (which it does according to a Lorentzian of distribution), another phonon will be re-emitted with certainty. On the other hand if a phonon is emitted with a Lorentzian distribution, then it subsequently may be absorbed (again with a Lorentzian distribution). Since the probability of the latter process involves the product of two Lorentzians, with integral half that of a single Lorentzian, the phonon population is favored by a factor of 2. (Indeed if we replace the Lorentzians $f(\nu)$ and $\alpha(\nu)$ by rectangular distributions the factors of 2 do not appear.) As one would expect, increasing the lifetime T_1 or the absorption probability $\alpha(\nu_0)b$ favors the $2\bar{A}$ states in the quasi-equilibrium.

In the limit $N^* \gg D_0$ Eq. (5.37b) becomes

$$\frac{N_2(\text{eq})}{N^*} = \frac{N_2(t=0) + n_{\text{ph}}(\nu_0, t=0) \sqrt{\alpha(\nu_0)b} \Delta\nu_0}{N^* + D(\nu_0) \sqrt{\alpha(\nu_0)b} \Delta\nu_0} . \quad (5.39a)$$

In this case all the initially injected phonons and phonon modes in the broad interval $\sqrt{\alpha(\nu_0)b} \Delta\nu_0$ (i.e. those

satisfying the condition $\alpha(v)b > 1$) participate in the quasi-equilibrium. The total phonon population is

$$N_{ph}(t) = \sqrt{\alpha(v_0)b} \Delta v_0 D(v_0) \frac{N_2(t)}{N^*} . \quad (5.39b)$$

We solve Eq. (5.37b) numerically and in Fig. 5.5 plot the quasi-equilibrium population $N_2(eq)/N^*$ vs N^*/D_0 for various values of T_1c/b assuming that no phonons are initially excited ($n_{ph}(v, t=0) = 0$). We see that for $N^* \ll D_0$ (see Eq. (5.38a)), $N_2(eq)/N^* = N_2(t=0)/(2D_0)$ which is independent of N^* . As N^* increases, the phonon band in quasi-equilibrium with the atoms broadens like $\Delta v = \sqrt{\alpha(v_0)b} \Delta v_0$ so that in this regime (see Eq. (5.39a)) $N_2(eq)/N^* \approx N_2(t=0)/(D_0 \sqrt{\alpha(v_0)b})$ which varies like $N^{*-1/2}$. Finally for $N^* \gg D_0$ the N^* term in the denominator of (5.39a) dominates so that $N_2(eq)/N^* \approx N_2(t=0)/N^*$ which varies like N^{*-1} .

These calculations can be compared to experiments of Pauli et al.^{20,21} if we note that in those experiments the initial laser pulse does excite phonons as well as Cr^{3+} ions. Indeed in their density regime $10^{16} \text{ cm}^{-3} \leq N^* \leq 10^{18} \text{ cm}^{-3}$ the appropriate curve, namely $T_1c/b = 1/5$, behaves like

$$N_2(eq)/N^* \propto N^{*-0.4} \quad (5.40)$$

in excellent agreement with their experiments assuming $n_{ph}(v, t=0) \Delta v_0 \approx 10^{14} \text{ cm}^{-3}$.

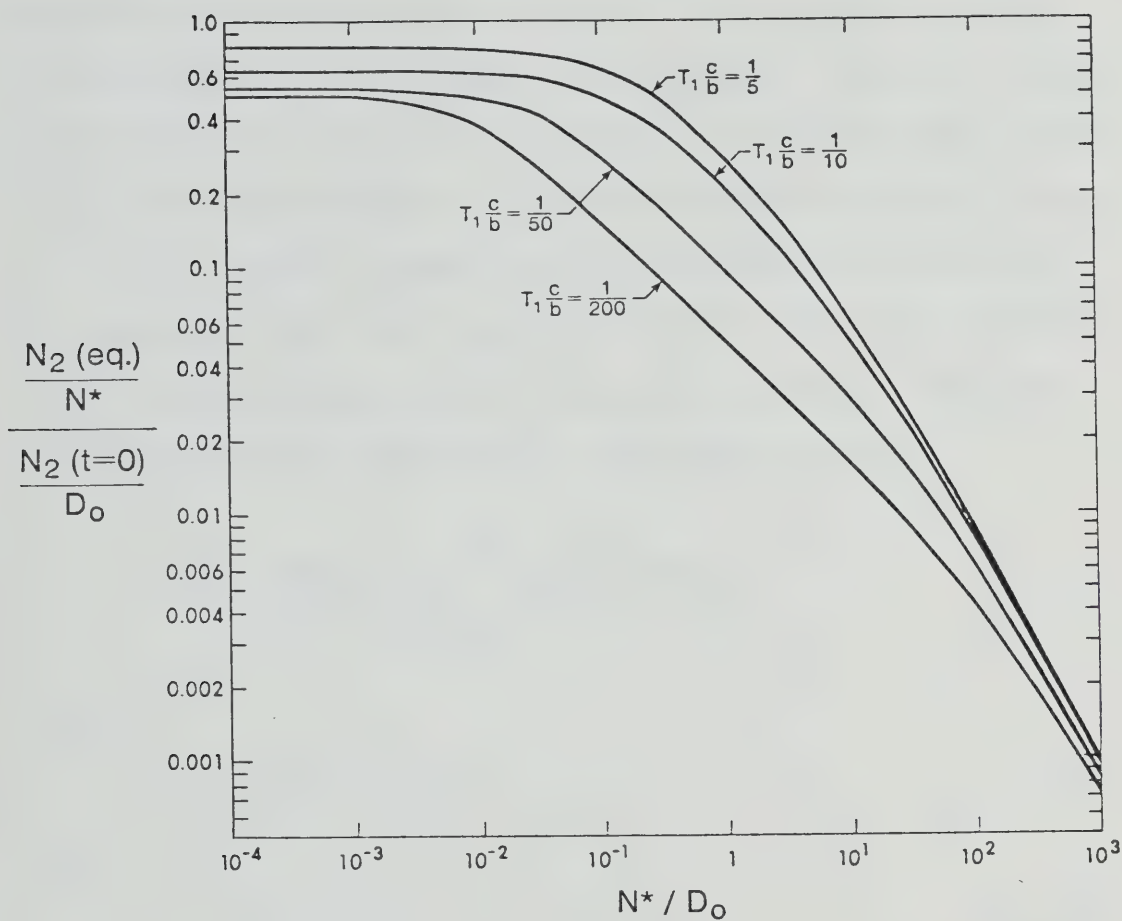


Fig. 5.5. Quasi-equilibrium population $N_2(\text{eq})/N^*$ vs N^*/D_0 for various values of $T_1 c/b$ assuming no phonons are initially excited.

5.2 Inclusion of Inhomogeneous Broadening

Until now we have assumed that the absorption and emission spectra are described by a Lorentzian profile centered about the resonance frequency ν_0 . However random static strains in the ruby crystal (or higher temperatures) can cause the resonance frequency to deviate locally from ν_0 . This results in so-called inhomogeneous broadening. The central limit theorem tells us that for large statistics the deviations have a Gaussian weighting. Thus we can replace the Lorentzian by the Voigt profile

$$f(\nu) = \frac{2 \ln 2}{\pi \sqrt{\pi}} \frac{\Delta \nu_0}{\Delta \nu_G^2} \int_{-\infty}^{\infty} \frac{e^{-y^2} dy}{a^2 + (\eta - y)^2}, \quad (5.41)$$

where

$$\eta = 2 \sqrt{\ln 2} \frac{\nu - \nu_0}{\Delta \nu_G}, \quad (5.42)$$

and

$$a = \frac{\Delta \nu_0}{\Delta \nu_G} \sqrt{\ln 2}. \quad (5.43)$$

$\Delta \nu_G$ measures the amount of Gaussian smearing of the original Lorentzian of width $\Delta \nu_0$. As before $f(\nu)$ is entered about ν_0 and normalized to unity. Using condition (5.5) we can write the absorption spectrum as

$$\alpha(\nu) = \frac{N^*}{D_0 c T_1} \frac{\ln 2}{\sqrt{\pi}} \left(\frac{\Delta \nu_0}{\Delta \nu_G} \right)^2 \int_{-\infty}^{\infty} \frac{e^{-y^2} dy}{a^2 + (\eta - y)^2}. \quad (5.44)$$

Note for $\Delta \nu_G = 0$ ($\Delta \nu_0 = 0$), $f(\nu)$ is pure Lorentzian

(Gaussian). Most importantly, for finite $\Delta\nu_G/\Delta\nu_0$, $f(\nu)$ is approximately Gaussian near $\nu = \nu_0$ and approximately the unbroadened Lorentzian in the wings.

We can now apply our method to the Voigt profile. For example solving Eqs. (5.23) and (5.24) numerically for the slow decay time T_s yields the results shown in Fig. 5.6a. Here we have plotted T_s vs N^*/D_0 (for $T_1 c/b = 1/200$) for various values of $\Delta\nu_G/\Delta\nu_0$. In all cases for small N^*/D_0 we see that the decay time T_s is smaller for the broadened than for the unbroadened spectrum simply because the broader the spectrum the smaller is the absorption $\alpha(\nu_0)$. For somewhat larger N^*/D_0 , T_s varies almost linearly with N^* . We will see shortly that this variation is characteristic of a Gaussian absorption and emission spectrum. For very large N^*/D_0 only phonons in the far wings of the spectrum can escape and at these frequencies the spectrum is almost Lorentzian. Thus as before we find in this regime that the decay time varies as $T_s \propto N^{*\frac{1}{2}}$. Since experimentally we do not find the linear variation of T_s with N^* at intermediate densities we conclude that inhomogeneous broadening is unimportant for the 29 cm^{-1} phonon line.

As a final simple calculation let us find the decay time T_s for a pure Gaussian spectrum for large N^* . In this case

$$\alpha(\nu)b = \alpha(\nu_0)b e^{-\eta^2}, \quad (5.45)$$

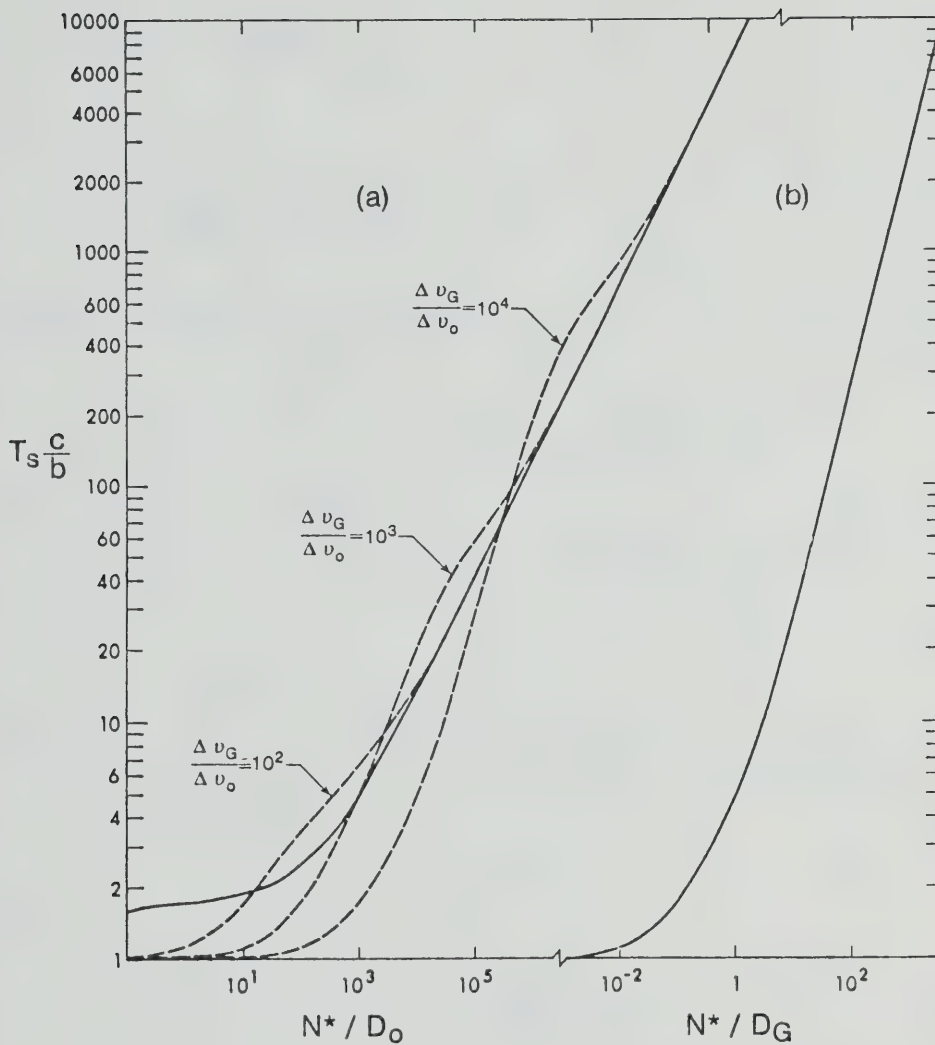


Fig. 5.6. (a) Dashed lines: Slow decay time T_s vs density N^*/D_0 for various amounts of inhomogeneous broadening. Solid line: pure Lorentzian, $\Delta \nu_G = 0$. (b) Pure Gaussian. (Note the different horizontal scale; D_G is defined in Eq. (5.46b).) For all curves $T_1 c/b = 1/200$.

where

$$\alpha(v_o) = \frac{N^*}{D_G c T_1} \quad (5.46a)$$

and

$$D_G = \frac{\Delta v_G}{2} \sqrt{\frac{\pi}{\ln 2}} D(v) ; \quad (5.46b)$$

so Eqs. (5.31)-(5.33) become

$$P_S(v) = \begin{cases} 1 & |\eta| < \sqrt{\ln(\alpha(v_o)b)} \\ 0 & |\eta| > \sqrt{\ln(\alpha(v_o)b)} \end{cases} \quad \text{when} \quad , \quad (5.47)$$

$$-T_1 s = \frac{2}{\sqrt{\pi}} \int_{\sqrt{\ln(\alpha(v_o)b)}}^{\infty} d\eta e^{-\eta^2} \approx \frac{2}{\pi} \cdot \frac{1}{\alpha(v_o)b} \cdot \frac{1}{\sqrt{\ln(\alpha(v_o)b)}} . \quad (5.48)$$

and

$$T_s = \frac{\pi}{2} \cdot T_1 \cdot \alpha(v_o)b \cdot \sqrt{\ln(\alpha(v_o)b)} . \quad (5.49)$$

Except for constants of order unity this is just the result found by Holstein⁶ and Veklenko⁷ for Gaussian spectra. As in the Lorentzian case, Eq. (5.48) clearly shows that T_s depends on the area under the wings of the emission spectrum where phonons escape ballistically. Again spatial diffusion is too slow and is thus irrelevant. Note that the radical varies so slowly that T_s varies almost linearly with N^* as we asserted above in the discussion of the Voigt

profile. The exact result for all densities for a pure Gaussian is shown in Fig. 5.6b.

5.3 Discussion

We have solved the set of coupled rate equation (5.1) describing the time evolution of a system of two-level atoms and phonons resonant with them, paying particular attention to the conditions obtaining during the final slow decay, i.e. during the phonon bottleneck.

One of our most important algebraic results is Eqs. (5.23), (5.24) which give a simple algorithm for the slow decay time T_s as a function of the concentration N^* of scatterers for any lineshape. Notice that for large N^* these equations reduce to the formal solution (1.8) of Holstein's integral equation. Because for large N^* the phonons from the center of the lineshape are effectively spatially trapped, T_s depends on the area under the wings of the lineshape where the phonons can escape ballistically. The system decays via 'spectral diffusion' with phonons from the center of the line being absorbed, their energy redistributed over the entire lineshape on emission, and finally phonons from the wings (obeying $\alpha(\nu) \cdot b < 1$) escaping ballistically. Hence the system decay rate $1/T_s$ equals the atomic decay rate $1/T_1$ times the fraction of the emitted phonons that escape ballistically.

During the slow decay of the system a quasi-equilibrium obtains²⁰, characterized by the two-level

atoms and all the phonon modes obeying $\alpha(\nu)b > 1$ reaching a uniform population of value $N_2(t)/N^*$. Thus if, for example, $\alpha(\nu)$ is Lorentzian the phonon population inside the excitation region is roughly rectangular with width $\Delta\nu = \Delta\nu_0 \sqrt{\alpha(\nu_0)b} \propto N^{*\frac{1}{2}}$ as in Fig. 5.4.

Let us now specialize our discussion to the $2\bar{A} \leftrightarrow \bar{E}$ transition of the Cr^{3+} ion in ruby. As evidenced by the experimentally observed dependence $T_s \propto N^{*\frac{1}{2}}$ for large N^* , the wings of the $2\bar{A} \rightarrow \bar{E}$ line are Lorentzian. There is insufficient inhomogeneous broadening to a Voigt profile to result in a linear dependence of T_s on N^* .

Our model applied to the phonon bottleneck in ruby (with Lorentzian intrinsic emission spectrum) reproduces the following experimental features:

- (1) the rapid initial decay of the system in time $t \approx T_1$,
- (2) the establishment of a bottleneck with a quasi-equilibrium excited atom population $N_2(\text{eq})/N^* N^{*-1/2}$,
- (3) the establishment of a broadened ($\Delta\nu \propto N^{*\frac{1}{2}}\Delta\nu_0$), flattened phonon population which has been observed by Dijkhuis et al.¹⁴ in CW Zeeman splitting experiments, and
- (4) the subsequent decay of the quasi-equilibrium in times $T_s \propto N^{*\frac{1}{2}}$ for large N^* .

To obtain quantitative agreement with the experiments by Pauli et al.^{20,21}, we must choose the $2\bar{A}$ state lifetime $T_1 \approx 20$ ns, if we take their estimates of N^* and b at face value and take the density of phonon states $D(\nu_0)$ according to Eq. (5.4). If we assume that N^* is actually underestimated by a factor of 3 (which is within the estimated uncertainty²¹) and that the Debye approximation of $D(\nu_0)$ is overestimated by a factor of 4, then a lifetime $T_1 = 5$ ns gives good agreement with experiment. In any case our T_1 is larger than the values in the literature: Lengfellner et al.²⁶ and Geschwind et al.¹⁹, $T_1 = .4$ ns; Rives and Meltzer¹³, $T_1 = 1.1$ ns; and Kurnit et al.²⁷, $T_1 = 2.8$ ns; which we note already differ by a factor of seven and which with the exception of Rives and Meltzer, are all only indirect estimates. (See Ref. 13 for a critique of these values.)

Rives and Meltzer¹³ treat the phonon bottleneck also via a rate equation approach. This model however precludes spectral or spatial diffusion and assumes that the system decays via phonon decay. They evaluated only the early time behavior of the system and used the concentration N^* and the anharmonic phonon decay time τ_{ph} as free parameters. Their best fit was obtained with $\tau_{ph} = 40$ ns which is far shorter than estimates of $2 \mu s$ previously cited^{15-18,20-22}. Furthermore their model cannot reproduce the experimentally found functional dependence of the

quasi-equilibrium population $N_2(\text{eq})/N^*$ or the decay time T_s as functions of N^* .

A second possible resolution of the lifetime discrepancy is the following: In a phenomenological theory such as ours, T_1 is the effective time in which, due to the decay of an atom, a free phonon is generated. Now for $N^* > D_0 \approx 10^{15} \text{ cm}^{-3}$, the concentration of scatterers is so large that a second atom has already reflected back a phonon before the first atom has finished emitting that phonon. Thus a cooperative effect can exist between the decaying atom and its neighbors, resulting in an effective decay time $T_1^{\text{eff}} \gg T_1$. This effect will be explored in Chapter 6.

CHAPTER 6

FIELD THEORETIC DESCRIPTION OF THE PHONON BOTTLENECK (II)

In Chapter 5 we solved a set of coupled rate equations for the time evolution of the electron-phonon system. These equations were derived from the quantum equations of motion (4.5a) and (4.7) under the assumption that $N^* \lesssim 10^{16} \text{ cm}^{-3}$ so that $T_1 < T_2(N^*)$, T_1 and T_2 being the time of interaction and the time between interactions respectively of the resonant phonons with Cr^{3+} ions. We have already indicated that under the opposite conditions when $T_2(N^*) < T_1$ cooperative effects between a decaying Cr^{3+} ion and its neighboring unexcited ions may exist, resulting in an increased effective lifetime T_1 . To explore this and other quantum effects not included in the rate equations we wish to study in this chapter the full quantum equations (4.5a) and (4.7).

6.1 General Description

Let us begin by writing down the Fourier transforms of the Heisenberg equations of motion (4.5a) and (4.7) for the annihilation operator $b_{\tilde{k}}(t)$ of the phonon mode of wave-number \tilde{k} and the lowering operator $S_n^-(t)$ of atom n , namely

$$B_{\tilde{k}}(x) = \frac{g}{x - \omega_{\tilde{k}}} \sum_{n=1}^N e^{-i\tilde{k} \cdot \tilde{r}_n} S_n^-(x) \quad (6.1a)$$

$$\begin{aligned}
 \mathcal{J}_n^-(x) = & \frac{i S_n^-(0)}{x - \Delta - \sum_{\tilde{k}} \frac{g^2}{x - \omega_{\tilde{k}}}} + \sum_{\substack{n'=1 \\ (n' \neq n)}}^N \frac{1}{x - \Delta - \sum_{\tilde{k}'} \frac{g^2}{x - \omega_{\tilde{k}'}}} \sum_{\tilde{k}} \frac{g^2 e^{-i\tilde{k} \cdot (\tilde{r}_n - \tilde{r}_{n'})}}{x - \omega_{\tilde{k}}} \\
 & \times \mathcal{J}_{n'}^-(x) .
 \end{aligned} \tag{6.1b}$$

In these equations we have dropped terms containing the phonon operator $b_{\tilde{k}}(0)$, under the assumption that initially at time $t=0$ only a single atom is excited and no phonons are present. We assume that there are N two-level atoms at positions $\tilde{r}_1, \tilde{r}_2, \dots, \tilde{r}_N$. Recall that the first term on the right hand side of (6.1b) describes the spontaneous decay of atom n and that the second term describes the influence on atom n of the excitations coming from other atoms n' . (To derive the rate equations we dropped this term.) We can solve (6.1b) formally by considering it to be a matrix equation with indices n, n' . Define the $N \times N$ path matrix (all matrices in this thesis denoted by carats)

$$\hat{P}_{n,n'}(x) \equiv \begin{cases} A^{\text{atom}}(x) \cdot \hat{A}_{n,n'}^{\text{ph}}(x) , & \text{for } n \neq n' \\ 0 & , \text{ for } n = n' , \end{cases} \tag{6.2}$$

where

$$A^{\text{atom}}(x) = \frac{1}{x - \Delta - \sum_{\tilde{k}} \frac{g^2}{x - \omega_{\tilde{k}}}} \tag{6.3}$$

is (the Fourier transform of) the amplitude that an initially excited atom is still excited, and

$$A_{n,n'}^{\text{ph}}(x) = \sum_{\vec{k}} \frac{g^2 e^{i\vec{k} \cdot (\vec{r}_n - \vec{r}_{n'})}}{x - \omega_{\vec{k}}} \quad (6.4)$$

is the amplitude that a phonon is emitted by atom n' and absorbed by atom n . We can write (6.1b) as

$$\mathcal{J}_n^-(x) = iA^{\text{atom}}(x)S_n^-(0) + \sum_{n' \neq 1}^N \hat{P}_{nn'}(x) \mathcal{J}_{n'}^-(x). \quad (6.5)$$

This matrix equation can be formally inverted to yield

$$\mathcal{J}_{n_2}^-(x) = (\hat{1} - \hat{P})_{n_2, n_1}^{-1} iA^{\text{atom}}(x)S_{n_1}^-(0). \quad (6.6)$$

Here $\hat{1}$ is the unit matrix $\hat{1}_{ij} = \delta_{ij}$.

Eq. (6.6) has the following interpretation: $iS_{n_1}^-(0)$ is the probability amplitude that atom n_1 is excited at time $t=0$. $(\hat{1} - \hat{P})_{n_2, n_1}^{-1}$ is the probability amplitude that an excitation leaves atom n_1 and reaches atom n_2 . A^{atom} is then the amplitude that atom n_2 does not decay. The product of these amplitudes gives (after a Fourier transform) the amplitude that atom n_2 is excited at time t . Eq. (6.6) can be given an interesting pictorial representation.

Denote

$$\textcircled{\text{O}} \equiv A^{\text{atom}} \quad (6.7)$$

and

$$\overset{\curvearrowright}{n_1 \quad n_2} \equiv \hat{A}_{n_2, n_1}^{\text{ph}} \quad (6.8)$$

so that

$$\begin{array}{c} \text{---} \circ \text{---} \\ n_1 \qquad n_2 \neq n_1 \end{array} \equiv \hat{P}_{n_2, n_1}^n . \quad (6.9)$$

Then Eq. (6.6) can be represented pictorially as

$$\begin{aligned}
 \mathcal{S}_{n_2}^-(x) = & -i S_{n_1}^-(0) \left\{ \delta_{n_1, n_2} \cdot \begin{array}{c} \text{---} \circ \text{---} \\ n_1 \end{array} + \begin{array}{c} \text{---} \circ \text{---} \text{---} \circ \text{---} \\ n_1 \qquad n_2 \neq n_1 \end{array} + \right. \\
 & + \sum_{n' \neq n_1, n_2} \begin{array}{c} \begin{array}{c} \text{---} \circ \text{---} \\ n_1 \end{array} \text{---} \begin{array}{c} \text{---} \circ \text{---} \\ n_2 \end{array} \\ \qquad \qquad \qquad \downarrow \\ \qquad \qquad \qquad \begin{array}{c} \text{---} \circ \text{---} \\ n' \end{array} \end{array} + \sum_{\substack{n' \neq n_1, n'' \\ n'' \neq n', n_2}} \begin{array}{c} \begin{array}{c} \text{---} \circ \text{---} \\ n_1 \end{array} \text{---} \begin{array}{c} \text{---} \circ \text{---} \\ n' \end{array} \text{---} \begin{array}{c} \text{---} \circ \text{---} \\ n'' \end{array} \text{---} \begin{array}{c} \text{---} \circ \text{---} \\ n_2 \end{array} \\ \qquad \qquad \qquad \downarrow \qquad \qquad \downarrow \\ \qquad \qquad \qquad \begin{array}{c} \text{---} \circ \text{---} \\ n' \end{array} \qquad \begin{array}{c} \text{---} \circ \text{---} \\ n'' \end{array} \end{array} \\
 & \left. + \dots \right\} \quad (6.10)
 \end{aligned}$$

where we have made the binomial expansion

$$(\hat{1} - \hat{P})^{-1} = \hat{1} + \hat{P} + \hat{P}^2 + \hat{P}^3 + \dots \quad (6.11)$$

In other words the amplitude that atom n_2 becomes excited is given by the sum of the amplitudes over all possible paths by which the excitations can go from atom n_1 to n_2 . Eqs. (6.9) and (6.10) show that \hat{P}_{n_2, n_1}^n is the amplitude for an excitation to have exactly n interactions before arriving at atom n_2 , the emission from atom n_1 counting as the first interaction.

Notice that in (6.10) an arrow representing a phonon cannot begin and end on the same atom (without going

through at least one other atom first; cf. (6.2)). The reason is that those diagrams would represent self-interactions causing the process of spontaneous decay, and they have already been included in the amplitude A^{atom} to all orders. This can be seen by denoting the amplitude of a free uncoupled atom by

$$\bullet \equiv A_O^{\text{atom}}(x) \equiv \frac{1}{x - \Delta} \quad , \quad (6.12)$$


and expanding the amplitude $A^{\text{atom}}(x)$ (cf. (6.3)) about A_O^{atom} to get

$$A^{\text{atom}}(x) = \frac{1}{x - \Delta} \sum_{n=0}^{\infty} \left[\frac{\sum_{\tilde{k}} \frac{g^2}{x - \omega_{\tilde{k}}} }{x - \Delta} \right]^n = \sum_{n=0}^{\infty} (A_O^{\text{atom}}(x))^{n+1} (\hat{A}_{1,1}^{\text{ph}}(x))^n$$

$$= \textcircled{\bullet} = \bullet + \textcircled{\bullet} + \textcircled{\textcircled{\bullet}} + \textcircled{\textcircled{\textcircled{\bullet}}} + \dots \quad (6.13)$$

To find $S_{n_2}^-(t)$, i.e. to inverse-Fourier transform Eq. (6.6), we note that $\mathcal{S}_{n_2}^-(x)$ can be expressed as some complicated function of $A^{\text{atom}}(x)$ and $\hat{A}^{\text{ph}}(x)$. Thus $\mathcal{S}_{n_2}^-(x)$ must have a branch cut along the interval $0 < x < \omega_D$.

Assuming that the resonance frequency Δ lies well inside this interval we can ignore any poles along the real axis outside this interval and evaluate $S_{n_2}^-(t)$ using the deformed contour



complex
x-plane (6.14)

This yields

$$\begin{aligned}
S_{n_2}^-(t) &\equiv -\frac{1}{2\pi} \oint_{\mathcal{C}} dx e^{-ixt} \varphi_{n_2}^-(x) \\
&= \lim_{\varepsilon \rightarrow 0} \frac{1}{2\pi i} S_{n_1}^-(0) \int_0^{\omega_D} dx e^{-ixt} \left\{ A^{\text{atom}}(x-i\varepsilon) (\hat{1} - \hat{P}(x-i\varepsilon))_{n_2, n_1}^{-1} \right. \\
&\quad \left. - \text{c.c.} \right\} \quad (6.15)
\end{aligned}$$

(6.15) is our fundamental equation giving the probability amplitude that atom n_2 is excited at time t given that atom n_1 alone was excited at time $t=0$ in the electron-phonon system. Our program now is to evaluate the amplitude A^{atom} and the amplitude matrix \hat{A}^{ph} which occur in the integrand of (6.15).

From Chapter 3 we know that the amplitude $A^{\text{atom}}(x \pm i\varepsilon)$ (where $0 < x < \omega_D$; $\varepsilon \rightarrow 0^+$) that the atom is excited is given by

$$\begin{aligned}
A^{\text{atom}}(x \pm i\varepsilon) &= \frac{1}{x - \Delta - \sum_{\tilde{k}} \frac{g^2}{x \pm i\varepsilon - \omega_{\tilde{k}}}} \\
&= \frac{1}{x - \Delta - g^2 \int_0^{\omega_D} \frac{D(\omega) d\omega}{x \pm i\varepsilon - \omega}} \\
&\approx \frac{1}{x - \Delta' \pm \frac{i\Gamma}{2}} \quad , \quad (6.16)
\end{aligned}$$

where

$$\Delta' = \Delta - g^2 \rho \int_0^{\omega_D} \frac{d\omega D(\omega) \Omega}{\omega - \Delta} \quad , \quad (6.17a)$$

and

$$\Gamma = 2\pi g^2 \Omega D(\Delta) \quad . \quad (2.17b)$$

We recall that the density of phonon modes $D(\omega)d\omega$ per unit volume in frequency interval $d\omega$ is given in one dimension by

$$D(\omega)d\omega = \frac{N}{\omega_D \Omega} d\omega \quad (6.17c)$$

(Ω is the length of the crystal), and in 3 dimensions by

$$D(\omega)d\omega = \sum_s D_{(s)}(\omega)d\omega \quad (6.17d)$$

where the density of branch s is (see Eq. (5.4))

$$D_{(s)}(\omega)d\omega = \frac{\omega^2}{2\pi^2 c_{(s)}^3} d\omega \quad . \quad (6.17e)$$

$c_{(s)}$, $s = L, T_1, T_2$, is the speed of sound of phonon branch s .

The Phonon Amplitude Matrix $\hat{A}^{ph}_{n,n'}(x)$

Let us now evaluate the amplitude $\hat{A}_{n,n'}(x \pm i\varepsilon)$ ($0 < x < \omega_D$; $\varepsilon \rightarrow 0^+$) that a phonon emitted by atom n' is absorbed by atom n . We first do the 1-dimensional case.

1-Dimension:

In this case denoting $|r_n - r_{n'}| \equiv r$, $\omega = c|k|$, and $\Gamma \equiv 2\pi g^2 N / \omega_D$, we get

$$\begin{aligned} \hat{A}_{n,n'}^{ph}(x \pm i\varepsilon) &= \sum_k \frac{g^2 e^{ik \cdot (r_n - r_{n'})}}{x \pm i\varepsilon - \omega_k} = \frac{N}{\omega_D} \int_0^{\omega_D} \frac{g^2 \cos \frac{\omega r}{c} d\omega}{x - \omega \pm i\varepsilon} \\ &= -\frac{\Gamma}{2\pi} \left\{ \cos\left(\frac{xr}{c}\right) \cdot \left[\text{Ci}\left(\frac{\omega_D - x}{c} r\right) - \text{Ci}\left(\frac{x}{c} r\right) \right] - \sin\left(\frac{xr}{c}\right) \cdot \right. \\ &\quad \left. \cdot \left[\text{Si}\left(\frac{xr}{c}\right) + \text{Si}\left(\frac{\omega_D - x}{c} r\right) \right] \pm i\pi \cos\left(\frac{xr}{c}\right) \right\} , \end{aligned} \quad (6.18)$$

where $\text{Si}(x)$ and $\text{Ci}(x)$ are the sine and cosine integrals⁵⁵ defined by

$$\text{Si}(x) \equiv \int_0^x \frac{\sin t}{t} dt \approx \begin{cases} x & \text{for } x \ll 1 \\ \frac{\pi}{2} - \frac{\cos x}{x} & \text{for } x \gg 1, \end{cases} \quad (6.19)$$

and

$$\begin{aligned} \text{Ci}(x) &\equiv \gamma + \ln x + \int_0^x \frac{\cos(t) - 1}{t} dt \\ &\equiv - \int_x^\infty \frac{\cos t}{t} dt \approx \begin{cases} \ln x & \text{for } x \ll 1 \\ \frac{\sin x}{x} & \text{for } x \gg 1. \end{cases} \end{aligned} \quad (6.20)$$

In the limits of small and large separations $|r_n - r_{n'}|$ we get respectively

$$\hat{A}_{n,n'}^{\text{ph}}(x \pm i\epsilon) = \begin{cases} -\frac{\Gamma}{2\pi} \left(\ln \frac{\omega_D^{-x}}{x} \pm i\pi \right) & \text{for } r \equiv |r_n - r_{n'}| < \frac{c}{x} \quad (6.21a) \\ \mp \frac{i\Gamma}{2} e^{i\frac{x}{c}r} & \text{for } r \equiv |r_n - r_{n'}| > \frac{c}{x} \quad (6.21b) \end{cases}$$

3-Dimensions:

In the 3-dimensional case we use the geometry shown below where $r_{\tilde{n}} - r_{\tilde{n}'}$ is along the z-axis:

$$(6.22)$$

In the continuum limit we replace

$$\sum_{\tilde{k}} \rightarrow \frac{\Omega}{4\pi} \sum_{s=L, T_1, T_2} \int_0^{\omega_D} D(s)(\omega) \int_0^{2\pi} d\phi \int_{-1}^1 d(\cos \theta), \quad (6.23)$$

where

$$D(s)(\omega) = \frac{\omega^2 d\omega}{2\pi^2 c(s)^3} \quad (6.24)$$

is the density per cm^3 of phonon modes of type s in the interval $d\omega$, and $c(s)$ is the speed of sound of mode type s . The phonon amplitude (6.4) becomes, after integrating over θ and ϕ ,

$$\hat{A}_{n,n'}^{\text{ph}}(x \pm i\epsilon) = \sum_{s=L, T_1, T_2} A_{n,n',(s)}^{\text{ph}}(x \pm i\epsilon), \quad (6.25)$$

where the amplitude for phonons of type s is

$$\hat{A}_{n,n',(s)}^{\text{ph}}(x \pm i\epsilon) = -\frac{\Omega c(s) g^2}{r} \int_0^{\omega_D} d\omega D(s)(\omega) \frac{\sin \frac{\omega}{c(s)} r}{\omega(\omega - x \mp i\epsilon)}, \quad (6.26)$$

where $r \equiv |\mathbf{r}_n - \mathbf{r}_{n'}|$. After some algebra we find that in the

limit of small and large separations respectively this amplitude becomes

$$\hat{A}_{n,n', (s)}^{\text{ph}}(x \pm i\varepsilon) = \begin{cases} -\Omega g^2 \left(\int_0^\omega d\omega \frac{D_{(s)}(\omega)}{\omega - x} \pm i\pi D_{(s)}(x) \right), & \text{for } r \ll \frac{c(s)}{x} \\ -\Omega g^2 D_{(s)}(x) \frac{e^{\pm i \frac{xr}{c(s)}}}{\frac{xr}{c(s)}}, & \text{for } r \gg \frac{c(s)}{x} \end{cases} \quad (6.27a)$$

Let us make the usual approximation that only frequencies near resonance are important so that we may replace $x \rightarrow \Delta$ everywhere except in the phases in the phonon amplitudes $\hat{A}_{n,n'}^{\text{ph}}$, given by (6.21) and (6.27) for 1- and 3-dimensions respectively. Then we get for small separations $|r_{\tilde{n}} - r_{\tilde{n}}| \ll c/\Delta$ that (see (6.17a,b))

$$\hat{A}_{n,n'}^{\text{ph}}(x \pm i\varepsilon) = \Delta' - \Delta \mp \frac{i\Gamma}{2} \quad (6.28)$$

in both one and three dimensions, and for large separations $|r_{\tilde{n}} - r_{\tilde{n}}| \equiv r \gg c/\Delta$, that

$$\hat{A}_{n,n'}^{\text{ph}}(x \pm i\varepsilon) = \mp \frac{i\Gamma}{2} e^{\pm i \frac{x}{c} r} \quad (6.29)$$

in one dimension, and

$$\hat{A}_{n,n', (s)}^{\text{ph}}(x \pm i\varepsilon) = -\frac{\Gamma}{2} \frac{e^{i \frac{x}{c(s)} r}}{\frac{\Delta}{c(s)} r} \quad (6.30)$$

in three dimensions. In Eqs. (6.28)-(6.30), Δ' and Γ are given by (6.17a-e).

Notice the following features of (6.28)-(6.30). We first suppose that $|\mathbf{r}_{\tilde{n}} - \mathbf{r}_{\tilde{n}'}| \gg c/\Delta = \lambda(\Delta)/(2\pi)$, i.e. that atoms n and n' are separated by a distance large compared to a resonance wavelength $\lambda(\Delta)$. Then the phonon amplitude $\hat{A}_{n,n'}^{\text{ph}}(\mathbf{x} + i\epsilon)$ has the form of a plane wave $\propto e^{\frac{i\mathbf{x}}{c}|\mathbf{r}_{\tilde{n}} - \mathbf{r}_{\tilde{n}'}|}$ in 1-dimension and of a spherical wave $\propto e^{\frac{i\mathbf{x}}{c}|\mathbf{r}_{\tilde{n}} - \mathbf{r}_{\tilde{n}'}|}/|\mathbf{r}_{\tilde{n}} - \mathbf{r}_{\tilde{n}'}|$ in 3-dimensions, propagating from atom n' to n . Next suppose that $|\mathbf{r}_{\tilde{n}} - \mathbf{r}_{\tilde{n}'}| \ll c/\Delta = \frac{\lambda(\Delta)}{2\pi}$, i.e. that atoms n and n' are separated by a distance less than $\frac{1}{2\pi}$ times the resonance wavelength. Then the amplitude $\hat{A}_{n,n'}^{\text{ph}}(\mathbf{x})$ has the form of a virtual phonon cloud rather than a plane wave. This is evidenced by the fact that $\hat{A}_{n,n'}^{\text{ph}}(\mathbf{x} + i\epsilon)$ is just the shift $\Delta' - \Delta - \frac{i\Gamma}{2}$ of the resonance frequency of a single atom undergoing spontaneous decay. Thus at these short distances the two atoms n and n' sit in the same phonon cloud and we expect that the evolution of the decaying atom is greatly affected by the second atom. Indeed we will show presently that under these circumstances we regain Dicke's results on radiation trapping (see Section 2.2).

Having evaluated the amplitude A^{atom} and the amplitude matrix \hat{A}^{ph} in both one and three dimensions, we proceed and evaluate the matrix quantity $(\hat{1} - \hat{P}(\mathbf{x} + i\epsilon))^{-1}$ occurring in the integrand of (6.15). In one dimension we get

$$(\hat{l} - \hat{P}(x+i\varepsilon))^{-1} = \begin{pmatrix} 1 & \frac{\frac{i\Gamma}{2} e^{i\frac{x}{c}r_{ij}}}{x - \Delta' + \frac{i\Gamma}{2}} & & \\ & 1 & & \\ & & \ddots & \\ & & & 1 \end{pmatrix} \quad (6.31)$$

where the separation $r_{ij} \equiv |r_i - r_j|$ of atom i and atom j is assumed large enough that the phonon amplitude has the form of a plane wave. Note the following features. For frequencies x far from the resonance frequency Δ' the off-diagonal elements of $(\hat{l} - \hat{P})$ are small and the binomial series expansion of $(\hat{l} - \hat{P})^{-1}$ will converge fairly rapidly. Physically this means that phonons far from resonance may escape from the system after interacting with only a few atoms. Various authors⁵⁶ have studied the simplest model of a single atom perturbing the lineshape emitted by an excited atom (the single particle approximation). This model gives a good description of the wings of the lineshape but breaks down near resonance. Exactly on resonance the ij element of $\hat{l} - \hat{P}$ is given by

$$(\hat{l} - \hat{P})_{ij} = e^{i\frac{x}{c}r_{ij}} \quad , \quad (6.32)$$

with modulus one. Thus on resonance the binomial expansion of $(\hat{l} - \hat{P})^{-1}$ will not converge because all numbers of interactions become important⁵⁷. The only recourse then is to look for exact solutions of (6.32), i.e. solutions to all orders of perturbation theory, which we do in the next section. It should be noted that in three dimensions the ij element ($i \neq j$) of $(\hat{l} - \hat{P}(x+i\epsilon))$ on resonance is given by

$$(\hat{l} - \hat{P})_{ij} = \frac{-i \frac{c}{\Delta} e^{i \frac{x}{c} r_{ij}}}{r_{ij}} . \quad (6.33)$$

Although this matrix element is inversely proportional to the separation r_{ij} of the atoms, and therefore is small for low densities of Cr^{3+} ions, it is compensated by the fact that the number of atoms in a shell of radius r_{ij} about atom i is proportional to r_{ij}^2 . Thus also in three dimensions we expect the expansion of $(\hat{l} - \hat{P})^{-1}$ to diverge on resonance.

Besides the divergence problem, the expansion of $(\hat{l} - \hat{P})^{-1}$ does not conserve probability (i.e. the number of excitations or energy of the system) if the series is cut off at any finite order. For example cutting the series off at first order, we get

$$(\hat{1} - \hat{P}(x+i\epsilon))^{-1} \approx \hat{1} + \hat{P}(x+i\epsilon)$$

$$= \begin{pmatrix} 1 & \frac{-\frac{i\Gamma}{2} e^{i\frac{x}{c} r_{ij}}}{x - \Delta' + \frac{i\Gamma}{2}} \\ & \ddots \\ \frac{-\frac{i\Gamma}{2} e^{i\frac{x}{c} r_{ij}}}{x - \Delta' + \frac{i\Gamma}{2}} & 1 \end{pmatrix} \quad (6.34)$$

Plugging (6.34) for $(\hat{1} - \hat{P})^{-1}$ and (6.16) for A^{atom} into (6.15) we find that the probability that atom j is excited at time t given that atom i was excited at time $t=0$ is given by

$$\begin{aligned} N_j^\uparrow(t) \Big|_{\text{to first order}} &= \langle \begin{pmatrix} 1 \\ 0 \end{pmatrix}_i | S_j^+(t) S_j^-(t) | \begin{pmatrix} 1 \\ 0 \end{pmatrix}_i \rangle \\ &= \left| \int_0^\omega dx e^{-ixt} \frac{1}{2\pi i} \left\{ \frac{-\frac{i\Gamma}{2} e^{i\frac{x}{c} r_{ij}}}{x - \Delta' - \frac{i\Gamma}{2}} - \text{c.c.} \right\} \right| \quad (6.35) \end{aligned}$$

regardless of the number $N-2$ of other atoms in the system. But this is nonsensical because if there are for example N_j atoms in the system under conditions identical to those of atom j then the probability that any particular one of them becomes excited must be proportional to $1/N_j$.

Evidently the higher order terms of the expansion of $(\hat{l} - \hat{P})^{-1}$ are essential in that they contribute probability amplitudes which interfere with the lowest order amplitude in such a way that overall probability is conserved.

6.2 Exact Results

We saw in Section 6.1 that a series expansion of $(\hat{l} - \hat{P})^{-1}$ in powers of \hat{P} cut off at any finite order diverges as well as gives incorrect results. Thus in this section we attempt to find $(\hat{l} - \hat{P})^{-1}$ exactly. This can be done for several special cases.

Two-Atom System in One Dimension

Consider the case of two two-level atoms, labelled 1 and 2, separated by a distance $r_{12} \equiv |r_1 - r_2| \gg c/\Delta$, i.e. large compared to the resonance wavelength. In this case the phonon amplitude is a plane wave and we find that

$$\hat{l} - \hat{P}(x+i\epsilon) = \begin{pmatrix} 1 & -p \\ -p & 1 \end{pmatrix}, \quad (6.36)$$

where

$$p = \frac{-\frac{i\Gamma}{2} e^{i\frac{x}{c}r_{12}}}{x - \Delta' + \frac{i\Gamma}{2}}. \quad (6.37)$$

Although $\hat{l} - \hat{P}$ can easily be inverted exactly, namely

$$(\hat{l} - \hat{P})^{-1} = \frac{1}{1-p^2} \begin{pmatrix} 1 & p \\ p & 1 \end{pmatrix} \quad (6.38)$$

we may also find it by expanding in powers of \hat{P} to give

$$\begin{aligned}
 (\hat{1} - \hat{P})^{-1} &= \hat{1} + \hat{P} + \hat{P}^2 + \hat{P}^3 + \dots \\
 &= \begin{pmatrix} 1 & 0 \\ 0 & 1 \end{pmatrix} + \begin{pmatrix} 0 & p \\ p & 0 \end{pmatrix} + \begin{pmatrix} p^2 & 0 \\ 0 & p^2 \end{pmatrix} + \begin{pmatrix} 0 & p^3 \\ p^3 & 0 \end{pmatrix} + \dots \\
 \text{order:} \quad & \quad (0) \quad \quad (1) \quad \quad (2) \quad \quad (3) \quad \dots \quad (6.39)
 \end{aligned}$$

The probability that atom n ($n=1,2$) is excited at time t , given that atom 1 was excited at time $t=0$, is given by

$$\begin{aligned}
 N_n^\uparrow(t) &= \langle \begin{pmatrix} 1 \\ 0 \end{pmatrix}_1 | S_n^+(t) S_n^-(t) | \begin{pmatrix} 1 \\ 0 \end{pmatrix}_1 \rangle \\
 &= \left| \int_0^\omega dx e^{-ixt} F_n(x) \right|^2, \quad (6.40)
 \end{aligned}$$

where

$$F_n(x) = \lim_{\varepsilon \rightarrow 0} \frac{-1}{2\pi i} \left[\frac{(\hat{1} - \hat{P}(x+i\varepsilon))_{n,1}^{-1}}{x - \Delta' + \frac{i\Gamma}{2}} - \text{c.c.} \right]. \quad (6.41)$$

We can compare the results of the exact inversion and the series expansion inversion of $(\hat{1} - \hat{P})$ by looking at Figs. 6.1 and 6.2. Fig. 6.1a and b respectively show the quantities $F_1(x)$ and $F_2(x)$ (which are proportional to the Fourier transforms of the amplitudes $S_1^-(t)$ and $S_2^-(t)$ of the two atoms) with the matrix $(\hat{1} - \hat{P})^{-1}$ calculated to various orders. For example in Figs. 6.1a_{1,2,3} the series $(\hat{1} - \hat{P})^{-1} = \sum_{n=0}^{\infty} \hat{P}^n$ has been cut off after the terms $n=1,3$, and ∞ respectively. Figs. 6.2a and b then show respectively the probabilities $N_1^\uparrow(t)$ and $N_2^\uparrow(t)$ that the first

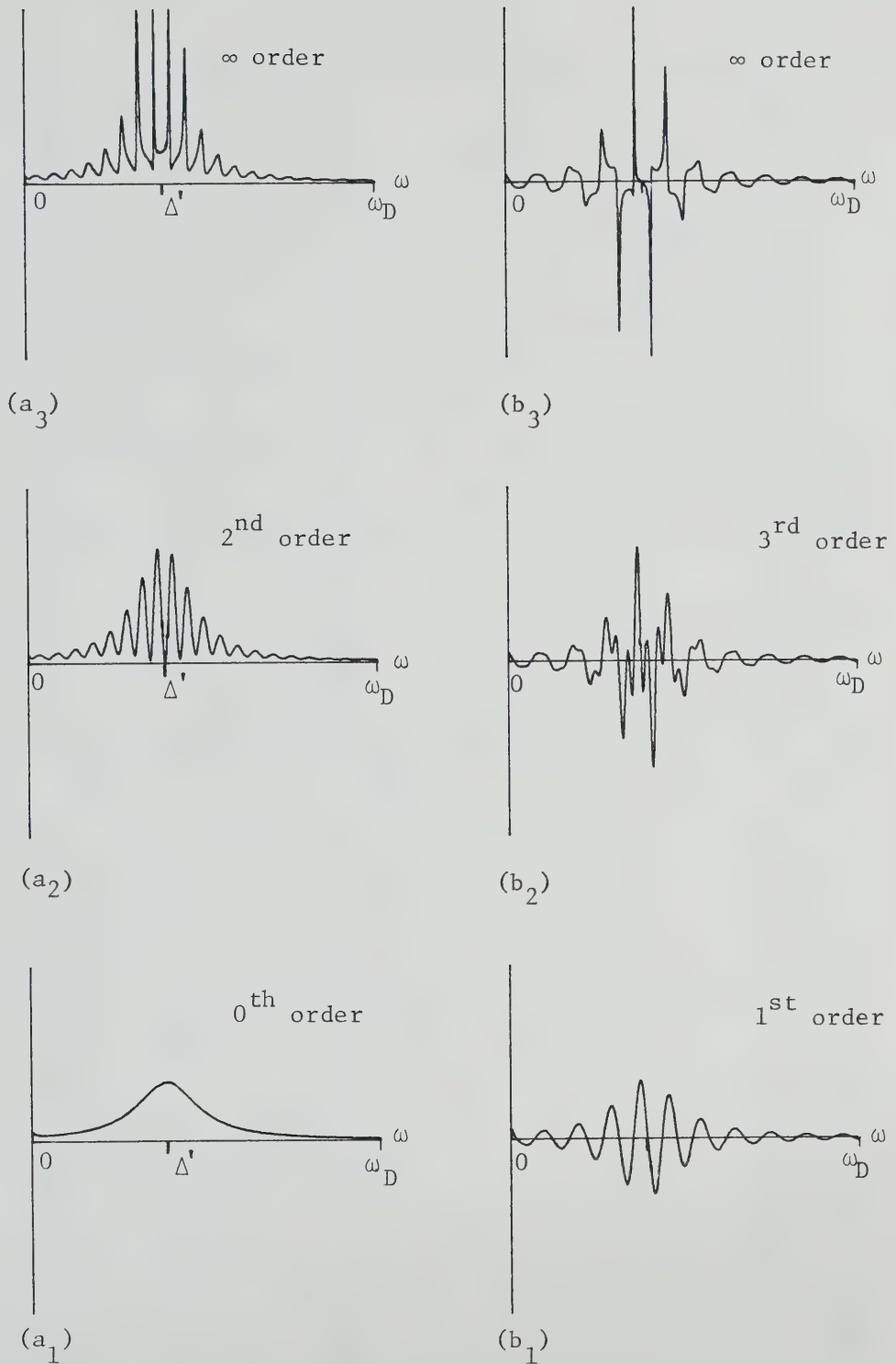


Fig. 6.1. (a_{1,2,3}) The Fourier transform of the probability amplitude that the initially excited atom 1 is still excited at time t , calculated to order 0, 2, and ∞ in \hat{P} respectively; (b_{1,2,3}) The same quantity for the initially unexcited atom 2 to order 1, 3 and ∞ respectively. Parameters: $\Delta = .4\omega_D$, $\Gamma = .2\omega_D$, and $r_{12} = 60 \text{ c}/\omega_D$.

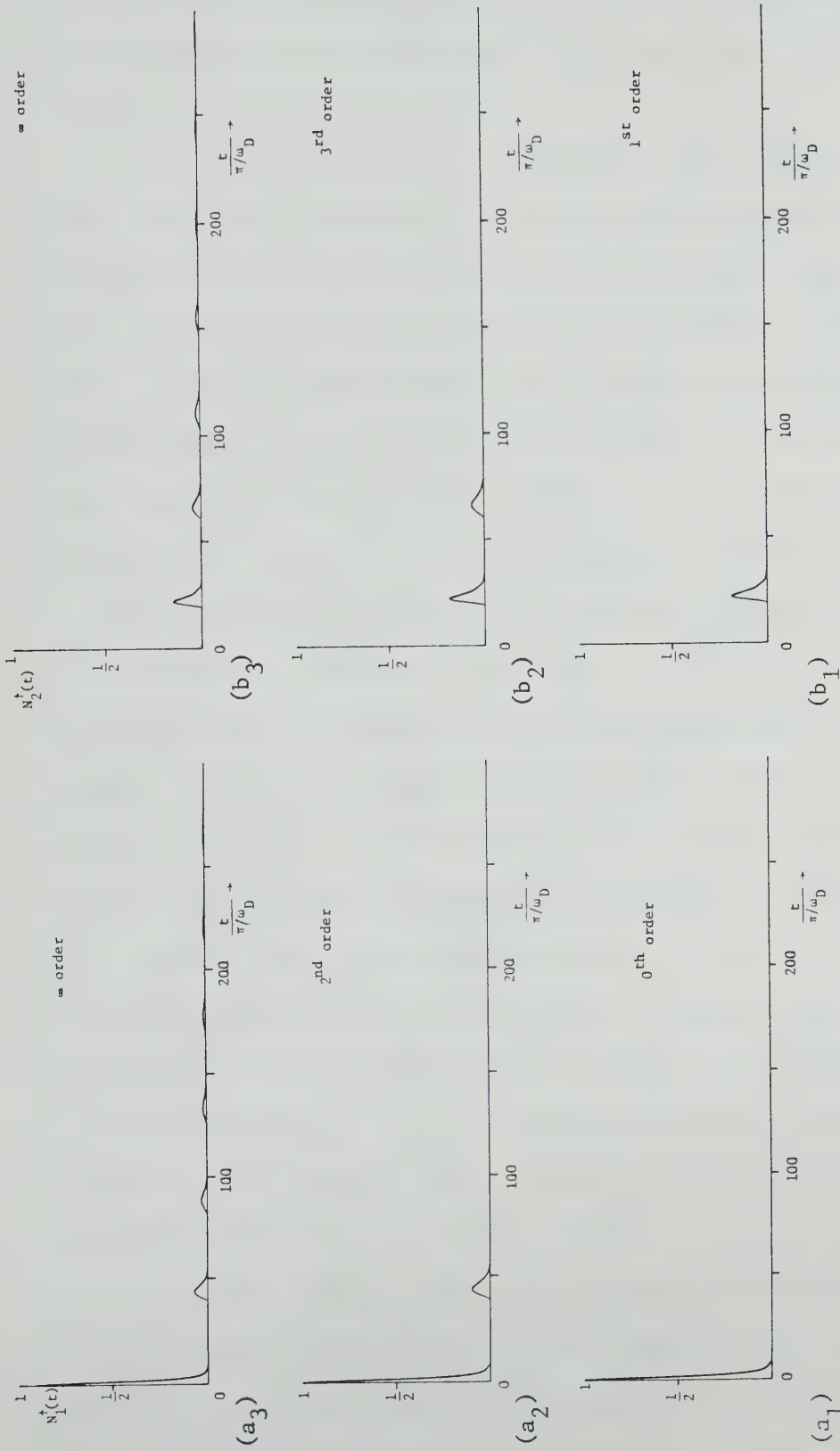


Fig. 6.2 The probability that atoms 1 and 2 are excited at time t , calculated to the various orders in \hat{p} indicated, from the inverse Fourier transforms of the respective diagrams of Fig. 6.1. See Fig. 6.1 and text.

and second atoms are excited at time t , calculated from the corresponding quantities $F_1(x)$ and $F_2(x)$ of Figs. 6.1a and b.

Notice the following features. Eq. (6.39) shows that only even (odd) powers of P in the expansion of $(\hat{l} - \hat{P})^{-1}$ contribute to the probability amplitude for atom one (two). Fig. 6.2a shows that to zeroth order in the expansion, atom 1 decays exponentially and is never re-excited. To second order, atom 1 has a probability of being re-excited once more at time $t = \frac{2r_{12}}{c}$, which is just the time it takes a phonon to travel to atom 2 and back. Keeping all orders in the expansion of $(\hat{l} - \hat{P})^{-1}$ yields the result that atom 1 is repeatedly re-excited at times $t = \frac{2r_{12}}{c} \cdot n$, $n = 1, 2, 3, \dots$ as the phonon is repeatedly reflected between the two atoms. After each transit the probability of the atom becoming excited is less because the phonon has a finite probability of being transmitted as well as reflected back.

Notice that the single pulse in Fig. 6.2a₂ is higher than the same pulse of Fig. 6.2a₃. This is an example showing that the probability (of the first re-excitation) is incorrect when $(\hat{l} - \hat{P})^{-1}$ is cut off after second order. Evidently the higher order terms in the series reduce the probability as we said after (6.35).

All features of Fig. 6.2 can be understood in terms of the Fourier transforms of the probability amplitudes shown in Fig. 6.1. Let us discuss the Fourier transforms for atom 1 which are shown in Fig. 6.1a. To zeroth order

the transform is just a Lorentzian leading to simple exponential decay. To second order Eqs. (6.37) and (6.39) show that the Lorentzian has an oscillation

$$\left(\frac{i\Gamma/2}{x - \Delta' + \frac{i\Gamma}{2}} \right)^2 e^{\frac{ix}{c} 2r_{12}} \quad (6.42)$$

added to it. The envelope of the oscillation is largest on resonance and the maxima occur at frequencies satisfying the condition

$$e^{\frac{ix}{c} 2r_{12}} = e^{2\pi i n} = 1$$

$$\longleftrightarrow x = \frac{\pi n c}{r_{12}}, \quad n = 1, 2, \dots, \infty \quad (6.43)$$

The wavelengths corresponding to these frequencies satisfy

$$\lambda(x) \equiv \frac{2\pi c}{x} = \frac{2r_{12}}{n}, \quad n = 1, 2, \dots, \infty,$$

i.e. the n^{th} peak in the spectrum occurs at a wavelength such that exactly n wavelengths fit in the distance $2r_{12}$. In other words a peak in the spectrum occurs when a standing wave is set up between atom 1 and 2, the height of the peak being the greatest for wavelengths near resonance. Finally including all the higher numbers of phonon reflections gives the spiked spectrum of Fig. 6.1a₃. Simple Fourier analysis gives the result that the spacing between the peaks in frequency space is inversely proportional to the period of the system. Specifically the re-excitation

pulses of atom 1 shown in Fig. 6.2a₃ occur at times

$$t = \frac{2\pi}{x_{i+1} - x_i} \cdot n = \frac{2r_{12}}{c} \cdot n, \quad n = 1, 2, \dots, \infty. \quad (6.45)$$

The narrowness of the spikes in Fig. 6.1a₃ yields the large number of re-excitation of Fig. 6.2a₃.

An important case occurs when $T_1 > 2r_{12}/c$, i.e. when the lifetime T_1 of the decaying atom is longer than the time it takes the emitted phonon to be reflected back to the atom. Then the Lorentzian is narrower than the spacing between the spikes, and the decay of the atom depends crucially on whether or not the Lorentzian overlaps with one of the spikes. In the case that it does not, the resulting lineshape is approximately the original Lorentzian and the excited atom decays in a time $t \approx T_1$ more or less unaffected by the second atom. However in the case that the Lorentzian does overlap with one of the spikes, the resulting lineshape is much narrower than the original Lorentzian. Physically this means that the resonant phonon has formed a strong standing wave between the two atoms and the two-atom system decays very slowly in a time $T_1^{\text{eff}} \gg T_1$.

Let us consider whether or not this phenomenon can occur in optically pumped ruby. It must be noted that since ruby is a three-dimensional system, the amplitude for a phonon to be emitted by atom 1 and absorbed by atom 2 is given by

$$\hat{P}(x+i\epsilon)_{12} = \frac{-\frac{\Gamma}{2} e^{+i\frac{x}{c}r_{12}}}{\frac{\Delta r_{12}}{c} (x - \Delta' + \frac{i\Gamma}{2})} .$$

This is the same as the one-dimensional amplitude (6.37) except that in this case the amplitude decreases with the atom separation r_{12} . Therefore for a resonance to occur between two atoms in three dimensions we have in addition to the former standing wave conditions that $r_{12} = n/2$ and $r_{12} < T_1 c/2$, the new condition that $r_{12} \lesssim c/\Delta$ i.e. that the separation r_{12} is not much larger than a resonance wavelength. The wavelength of phonons resonant between the $2\bar{A}$ and \bar{E} levels in ruby is $\lambda_0 \approx 10^{-6}$ cm. Assuming that the average distance between neighboring Cr^{3+} ions at a density N^* is $\langle r_{n.n.} \rangle = N^{*-1/3}$, we see that at a density $N^* \approx 10^{18} \text{ cm}^{-3}$, $\langle r_{n.n.} \rangle = \lambda_0$, i.e. nearest neighbors are on the average a resonance wavelength apart. Thus at this density we expect many Cr^{3+} ion pairs to satisfy the standing wave conditions. It should be pointed out that a proper calculation would involve studying the radial distribution function for excited Cr^{3+} ions in ruby. The radial distribution function $n_2(r_{12})$ is proportional to the probability that given a Cr^{3+} ion is located at some position r_1 , a second ion is located a distance r_{12} from that ion. This function would depend on how the crystal was grown, etc. In general $n_2(r_{12})$ is a maximum near

$r_{12} = \langle r_{n.n.} \rangle$. If we assume, as is the case in liquids⁵⁷, that this maximum is rather broad, then even at densities lower than $N^* \approx 10^{18} \text{ cm}^{-3}$ we expect the standing wave condition to be satisfied for many ion pairs. Although more study is required, we conclude that this phenomenon could account for the long effective lifetime T_1^{eff} noted in the rate equation analysis of Chapter 5.

N Atoms, All at the Same Position

Another case that can be solved exactly is the system of N distinguishable atoms all at the same position. In practice this would occur if the atoms were more than a deBroglie wavelength apart (i.e. distinguishable) but less than a resonance radiation wavelength apart. This is the system studied by Dicke³⁰ (see Section 2.2). It is easy to verify that for this case the inverse of the matrix

$$\frac{1}{A^{\text{atom}}(x+i\epsilon)} (\hat{1} - \hat{P}(x+i\epsilon)) = \begin{pmatrix} a & & & & \\ & b & & & \\ & & \ddots & & \\ & & & \ddots & \\ b & & & & a \end{pmatrix} \quad (6.46a)$$

where

$$a = x - \Delta' + \frac{i\Gamma}{2} \quad , \quad (6.46b)$$

and

$$b = \Delta - \Delta' + \frac{i\Gamma}{2} \quad , \quad (6.46c)$$

is the matrix

$$A^{\text{atom}}(x+i\epsilon) (\hat{1} - \hat{P}(x+i\epsilon))^{-1} = \left(\begin{array}{c} \text{diagram} \end{array} \right) \quad (6.47a)$$

where

$$c = \frac{\frac{N-1}{N}}{x - \Delta} + \frac{\frac{1}{N}}{x - \Delta + N(\Delta - \Delta' + \frac{i\Gamma}{2})} \quad , \quad (6.47b)$$

and

$$d = \frac{-\frac{1}{N}}{x - \Delta} + \frac{\frac{1}{N}}{x - \Delta + N(\Delta - \Delta' + \frac{i\Gamma}{2})} \quad . \quad (6.47c)$$

Plugging (6.47a,b,c) into (6.15) we find that the probability that atom n is excited at time t given that atom 1 was excited at time $t=0$ is

$$\begin{aligned} N_n^{\uparrow}(t) &= \langle \begin{pmatrix} 1 \\ 0 \end{pmatrix}_1 | S_n^+(t) S_n^-(t) | \begin{pmatrix} 1 \\ 0 \end{pmatrix}_1 \rangle \\ &= \left| \left(\delta_{1n} - \frac{1}{N} \right) e^{-i\Delta t} + \frac{1}{N} e^{-i(\Delta - N(\Delta - \Delta'))t} e^{-N\Gamma t/2} \right|^2 \\ &= \begin{cases} e^{-\Gamma t} & , \quad \text{for } t \approx 0 \quad , \quad \text{for } n = 1 \quad , \\ \left(\frac{N-1}{N} \right)^2 & , \quad \text{for } t \rightarrow \infty \quad \text{for atom 1} \quad , \\ \frac{1}{N^2} & , \quad \text{for } t \rightarrow \infty \quad \text{for all } N-1 \text{ other atoms.} \end{cases} \quad (6.48) \end{aligned}$$

(6.48) shows that the probability of non-decay of atom 1 decreases initially at the rate Γ of a single isolated atom but soon becomes fixed at the non-zero value

$N_1^\uparrow(t \rightarrow \infty) = \left(\frac{N-1}{N}\right)^2$. Similarly the other $N-1$ atoms have a probability $1/N^2$ of becoming excited. Hence the probability that a phonon is eventually emitted is only $N_{ph} = 1/N$. This is in complete agreement with Dicke's results on radiation trapping which we presented in Section 2.2

Let us look at the phonon spectrum that is emitted. Plugging (6.1a) and (6.6) into the Fourier transform formula (3.3) we can write

$$b_k(t) = \frac{S_1^-(0)}{2\pi i} \oint_C dx e^{-ixt} \frac{g}{x - \omega_k} \sum_{n=1}^N e^{-ikr_n} A^{\text{atom}}(x) (\hat{1} - \hat{P}(x))_{n,1}^{-1}, \quad (6.49)$$

where C is the contour (3.3a) around the lower half-plane. In this equation, since all atoms are at the same position, we find that

$$\sum_{n=1}^N e^{-ikr_n} A^{\text{atom}}(x+i\epsilon) (\hat{1} - \hat{P}(x+i\epsilon))_{n,1}^{-1} = \frac{1}{x - \Delta + N(\Delta - \Delta' + \frac{i\Gamma}{2})}. \quad (6.50)$$

Thus doing the contour integration we find that

$$b_k(t) = \frac{S_1^-(0) g}{\omega_k - \Delta + N(\Delta - \Delta' + \frac{i\Gamma}{2})} (e^{-i\omega_k t} - e^{-i(\Delta - N(\Delta - \Delta'))t} e^{-N\Gamma t/2}). \quad (6.51)$$

The total number of phonons in the system at time t is given by

$$\begin{aligned}
N_{\text{ph}}(t) &\equiv \sum_k \langle \begin{pmatrix} 1 \\ 0 \end{pmatrix}_1 | b_k^\dagger(t) b_k(t) | \begin{pmatrix} 1 \\ 0 \end{pmatrix}_1 \rangle \\
&= \int_0^\omega d\omega \frac{\Gamma/2\pi}{(\omega - \Delta + N(\Delta - \Delta'))^2 + (\frac{N\Gamma}{2})^2} \left\{ 1 + e^{-N\Gamma t} - 2e^{-N\Gamma t/2} \right. \\
&\quad \left. \times \cos(\omega - \Delta + N(\Delta - \Delta'))t \right\}. \quad (6.52a)
\end{aligned}$$

By either expanding the quantities in braces for $t=0$ or by integrating over ω we can write (6.52a) in the following forms

$$N_{\text{ph}}(t) = \begin{cases} \int_0^\omega d\omega \frac{\Gamma}{2\pi} t^2 & \text{for } t = 0 \end{cases} \quad (6.52b)$$

$$\frac{1}{N} (1 - e^{-N\Gamma t}) = \begin{cases} \Gamma t, & \text{for } t \approx 0 \\ \frac{1}{N}, & \text{for } t \rightarrow \infty \end{cases} \quad (6.52c)$$

Eq. (6.52b) shows that for time $t=0$ a uniform spectrum of phonons is emitted in agreement with the uncertainty relation $\Delta\omega \cdot \Delta t \gtrsim 1$. (6.52b) is identical to the result for the emission spectrum of a single atom for time $t=0$ (see discussion of Eq. (4.13)). (6.52c) shows that for finite but small times the rate of phonon emission is Γ , again the same result as for a single isolated atom. Finally (6.52a and d) together show that after a long time the N atom system has emitted a phonon with probability $1/N$, and that the phonon emission spectrum is Lorentzian with width and shift N times that of the Lorentzian emission spectrum of

a single isolated atom. This is an extreme example of the well-known phenomenon of pressure broadening, i.e. the broadening of the emission spectrum of an atom due to the perturbations of nearby atoms.

N Near Atoms

Having obtained the exact solution to the problem of N atoms at the same position, we can do perturbation theory around that result and consider the case where the N atoms are only near each other. (By near we mean that $\text{Max}(r_{ij}) \ll c/\Delta$ where $\text{Max}(r_{ij})$ is the maximum separation of any two atoms.)

From a mathematical point of view the radiation trapping that occurred in the former exact case is due to the pole at $x = \Delta$ in the probability amplitudes (6.47b and c). When the atoms are separated slightly we expect this pole to move slightly off the real axis to a new position $x = -\frac{\Gamma_{\text{slow}}}{2}$ with the consequence that the trapped radiation slowly leaks away at the rate $\text{Im}(\Gamma_{\text{slow}})$.

Let us begin by defining the matrices

$$\hat{\mathcal{L}}_0(x) \equiv \frac{1}{A_{\text{atom}}(x)} (\hat{1} - \hat{P}_0(x)) , \quad (6.53)$$

and

$$\hat{\mathcal{L}}(x) \equiv \frac{1}{A_{\text{atom}}(x)} (\hat{1} - \hat{P}(x)) . \quad (6.54)$$

$\hat{\mathcal{L}}_0$ and $\hat{\mathcal{L}}$ are respectively the zero-order matrix (i.e. the matrix of the former problem defined in (6.46)) and the new perturbed matrix. The difference between these matrices

defines the matrix

$$\begin{aligned}\hat{\varepsilon}(x) &= \hat{\mathcal{L}}(x) - \hat{\mathcal{L}}_0(x) = \frac{1}{A^{\text{atom}}(x)} (\hat{P}_0(x) - \hat{P}(x)) \\ &= \hat{A}_0^{\text{ph}}(x) - \hat{A}^{\text{ph}}(x)\end{aligned}\quad (6.55)$$

$\hat{\mathcal{L}}$ can be inverted by using the fact that

$$\begin{aligned}\hat{\mathcal{L}}_0^{-1} - \hat{1} &= \hat{\varepsilon} \hat{\mathcal{L}}_0^{-1} \\ \longleftrightarrow \hat{\mathcal{L}}^{-1} &= \hat{\mathcal{L}}_0^{-1} (\hat{1} + (\hat{\varepsilon} \hat{\mathcal{L}}_0^{-1}))^{-1} = \hat{\mathcal{L}}_0^{-1} - \hat{\mathcal{L}}_0^{-1} \hat{\varepsilon} \hat{\mathcal{L}}_0^{-1} + \dots\end{aligned}\quad (6.56)$$

It is convenient to define the matrix \hat{E} , such that $\hat{E}_{ij} = 1$ for all i, j , and the quantity $\beta \equiv \Delta - \Delta' + \frac{i\Gamma}{2}$. Then we may write

$$\begin{aligned}\hat{\mathcal{L}}_0^{-1}(x+i\varepsilon) &= A^{\text{atom}}(x+i\varepsilon) (\hat{1} - \hat{P}_0(x+i\varepsilon))^{-1} \\ &= \frac{1}{x - \Delta} \left(\hat{1} - \frac{\beta}{x - \Delta + N\beta} \hat{E} \right)\end{aligned}\quad (6.57)$$

and Eq. (6.56) becomes

$$\begin{aligned}\hat{\mathcal{L}}^{-1}(x+i\varepsilon) &= A^{\text{atom}}(x+i\varepsilon) (\hat{1} - \hat{P}(x+i\varepsilon))^{-1} \\ &= \frac{1}{x - \Delta} \left(\hat{1} - \frac{\beta}{x - \Delta + N\beta} \hat{E} \right) \left(1 - \frac{\hat{\gamma}^s}{x - \Delta} \right)\end{aligned}\quad (6.58)$$

where

$$\hat{\gamma}^s = 2 \left(\hat{\varepsilon} - \frac{\beta}{x - \Delta + N\beta} \hat{\varepsilon} \hat{E} + O(\hat{\varepsilon}^2) \right) \quad (6.59)$$

The shift of the pole from $x = \Delta$ to $x = \Delta - \frac{\Gamma^s}{x}$ is described by the formula

$$\frac{1}{x - \Delta + \frac{\Gamma^S}{2}} = \frac{1}{x - \Delta} \left(1 - \frac{\Gamma^S/2}{x - \Delta} + O((\Gamma^S)^2) \right) . \quad (6.60)$$

Comparing (6.58) to (6.60) we find after some algebra that

$$\begin{aligned} \sum_{ij}^{-1}(x+i\varepsilon) &= A^{\text{atom}}(x+i\varepsilon) \left(1 - P(x+i\varepsilon) \right)_{ij}^{-1} \\ &= \frac{\delta_{ij} - \frac{1}{N}}{x - \Delta + \frac{\Gamma_{ij}^S}{2}} + \frac{1/N}{x - \Delta + N(\Delta - \Delta' + \frac{i\Gamma}{2})} , \end{aligned} \quad (6.61)$$

where the shift of the pole in the ij matrix element is given by

$$\frac{\Gamma_{ij}^S}{2} = \frac{\varepsilon_{ij} - \frac{1}{N} \sum_k (\varepsilon_{ik} + \varepsilon_{jk}) + \frac{1}{N^2} \sum_{k,l} \varepsilon_{k,l}}{\delta_{ij} - \frac{1}{N}} , \quad (6.62)$$

with $\varepsilon_{ij}(x)$ evaluated at $x = \Delta$.

Two Near Atoms

Consider the simplest non-trivial example, namely that of two near atoms in one dimension, with atom 1 initially excited and atom 2 initially unexcited. In this case it is easy to show that

$$\varepsilon_{12} \approx \text{Re}(\varepsilon_{12}) - i\Gamma \left(\frac{r_{12}\Delta}{2c} \right)^2 , \quad (6.63)$$

(for $\frac{r_{12}\Delta}{2c} \ll 1$, where r_{12} is the separation of the atoms) and that

$$\Gamma_{ij}^S = -2\varepsilon_{12} = 2i\Gamma \left(\frac{r_{12}\Delta}{2c} \right)^2 , \quad (6.64)$$

for all ij . (We ignore the real part of the shift Γ_{ij}^S .)

Combining (6.64) with (6.61) and (6.15) we find that the

probability that atom n , $n=1,2$, is excited at time t , given that atom 1 was excited at time $t=0$, is given by

$$N_n^\dagger(t) = \left| \frac{1}{2\pi i} \int_0^\omega dx e^{-ixt} \left\{ \sum_{n,1}^{-1}(x-i\epsilon) - \sum_{n,1}^{-1}(x+i\epsilon) \right\} \right|^2$$

$$= \left| \left(\delta_{1,n} - \frac{1}{2} \right) e^{-i\Delta t} e^{-\Gamma_{\text{slow}} t/2} + \frac{1}{2} e^{-i(\Delta - 2(\Delta - \Delta'))t} e^{-\Gamma t} \right|^2 .$$
(6.65a)

The slow decay rate for both atoms is

$$\Gamma_{\text{slow}} = 2\Gamma \left(\frac{r_{12}\Delta}{2c} \right)^2 .$$
(6.65b)

These probabilities are shown in Fig. 6.3a and b for two different separations r_{12} of the atoms. Note that the decay rate Γ_{slow} increases as the separation increases. The inset of Fig. 6.3(a) shows the Fourier transform of the probability amplitude for atom n , namely the quantity

$$\frac{\sum_{n,1}^{-1}(x-i\epsilon) - \sum_{n,1}^{-1}(x+i\epsilon)}{2\pi i} .$$
(6.66)

We see that the former pole at $x=\Delta$ has become a narrow resonance.

N Randomly Distributed Near Atoms

Suppose there are a large number N of two-level atoms randomly distributed in a one-dimensional box of length L , with only atom 1 initially excited. It is easy to show that the average square distance $\langle r_{12}^2 \rangle$ between any two atoms is given by

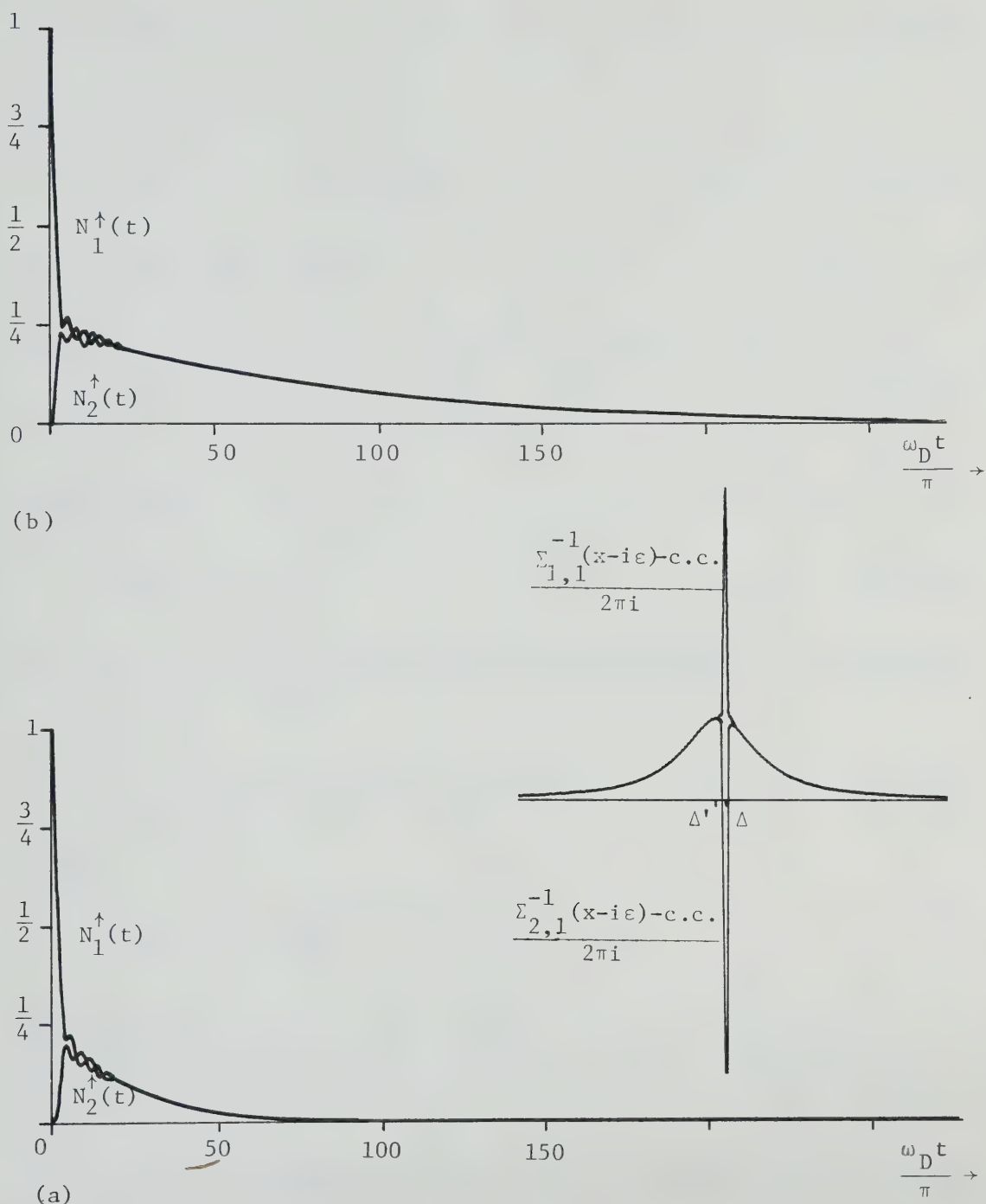


Fig. 6.3 (a) The probabilities $N_1^\uparrow(t)$ and $N_2^\uparrow(t)$ that atoms 1 and 2 are excited at time t . System parameters: $\Delta = .4\omega_D$, $\Gamma = .2\omega_D$, and atom separation $r_{1,2} = c/\omega_D$. (b) Same as (a) with atom separation $r_{1,2} = \frac{1}{2}c/\omega_D$. The inset of (a) shows the Fourier transform of the probability amplitude for the two atoms.

$$\langle r_{12}^2 \rangle = L^2/6 \quad . \quad (6.67)$$

Thus from (6.63)

$$\langle \text{Im}(\epsilon_{12}) \rangle = - \frac{\Gamma}{6} \left(\frac{L\Delta}{2c} \right)^2 \quad . \quad (6.68)$$

If we now assume that

$$\epsilon_{ij} = \begin{cases} \langle \epsilon_{12} \rangle & , \quad \text{for } i \neq j \\ 0 & , \quad \text{for } i = j \end{cases} \quad (6.69)$$

we find that

$$\frac{\Gamma_{ij}^S}{2} = - \langle \epsilon_{12} \rangle \quad , \quad (6.70)$$

for all i, j . Thus the probability that atom 1 is excited at time t is

$$N_1^\uparrow(t) \approx e^{-\Gamma_{\text{slow}} t} \quad (6.71a)$$

where

$$\Gamma_{\text{slow}} = \frac{\Gamma}{3} \left(\frac{L\Delta}{2c} \right)^2 \quad . \quad (6.71b)$$

The probability that any of the other $N-1$ atoms become excited is negligible for large N . Let us now find the phonon spectrum that is emitted in this case. The density $n_{\text{ph}}(\omega_k) d\omega_k$ of phonons emitted into frequency interval $d\omega_k$ is given by

$$n_{\text{ph}}(\omega_k, t) d\omega_k = D(\omega_k) \Omega \langle \begin{pmatrix} 1 \\ 0 \end{pmatrix}_1 | b_k^\dagger(t) b_k(t) | \begin{pmatrix} 1 \\ 0 \end{pmatrix}_1 \rangle \quad , \quad (6.72)$$

where $b_k(t)$ is given by (6.49). To find $b_k(t)$ we must evaluate the quantity (see Eq. (6.50))

$$\begin{aligned}
& \sum_{n=1}^N e^{-ikr_n} A^{\text{atom}}(x+i\epsilon) (\hat{1} - \hat{P}(x+i\epsilon))_{n,1}^{-1} \\
&= \sum_{n=1}^N e^{-ikr_n} \left\{ \frac{\delta_{n,1} - \frac{1}{N}}{x - \Delta + \frac{\Gamma_{ij}^s}{2}} + \frac{1/N}{x - \Delta + N(\Delta - \Delta' + \frac{i\Gamma}{2})} \right\}. \quad (6.73)
\end{aligned}$$

In the previous case where all atoms were at the same position, the contribution from the first term in braces vanished identically. However in the present case with N large, this term gives the dominant contribution. Thus neglecting the second term and using the expression (6.70) for Γ_{ij}^s we find that (6.73) becomes

$$\frac{C}{x - \Delta + i \frac{\Gamma_{\text{slow}}}{2}}, \quad (6.74)$$

where C is an undetermined constant. Plugging (6.74) into (6.49) we find that

$$b_k(t \rightarrow \infty) = \frac{C g S_1^-(0) e^{-i\omega_k t}}{\omega_k - \Delta + i \frac{\Gamma_{\text{slow}}}{2}}. \quad (6.75)$$

The condition that a phonon is emitted with certainty as $t \rightarrow \infty$ determines the constant $|C|^2$ to be

$$|C|^2 = \frac{\Gamma_{\text{slow}}}{\Gamma}. \quad (6.76)$$

The phonon spectrum emitted after long times is thus

$$n_{\text{ph}}(\omega, t \rightarrow \infty) d\omega = \frac{\frac{\Gamma_{\text{slow}}}{2\pi}}{(\omega - \Delta)^2 + \left(\frac{\Gamma_{\text{slow}}}{2}\right)^2}. \quad (6.77)$$

Let us paraphrase these results. If a single atom of a collection of N atoms randomly distributed along a length $L < c/\Delta$ is initially excited, then that atom decays at the rate

$$\Gamma_{\text{slow}} = \frac{\Gamma}{12} \left(\frac{L\Delta}{c} \right)^2, \quad (6.78)$$

emitting a Lorentzian phonon spectrum (6.77) of width Γ_{slow} . This decay is indistinguishable from the decay of a single isolated atom whose effective lifetime is $T_1^{\text{eff}} = 1/\Gamma_{\text{slow}}$. It is interesting to note that the rate Γ_{slow} is independent of the number of atoms N (for large N) in the system. If we imagine that the length L of the system is just the range of the virtual phonon cloud surrounding the excited atom (i.e. the range for which the near-field form of the phonon amplitude (6.28) is valid); namely

$$L = c/\Delta, \quad (6.79)$$

then we find that

$$\Gamma_{\text{slow}} = \frac{\Gamma}{12}. \quad (6.80)$$

This result holds whenever the number N of atoms in the range (6.79) is large compared to unity.

Assuming that these results hold also in the three-dimensional ruby system where $L = \frac{10^6 \text{ cm/sec}}{2 \times 10^{12} \text{ Hz}} \approx 10^{-7} \text{ cm}$, we expect (6.80) to obtain for densities of excited Cr^{3+} ions $N^* \gtrsim 1/L^3 \approx 10^{20} \text{ cm}^{-3}$. Unfortunately these densities are beyond the range of the present phonon bottleneck

experiments in ruby. To our knowledge this phenomenon has not been looked for or observed in optical radiation trapping experiments.

CHAPTER 7

CONCLUSION

We have studied the phenomenon of resonance radiation trapping by a system of two-level states paying particular attention to the example of the bottlenecking of 29 cm^{-1} phonons by excited Cr^{3+} ions in optically pumped ruby. In Chapter 2 we found the field theoretic form of the electron-phonon interaction in ruby, and in Chapter 3 we studied the time evolution of a single two-level state coupled to a phonon field. With this experience we proceeded to solve the problem of the time evolution of a system of many atoms coupled to a phonon field by deriving in Chapter 4 a set of rate equations describing the system. These equations were shown to be valid for small numbers of excitations and at low density of two-level states. The former restriction allowed us to neglect stimulated phonon emission and the latter to neglect the quantum interference effects due to phonon reflections by nearby atoms. In other words an electron-phonon interaction could be viewed as a two-step process with the phonon emission by an atom independent of the preceding phonon absorption. With these limitations in mind we solved the rate equations in Chapter 5 and compared the results with recent experiments on the phonon bottleneck in ruby. The rate equations were able to reproduce the following experimental features:

(1) the rapid decay of the system in time $t \approx T_1$ from its non-equilibrium initial conditions.

(2) the establishment of a bottleneck with a quasi-equilibrium excited atom population $N_2(\text{eq})/N^* \propto N^{*-1/2}$, and

(3) the subsequent decay of the quasi-equilibrium at the rate $1/T_s \propto 1/T_1 \times f$ where f is the fraction of the emitted phonon spectrum which is not resonantly reabsorbed. In the case of ruby where the emission spectrum is Lorentzian we had $f = 1/\sqrt{\alpha(\nu_0)b}$.

We saw that the $N^{*-1/2}$ behavior of the quasi-equilibrium excited atom population was a consequence of the fact that all phonon modes in the frequency band satisfying the condition $\alpha(\nu)b > 1$ came into equilibrium with (i.e. reached the same population as) the excited atoms, and that this band had a width $\Delta\nu_0 \sqrt{\alpha(\nu_0)b} \propto N^{*1/2}$.

The appendix shows that this broadened, flattened spectrum existing inside the system is the same as the spectrum that would be observed emerging from the system.

To obtain quantitative agreement with the experiments by Pauli et al.^{20,21} we had to choose the $2\bar{A}$ state lifetime $T_1 \approx 20$ ns in the rate equations, which is longer by an order of magnitude, than most previous estimates of T_1 . In Chapter 6 we showed that this large lifetime could be due to a quantum interference effect in which a standing wave or resonance is formed between the decaying atom and a neighboring unexcited atom. The duration of this resonance then

enters as the effective lifetime T_1^{eff} of an excited atom in the otherwise classical rate equations.

In Chapter 6 we found another quantum effect which occurs at densities so high that there are several other atoms within a resonance radiation wavelength, i.e. within the virtual phonon cloud, of an excited atom ($N^* \gtrsim 10^{20} \text{ cm}^{-3}$ in ruby). In this regime the radiation, which is perfectly trapped in Dicke's model, slowly leaks away in a time $T_1^{\text{eff}} = 12 T_1$, independent of the atom density.

Some of our assertions could be tested experimentally. For example the radiation leaking result of the preceding paragraph could be checked in impurity-doped crystals such as sapphire which have a longer resonance wavelength than ruby, and for which the effect should therefore appear at a lower density N^* . Also no experiments to date have examined the dependence of T_s on the size b of the excitation region. We predict a $b^{1/2}$ dependence where a theory due to Pauli et al.²⁰ predicts that $T_s \propto b^{3/2}$, and purely spatial diffusion implies that $T_s \propto b^2$.

REFERENCES

1. A.C.G. Mitchell and M.W. Zemansky, 'Resonance radiation and excited atoms' (Cambridge University Press, Cambridge, 1961).
2. H.W. Webb, 'The metastable state in mercury vapor', Phys. Rev. 24, 113 (1924).
3. M.W. Zemansky, 'The diffusion of imprisoned resonance radiation in mercury vapor', Phys. Rev. 29, 513 (1927).
4. K.T. Compton, 'Theory of ionization by cumulative action and the low voltage arc', Phys. Rev. 20, 283 (1922).
5. E. Milne, J. Lond. Math. Soc. 1, 1 (1926).
6. T. Holstein, 'Imprisonment of resonance radiation in gases. I and II', Phys. Rev. 72, 1212 (1947); 83, 1159 (1951).
7. V.A. Veklenko, 'Green's function for the resonance radiation diffusion equation', Soviet Physics JETP 9, 138 (1959).
8. G.W. Semenoff, private communication.
9. E.H. Jacobsen and K.W.H. Stevens, 'Interaction of ultrasonic waves with electron spins', Phys. Rev. 129, 2036 (1963).
10. A. Sommerfeld, 'Über die fortpflanzung des lichtes in dispergierenden medien', Ann. Physik 44, 177 (1914).
11. E.B. Tucker, 'Amplification of 9.3-kMc/sec ultrasonic pulses by maser action in ruby', Phys. Rev. Lett. 6, 547 (1961).

12. R.S. Meltzer and J.E. Rives, 'New high-energy monoenergetic source for nanosecond phonon spectroscopy', Phys. Rev. Lett. 38, 421 (1976).
13. J.E. Rives and R.S. Meltzer, 'Time resolved spectroscopic study of the excited-state spin-phonon interaction in ruby', Phys. Rev. B 16, 1808 (1977).
14. J.I. Dijkhuis, A. van der Pol, and H.W. DeWijn, 'Spectral width of optically generated bottlenecked 29-cm^{-1} phonons in ruby', Phys. Rev. Lett. 37, 1554 (1976).
15. J.I. Dijkhuis and H.W. DeWijn, 'Spatial diffusion of weakly bottlenecked 29-cm^{-1} phonons in ruby observed by quasi-stationary techniques', Sol. State. Commun. 31, 39 (1979).
16. J.I. Dijkhuis, K. Huibregtse, and H.W. deWijn, 'Optical detection and phonon bottleneck of the direct decay within the $\bar{E}(^2E)$ state of ruby', Phys. Rev. B 20, 1835 (1979).
17. J.I. Dijkhuis and H.W. deWijn, 'Optically induced 2-phonon processes connecting the $\bar{E}(^2E)$ states in ruby', Phys. Rev. B 20, 3615 (1979).
18. J.I. Dijkhuis and H.W. deWijn, 'Diffusion of bottlenecked 29-cm^{-1} phonons in optically excited ruby', Phys. Rev. B 20, 1844 (1979).
19. S. Geschwind, G.E. Devlin, R.L. Cohen, and S.R. Chinn, 'Orbach relaxation and hyperfine structure in the excited $\bar{E}(^2E)$ state of Cr^{3+} in Al_2O_3 ', Phys. Rev. 137, A1087 (1965).

20. G. Pauli, K.F. Renk, G. Klimke, and H.J. Kreuzer,
'Resonance interaction of electronic 2-level states
and short-wave phonon radiation in ruby', Phys. Stat.
Sol.(b) 95, 503 (1979).
21. G. Pauli, 'Resonanzstreuung von 29 cm^{-1} phononen in
optisch gepumptem rubin' Ph. D. thesis, Univ.
Regensburg, 1978.
22. G. Pauli and K.F. Renk, 'Spectral diffusion of resonantly
trapped 29-cm^{-1} phonons in ruby', Phys. Lett. 67A, 410
(1978).
23. R. Orbach and L.A. Vredevoi, 'The attenuation of high-
frequency phonons at low temperatures', Physics 1, 91
(1964).
24. P.G. Klemens, 'Decay of high-frequency longitudinal phonons',
J. Appl. Phys. 38, 4573 (1967).
25. A.A. Kaplyanskii, S.A. Basun, V.A. Rachin, and R.A. Titov,
'Anisotropy of resonant absorption of high frequency
 0.87×10^{12} Hz phonons in the excited state of Cr^{3+} ions
in ruby', JETP Lett. 21, 200 (1975).
26. H. Lengfellner, G. Pauli, W. Heisel and K.F. Renk, 'Tunable
quantum counter for far-infrared radiation', Appl. Phys.
Lett. 29, 566 (1976).
27. M.A. Kurnit, I.D. Abella and S.R. Hartmann in 'The physics
of quantum electronics conference proceedings, San
Juan, Puerto Rico, 1965', ed. P.L. Kelly, B. Lax and
P.E. Tannenwald (McGraw-Hill, New York, 1966), p. 267.

28. S. Sugano and Y. Tanebe, 'Absorption spectra of Cr^{3+} in Al_2O_3 Part A. Theoretical studies of the absorption bands and lines', J. Phys. Soc. Japan 13, 880 (1958).
29. B. DiBartolo, 'Optical interactions in solids', (J. Wiley and Sons, Inc., New York, 1968), p. 343.
30. R.H. Dicke, 'Coherence in spontaneous radiation processes', Phys. Rev. 93, 99 (1954).
31. S. Swain, 'A continued fraction solution to the problem of a single atom interacting with a single radiation mode in the electric dipole approximation', J. Phys. A 6, 192 (1973).
32. G. Scharf, 'Time evolution of a quantum mechanical maser model', Ann. Phys. 83, 71 (1974).
33. R. Prakash and N. Chandra, 'Theory of emission of radiation from an assembly of N two-level atoms', Phys. Rev. A 21, 1297 (1980).
34. W.R. Mallory, 'Cooperative interaction of atoms with a radiation field: Evolution of the field density matrix', Phys. Rev. A 11, 2036 (1975).
35. R. Bonifacio and G. Preparata, 'Coherent spontaneous emission', Phys. Rev. A 2, 336 (1970).
36. R. Bonifacio, P. Schwendimann and F. Haake, 'Quantum statistical theory of superradiance. I', Phys. Rev. A 4, 302 (1971).
37. C. Leonardi and F. Persico, 'Excitation spectrum of a linear chain of paramagnetic atoms with spin-phonon interaction', Phys. Rev. Lett. 19, 899 (1967).

38. C. Leonardi and F. Persico, 'Theory of the dynamical behavior of inverted spins linearly coupled to a lattice', Sol. Stat. Commun. 9, 1259 (1971).
39. C. Leonardi and F. Persico, 'Phonon bandwidth and rate equations in avalanche relaxation', Phys. Rev. B 8, 4975 (1973).
40. D. Walgraef, 'Quantum statistics of a monomode-laser model', Physica 72, 578 (1974).
41. E.S. Grinberg and R.R. Nigmatullin, 'Kinetics of dilute solid paramagnets under bottleneck conditions', Phys. Stat. Sol. B 82, 397 (1977).
42. I.L. Bukhbinder, I.S. Donskaya and A.R. Kessel, 'Kinetic equations for the dilute solid paramagnets', Physica 74, 75 (1974).
43. M.I. D'yakonov and V.I. Perel', 'Coherence relaxation during diffusion of resonance radiation', Soviet Physics JETP 20, 997 (1965).
44. V. Weisskopf and E. Wigner, 'Berechnung der natürlichen linienbreite auf grund der Diracshen lichttheorie', Z. Phys. 63, 54 (1930).
45. I.R. Senitzky, 'Interaction between a non-linear oscillator and a radiation field', Phys. Rev. A 6, 1175 (1972).
46. R. Teshima, private communication.
47. I. Gradshteyn and I. Ryzhik, 'Table of integrals, series and products', (Academic Press, New York, 1965).
48. S. Geschwind, 'Electron paramagnetic resonance', (Plenum Press, New York, 1972).

49. L. Fonda, G.C. Ghirardi and A. Rimini, 'Decay theory of unstable quantum systems', Rep. Prog. Phys. 41, 587 (1978).
50. M. Razavy and E. Henley, Jr., 'Model for gamma decay of atomic or nuclear systems', Can. J. Phys. 48, 2399 (1970).
51. H.J. Kreuzer, 'Non-equilibrium thermodynamics and its statistical foundations', (Oxford University Press, 1980).
52. H.J. Kreuzer and J.R. Beamish, 'Topics in non-equilibrium physics', unpublished, 1977.
53. N.N. Bogoliubov, in 'Studies in statistical mechanics, deBoer and Uhlenbeck, eds., (North Holland, Amsterdam, 1962).
54. J. Matthews and R. Walker, 'Mathematical methods of physics', (W. Benjamin, New York, 1965), pp. 223-225.
55. M. Abramowitz and I.A. Stegun, eds., 'Handbook of mathematical functions', (National Bureau of Standards, 1964).
56. R.G. Breene, Jr., 'The shift and shape of spectral lines', Handb. d. Phys. 27, 1, (Springer, 1964).
57. G. Reck, H. Takebe, and C. Mead, 'Theory of resonance absorption line shapes in monatomic gases', Phys. Rev. 137, A683 (1965).

APPENDIX

THE EMITTED PHONON SPECTRUM

Until now we have not discussed the spectrum of phonons that emerges from the excited region of the ruby crystal. This spectrum can be derived from a simple phenomenological argument. Suppose that we have a uniform distribution of two-level atoms in the upper energy level along a one-dimensional system of length b , as shown in Fig. A.1(a). Then each infinitesimal region of length dx about x , $0 < x < b$, of the system emits a spectrum $A \alpha(\nu) dx$ of phonons toward the observer located at $x=0$, where A is some constant and $\alpha(\nu)$ is the frequency dependent absorption coefficient (which is proportional to the emission spectrum). In travelling to the observer this emission is attenuated by the factor $e^{-\alpha(\nu)x}$. Integrating over the entire system we find the spectrum $P(\nu)$ arriving at $x=0$ from all parts of the system, namely

$$P(\nu) = A\alpha(\nu) \int_0^b dx e^{-\alpha(\nu)x} = A(1 - e^{-\alpha(\nu)b}) \quad . \quad (A.1)$$

If $\alpha(\nu)b \ll 1$, i.e. if the system is 'transparent', then $P(\nu) = Ab\alpha(\nu)$, which is just the unattenuated emission spectrum. On the other hand if $\alpha(\nu)b \gg 1$, i.e. if the system is opaque then, as shown in Fig. A.1(c), $P(\nu) = A =$ constant over a broad band of frequencies around resonance

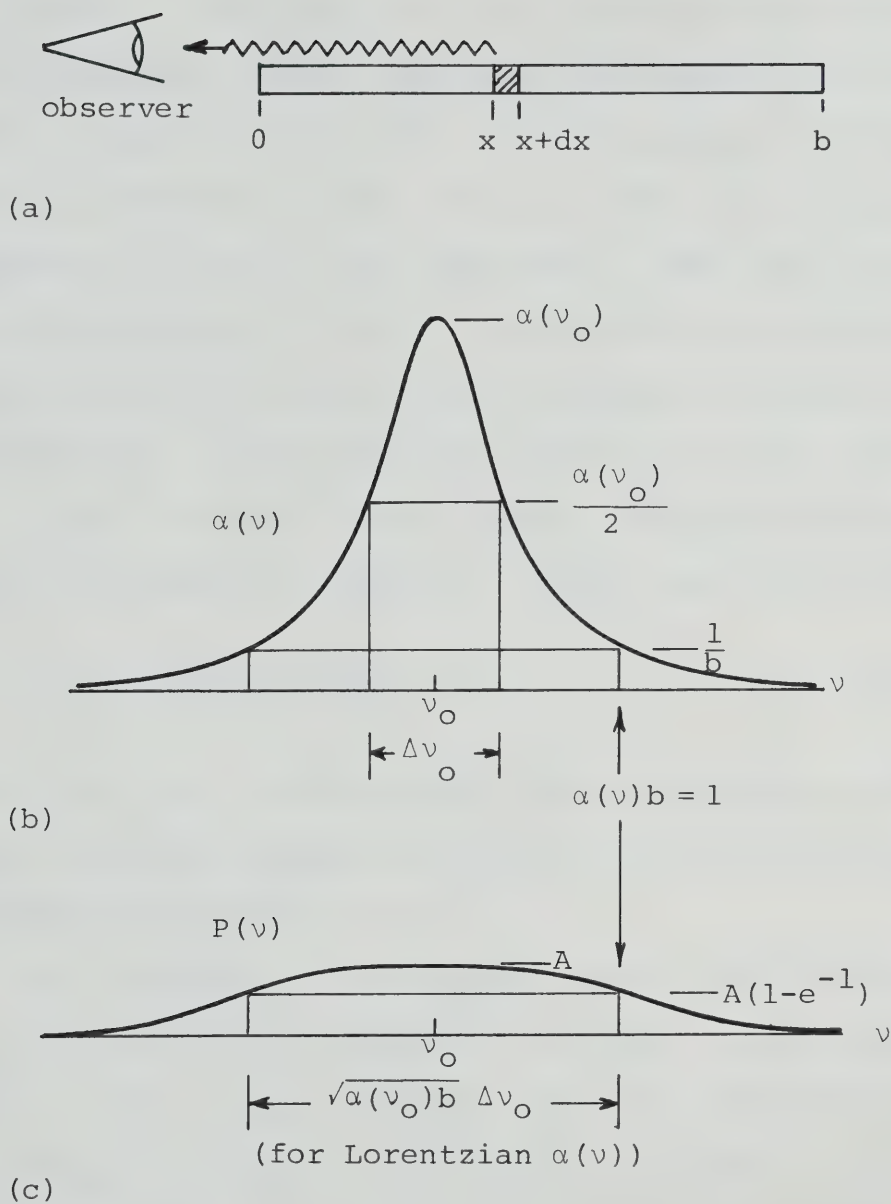


Fig.A.1 (a) Geometry of the one-dimensional radiation trapping system of size b . (b) The absorption coefficient $\alpha(\nu)$. (c) The phonon spectrum $P(\nu)$ emerging from the system in case $\alpha(\nu_0)b \gg 1$.

satisfying $\alpha(\nu)b > 1$, and $P(\nu) = Ab\alpha(\nu)$ in the far wings where $\alpha(\nu)b < 1$. In case $\alpha(\nu)$ is a Lorentzian of width $\Delta\nu_0$ then the emerging phonon spectrum is broadened to width $\sqrt{\alpha(\nu_0)b} \Delta\nu_0$ and flattened similar to the phonon spectrum inside the excitation region shown in Fig. 5.4, except for the absence of the dip near resonance. This self-reversal of the distribution in Fig. 5.4 is due to the vanishing of the density of Cr^{3+} ions in the $2\bar{A}$ state at the walls of the container. We can reproduce this by allowing the constant A in Eq. (A.1) to have a spatial dependence such as that of the system of Chapter 5, namely (see Eq. (5.12))

$$A(x) = J_0\left(\frac{4.8}{b} \left|x - \frac{b}{2}\right|\right) . \quad (\text{A.2})$$

Thus we find that in the steady state the phonon spectrum emerging from the excitation region is the same as that inside the excitation region.

Some features of the emitted phonon spectrum can be found via quantum field theoretic methods. Recall from Chapter 6 (Eqs. (6.1a) and (6.6)) that the probability amplitude that a phonon of wavenumber \underline{k} exists in the system is given by

$$B_{\underline{k}}(x) = \frac{g}{x - \omega_{\underline{k}}} \sum_{n=1}^N e^{-i\mathbf{k} \cdot \mathbf{r}_n} \mathcal{J}_n^-(x) , \quad (\text{A.3})$$

where the amplitude that atom n is excited is given by

$$\mathcal{J}_n^-(x) = (\hat{1} - \hat{P}(x))_{n,m}^{-1} A^{\text{atom}}(x) i S_m^-(0) . \quad (\text{A.4})$$

We have assumed that in the initial state $|i\rangle = |(\frac{1}{0})_m\rangle$, atom m is excited and that no phonons are present. From our work of Chapter 6 we know that whenever the two-level atoms are not all at the same position, then $\phi_n^-(x)$ has a branch cut along the real axis in the interval $0 < x < \omega_D$ and no poles. Hence its Fourier transform $S_n^-(t)$ decays in a finite time. Since we are interested in the spectrum of phonons existing in the infinite time limit (when all the phonons have escaped from the excitation region), we may find $b_k(t \rightarrow \infty)$ by simply evaluating $B_k(x)$ at the pole $x = \omega_k$, i.e.:

$$b_k(t \rightarrow \infty) = \lim_{\epsilon \rightarrow 0} \sum_{n=1}^N e^{-ik \cdot \tilde{r}_n} (\hat{1} - \hat{P}(\omega_k + i\epsilon))^{-1}_{n,m} A^{\text{atom}}(\omega_k + i\epsilon) S_m^-(0) . \quad (\text{A.5})$$

The number of phonons eventually emerging from the excitation region is given by

$$N_{\text{ph}} = \sum_k \langle i | b_k^\dagger(t \rightarrow \infty) b_k(t \rightarrow \infty) | i \rangle . \quad (\text{A.6})$$

Let us now specialize to a one dimensional continuum system. Then (A.6) can be written

$$N_{\text{ph}} = \int_0^{\omega_D} n_{\text{ph}}(\omega_k) d\omega_k , \quad (\text{A.7})$$

where

$$n_{\text{ph}}(\omega_k) d\omega_k = \frac{1}{2} \frac{\Gamma}{2\pi} d\omega_k \left\{ \left| \sum_{n=1}^N e^{+\frac{i\omega_k}{c} r_n} (\hat{1} - \hat{P}(\omega_k + i\varepsilon))_{nm}^{-1} A^{\text{atom}}(\omega_k + i\varepsilon) \right|^2 + \left| \sum_{n=1}^N e^{-\frac{i\omega_k}{c} r_n} (\hat{1} - \hat{P}(\omega_k + i\varepsilon))_{nm}^{-1} A^{\text{atom}}(\omega_k + i\varepsilon) \right|^2 \right\}. \quad (\text{A.8})$$

Here the first/second term in braces represents phonons emitted to the left/right. Let us arrange the atoms in the order shown below

$$\begin{array}{ccccccc} & r_1 & r_2 & \dots & r_m & \dots & r_{N-1} & r_N \\ & \times & \times & & \times & & \times & \times \\ \text{atom:} & 1 & 2 & \dots & m & \dots & N-1 & N \end{array} \quad r \quad (\text{A.9})$$

and assume that the distance r_{ij} between atoms i and j is large, i.e. $r_{ij} \gg c/\Delta$. Consider the spectrum of phonons emitted to the right by an interior atom m . Note that we may formally invert the matrix $(\hat{1} - \hat{P}(\omega_k + i\varepsilon))$ occurring in (A.8), yielding

$$(\hat{1} - \hat{P}(\omega_k + i\varepsilon))_{ij}^{-1} = \frac{\hat{C}_{ij}(\omega_k + i\varepsilon)}{\det(\hat{1} - \hat{P}(\omega_k + i\varepsilon))} \quad (\text{A.10})$$

where $\hat{C}_{ij}(\omega_k + i\varepsilon)$ is the cofactor matrix formed by multiplying $(-1)^{i+j}$ times the matrix formed by deleting the i^{th} row and the j^{th} column of $(\hat{1} - \hat{P}(\omega_k + i\varepsilon))$. Thus we can write the second term of (A.8) in the form

$$n_{ph}(\omega) d\omega \left| \begin{array}{l} \text{emitted to} \\ \text{the right} \\ \text{by atom } m \end{array} \right| = \frac{1}{2} \frac{\Gamma}{2\pi} \left| \frac{A^{atom}(\omega+i\epsilon)}{\det(\hat{1}-\hat{P}(\omega+i\epsilon))} \sum_{n=1}^N e^{-\frac{i\omega}{c} r_n} \hat{C}_{nm}(\omega+i\epsilon) \right|^2 \quad (A.11a)$$

$$= \frac{1}{2} \frac{\Gamma}{2\pi} \left| \frac{A^{atom}(\omega+i\epsilon)}{\det(\hat{1}-\hat{P}(\omega+i\epsilon))} \right|^2 \cdot \left| \det \hat{C}'(\omega+i\epsilon) \right|^2, \quad (A.11b)$$

where

$$\det \hat{C}'(\omega+i\epsilon) = \begin{vmatrix} 1 & \dots & \alpha e^{\frac{i\omega}{c} r_{ij}} \\ \vdots & \ddots & \vdots \\ e^{\frac{i\omega}{c} r_{1,N}} & e^{\frac{i\omega}{c} r_{2,N}} & \dots & 1 \end{vmatrix} \quad \begin{array}{l} \text{m}^{th} \text{ row} \\ \text{N} \times \text{N matrix} \end{array}$$

$$= |1-\alpha|^{N-m} e^{\frac{i\omega}{c} r_{m,N}} \det \hat{C}''(\omega+i\epsilon), \quad (A.12)$$

where

$$\det \hat{C}''(\omega+i\epsilon) = \begin{vmatrix} 1-\alpha & \dots & \alpha(e^{\frac{i\omega}{c} r_{ij}} - e^{-\frac{i\omega}{c} r_{ij}}) \\ \vdots & \ddots & \vdots \\ 0 & \dots & 1-\alpha \\ \vdots & \ddots & \vdots \\ e^{\frac{i\omega}{c} r_{1m}} & e^{\frac{i\omega}{c} r_{2m}} & \dots & 1 \end{vmatrix} \quad \begin{array}{l} \text{m} \times \text{m matrix,} \\ \end{array} \quad (A.13)$$

and

$$\alpha(\omega) \equiv \frac{i\Gamma/2}{\omega - \Delta' + \frac{i\Gamma}{2}} \quad . \quad (\text{A.14})$$

Eq. (A.11a) has the following interpretation:

At time $t=0$ atom m is excited.

A^{atom} is the probability amplitude for the non-decay of this atom.

$1/\det(1 - P) = \det(1 - P)^{-1}$ is the sum of the amplitudes over all possible paths (traversed all numbers of times) for a phonon to be emitted and to eventually return to the originally excited atom m .

C_{nm} is then the amplitude for a phonon to be emitted by atom m and absorbed by atom n , by traversing a simple non-repeating path from m to n . The product of the above amplitudes gives the amplitude that atom n is excited. Finally the amplitudes for phonons to be emitted by any of the N atoms add in phase to give the amplitude for the existence of a phonon.

Eqs. (A.11b) and (A.12) show that by factorizing $\det C'$ a different interpretation is possible:

$\det C''$ is the amplitude for a phonon to interact with the $m-1$ atoms to the left of atom m and to eventually return to atom m .

The factor

$$F_m(\omega) \equiv |1 - \alpha|^2 (N-m) = \left[\frac{(\omega - \Delta')^2}{(\omega - \Delta')^2 + (\frac{\Gamma}{2})^2} \right]^{N-m} \quad (\text{A.15})$$

is then the factor by which these phonons are attenuated in travelling the distance from atom m to the right to atom N .

To date it has proved impossible to evaluate $\det(1 - P(\omega + i\varepsilon))$ and $\det C''(\omega + i\varepsilon)$ in closed form for all ω . However if we approximate these quantities by their values far from resonance, namely

$$\det(1 - P(\omega \rightarrow \infty + i\varepsilon)) = 1, \quad (A.16)$$

$$\det C''(\omega \rightarrow \infty + i\varepsilon) = 1,$$

then Eq. (A.11b) becomes

$$n_{ph}(\omega) d\omega \Big|_{m;right} = \frac{1}{2} \frac{\Gamma}{2\pi} \frac{1}{(\omega - \Delta')^2 + (\frac{\Gamma}{2})^2} \cdot F_m(\omega) \quad (A.17)$$

The attenuating factor $F_m(\omega)$ and the spectrum $n_{ph}(\omega) \Big|_{m;right}$ emitted to the right by atom m are sketched in Figs. A.2(a,b) respectively. We see that the presence of $N-m$ atoms between atom m and the surface of the excitation region results in a 'hole' of width $= \Gamma\sqrt{N-m}$ in the center of the spectrum emitted by atom m .

If we assume that the one-dimensional system is uniformly excited, i.e. that each of the N atoms has a probability $1/N$ of being initially excited, then the averaged emission spectrum is given by

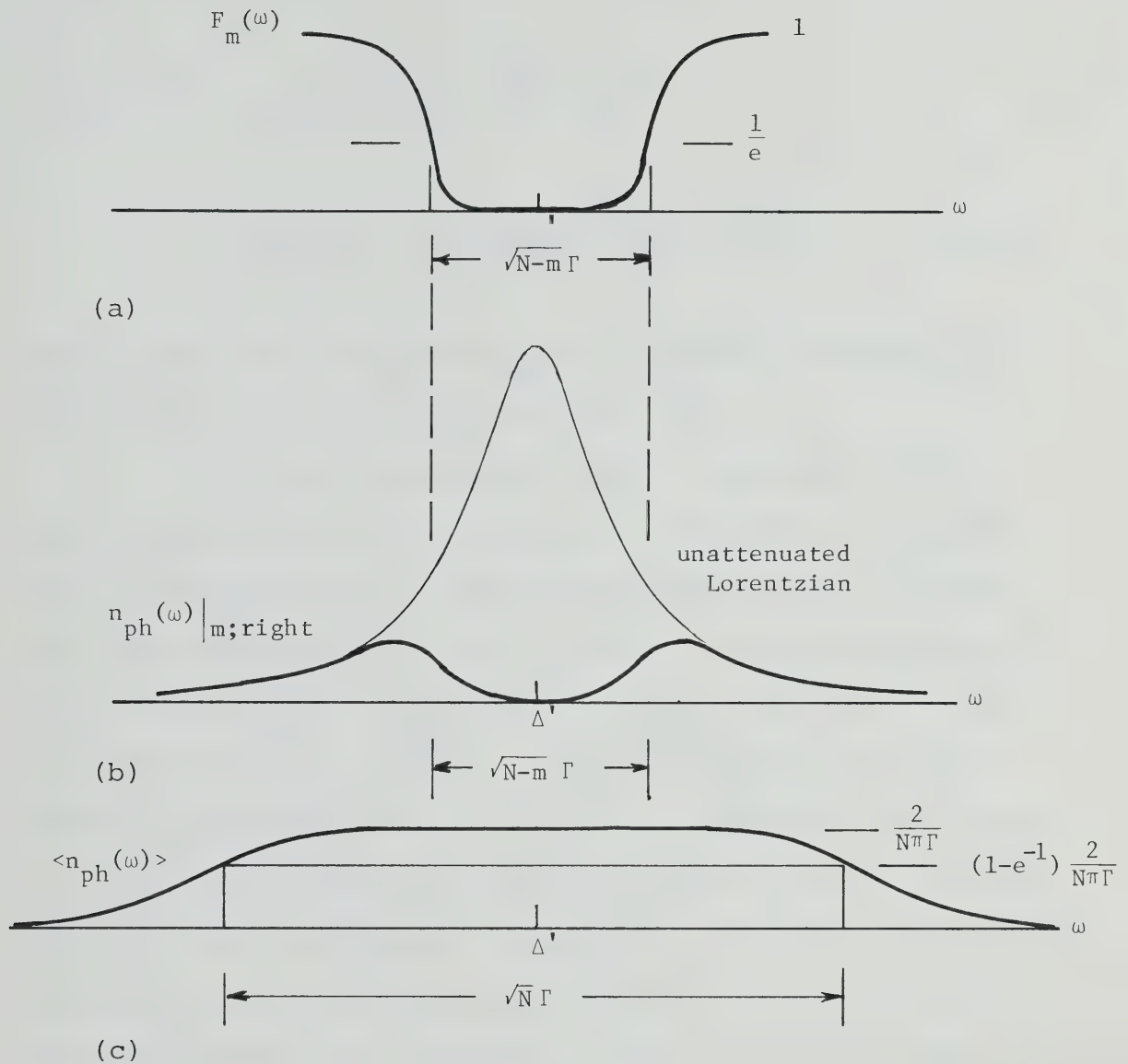


Fig. A.2 (a) The factor $F_m(\omega)$ by which phonons of frequency ω are attenuated in travelling from atom m past $N-m$ atoms to the right-hand boundary of the system (see Eq. (A.15)). (b) The phonon spectrum $n_{ph}(\omega)|_{m;right}$ emerging from the right-hand boundary of the system given that atom m was initially excited. (The light line is the unattenuated Lorentzian emitted by atom m) (see Eq. (A.17)). (c) The phonon spectrum $\langle n_{ph}(\omega) \rangle$ emerging from the system assuming that each two-level atom has probability $1/N$ of being initially excited (see Eq. (A.18)).

$$\begin{aligned}
\langle n_{\text{ph}}(\omega) d\omega \rangle &= \frac{\Gamma/2\pi}{(\omega - \Delta') + (\frac{\Gamma}{2})^2} \frac{\sum_{m=1}^N 1}{N} F_m(\omega) \\
&= \frac{2}{N\pi\Gamma} \left[1 - \left(\frac{(\omega - \Delta')^2}{(\omega - \Delta')^2 + (\frac{\Gamma}{2})^2} \right)^N \right] . \quad (\text{A.18})
\end{aligned}$$

We see that the spectrum $\langle n_{\text{ph}}(\omega) \rangle$, which is sketched in Fig. A.2(c), is flat and has width $\sqrt{N}\Gamma$.

In this one-dimensional system a resonant phonon undergoes exactly N absorptions in traversing the system. Thus it approximates a three-dimensional system in which the absorption probability $\alpha(\nu_0)b = N$. Thus this spectrum is similar to the one of width $\sqrt{\alpha(\nu_0)b} \Gamma$ derived in (A.1) by the elementary argument. (However due to the rather drastic approximations (A.16) it is normalized incorrectly.)

It is possible, by doing the calculation on a computer, to find the spectrum $\langle n_{\text{ph}}(\omega) d\omega \rangle$ emitted by a uniformly excited one-dimensional system without using the approximations for $\det(1-P)$ and $\det C''$ given in (A.16). The results for systems of $N=1,3,5$, and 8 two-level atoms are shown in Fig. A.3(a-d). Here a Monte-Carlo-type calculation was used: Positions for the N atoms were chosen by a random number generator 128 times, each time the resulting spectrum being found. The spectra of the 128 ensemble members were then averaged to produce the spectra of Fig. A.3. Also shown (light lines) are the approximate spectra

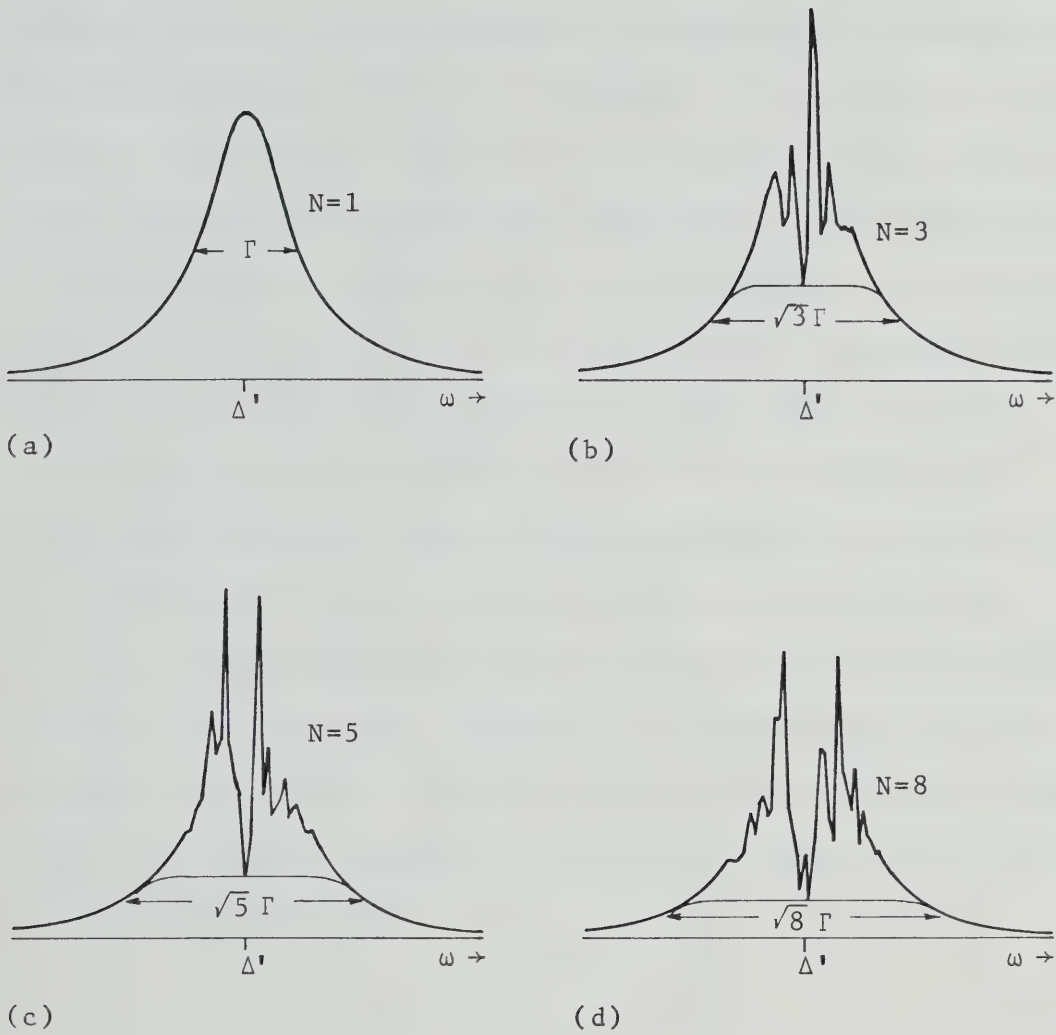


Fig. A.3(a-d) The exact phonon spectrum $\langle n_{ph}(\omega) \rangle$ emitted from a uniformly excited N atom system; $N=1, 3, 5, 8$ respectively. The light curves show $\langle n_{ph}(\omega) \rangle$ according to the approximate formula (A.18). Note the dip in the spectra on resonance.

according to Eq. (A.18). We see that the approximation underestimates the population of phonons with frequencies within a distance $\sqrt{N} \frac{\Gamma}{2}$ of resonance. The spikes in the spectra are due to long-lived resonances between various atoms of some of the systems, and have not yet disappeared in the averaging process. It is interesting to note that the spectra have a hole at the resonance frequency. This hole can be shown to be due to the fact that in a one-dimensional system, phonons exactly on resonance are reflected backwards from an unexcited two-level atom with 100% certainty. Since this phenomenon occurs for all phonons except those emitted outwards by the two end atoms 1 and N, the hole has a height $\frac{1}{2} \times \frac{2}{N} \times$ the height of the original Lorentzian. Since in three dimensions the reflectivity of resonant phonons is not 100%, this effect will not be observed there.

B30292